



THE UNIVERSITY OF  
**WAIKATO**  
*Te Whare Wānanga o Waikato*

Research Commons

<http://researchcommons.waikato.ac.nz/>

## Research Commons at the University of Waikato

### Copyright Statement:

The digital copy of this thesis is protected by the Copyright Act 1994 (New Zealand).

The thesis may be consulted by you, provided you comply with the provisions of the Act and the following conditions of use:

- Any use you make of these documents or images must be for research or private study purposes only, and you may not make them available to any other person.
- Authors control the copyright of their thesis. You will recognise the author's right to be identified as the author of the thesis, and due acknowledgement will be made to the author where appropriate.
- You will obtain the author's permission before publishing any material from the thesis.

# **Managed Aquifer Recharge in the Poverty Bay flats?**

A thesis submitted in fulfilment  
of the requirements for the degree  
of  
**Master of Science in Earth Sciences**  
at  
**The University of Waikato**  
by  
**George Hampton**



THE UNIVERSITY OF  
**WAIKATO**  
*Te Whare Wānanga o Waikato*

**2015**



## Abstract

---

Groundwater use within the Poverty Bay flats has increased over the past 35 years due to land use changes. As a result, groundwater levels within the Makauri and Matokitoki Gravel aquifers are declining at statistically significant rates. The GDC is investigating whether managed aquifer recharge (MAR) can be used to help achieve the sustainable management of groundwater resources within the Poverty Bay flats. The objective of this research is to identify whether an infiltration basin may be successfully used to artificially recharge the Makauri Gravel aquifer beneath the Poverty Bay flats.

Trend analyses were undertaken to provide updated information as to the current state of groundwater resources. Groundwater levels within the Te Hapara Sands, Shallow Fluvial Deposits, and Waipaoa Gravel aquifers are typically stable. However, further monitoring is needed within these aquifers to increase the spatial coverage of the bores monitored. Groundwater levels within the Makauri and Matokitoki Gravel aquifers are declining at statistically significant rates. These declines are probably due to groundwater abstractions.

Groundwater level changes as a result of rainfall event and associated changes in river stage were examined. Groundwater level changes in the Te Hapara Sands, Shallow Fluvial Deposits, and Waipaoa Gravel aquifer were all dependent on the location of each bore. Groundwater level increases in these aquifers were greatest in close proximity to the Waipaoa River. Groundwater level changes within the Makauri Gravel aquifer could be broken into two groups. In the northern and southern reaches of the Makauri Gravel aquifer groundwater levels increased and declined in conjunction with river stage, indicating little recharge occurs in these areas. In the middle reaches of the Makauri Gravel aquifer groundwater levels increased throughout the monitoring period, indicating that this area of the aquifer is subject to significant amounts of recharge.

A pumping test was undertaken to identify if a hydraulic connection existed between the Makauri Gravel aquifer and the overlying Waipaoa Gravel aquifer in the Caesar Road area. No hydraulic connection was identified. Further research is needed in this area to identify if a hydraulic connection does exist, and if so, to evaluate the vertical exchange of groundwater.

Surface-groundwater interactions were analysed via concurrent Waipaoa River flow gaugings. No consistent gaining or losing reaches were identified. Further gaugings should be undertaken regularly to help characterise surface-groundwater interactions.

Two sites were then identified within the Poverty Bay flats for MAR using infiltration basins using the “HIGGS Index”, which was developed to evaluate the MAR potential of an infiltration basin site. While the two sites showed initial promise via a desktop study, infiltrations tests at each site indicated low rates of saturated hydraulic conductivity due to the presence of sediments with low permeability. Subsequently, the MAR potential of both sites was low.

Hydrogeological modelling was undertaken to ascertain whether an infiltration basin may be successfully used as a MAR technique to artificially recharge the Makauri Gravel aquifer. Modelling indicated that an infiltration basin would result in hydraulic head increases of up to 0.85 m within the Makauri Gravel aquifer. However, infiltration rates must not exceed 0.0425 m/day (10.625 m<sup>3</sup>/day) to avoid inundation at the ground surface in close proximity to the infiltration basin. Therefore, given the low infiltration rates it is questionable whether the benefits of establishing and operating an infiltration basin within the Poverty Bay flats would outweigh the costs.

# Acknowledgements

---

This thesis could not have been completed without contributions from the following people:

- Associate Professor Earl Bardsley (primary supervisor, University of Waikato) for proposing and agreeing to supervise this project. Your advice throughout the duration of my research was invaluable.
- Paul White (secondary supervisor, GNS) for sharing your knowledge of the groundwater system within the Poverty Bay flats. Your expertise and advice throughout the duration of this project was much appreciated.
- Dennis Crone, Paul Murphy, Greg Hall, and Peter Hancock (Gisborne District Council). Without your input and help along the way I could not have completed this project. It has been an enjoyable experience working with you. I hope that this thesis is in some manner beneficial to you.
- Clare Houlbrooke, Bob Bower, and Brett Sinclair (Golder Associates) for the providing advice and generously allowing me to use some of your infiltrometer.
- To the landowners who gave me access to their bores and in some cases allowed me to dig up their land. I appreciate your generosity.
- My family and friends for encouraging me to chase my dreams. Your support is valued.
- Kelsey for your unwavering support for which I am incredibly grateful to have.
- Lastly, this project was not possible without the generous financial support provided by the University of Waikato Masters Research Scholarship, the Broad Memorial Fund, and the New Zealand Hydrological Society Project Fund grant. Thank you for thinking I was worthy of your funding.

# Table of Contents

---

<b>Abstract</b> .....	<b>i</b>
<b>Acknowledgements</b> .....	<b>iii</b>
<b>Table of Contents</b> .....	<b>iv</b>
<b>List of Figures</b> .....	<b>vii</b>
<b>List of Tables</b> .....	<b>x</b>
<b>Chapter 1 – Introduction</b> .....	<b>1</b>
<b>1.1. Groundwater in New Zealand</b> .....	<b>1</b>
<b>1.2. Groundwater Management</b> .....	<b>2</b>
<b>1.3. The Poverty Bay flats</b> .....	<b>3</b>
<b>1.4. Research Objective</b> .....	<b>4</b>
<b>1.5. Thesis Structure</b> .....	<b>4</b>
<b>Chapter 2 – Theoretical Review</b> .....	<b>5</b>
<b>2.1. Introduction</b> .....	<b>5</b>
<b>2.2. Groundwater</b> .....	<b>5</b>
2.2.1 Groundwater & aquifer properties.....	5
2.2.2 Groundwater recharge & discharge .....	10
2.2.3 Groundwater flow .....	11
<b>2.3 Groundwater management in New Zealand</b> .....	<b>15</b>
<b>2.4 Managed aquifer recharge</b> .....	<b>16</b>
2.4.1 Managed aquifer recharge methods.....	17
2.4.2 Infiltration basins.....	19
2.4.3. Case Study – Roys Hill artificial recharge scheme .....	20
<b>Chapter 3 – The Poverty Bay Flats</b> .....	<b>24</b>
<b>3.1 Introduction</b> .....	<b>24</b>
<b>3.2 Geology</b> .....	<b>26</b>
<b>3.3 Groundwater system</b> .....	<b>27</b>
3.3.1 Te Hapara Sands .....	31
3.3.2 Shallow Fluvial Deposits .....	32
3.3.3 Waipaoa Gravel Aquifer.....	32
3.3.4 Makauri Gravel Aquifer .....	36
3.3.5 Matokitoki Gravel Aquifer .....	37
<b>3.4 Land use changes</b> .....	<b>38</b>

<b>3.5 Groundwater resources</b> .....	<b>39</b>
<b>Chapter 4 – The HIGGS Index</b> .....	<b>42</b>
<b>4.1 Weights</b> .....	<b>43</b>
<b>4.2 Ranges</b> .....	<b>44</b>
<b>4.3 Ratings</b> .....	<b>46</b>
<b>4.4 Parameters</b> .....	<b>46</b>
4.4.1 Hydraulic connection .....	46
4.4.2 Impact of the vadose zone.....	47
4.4.3 Groundwater depth.....	49
4.4.4 Groundwater flow direction.....	51
4.4.5 Saturated hydraulic conductivity.....	52
<b>4.5 Assumptions</b> .....	<b>52</b>
<b>4.6 Site Selection</b> .....	<b>53</b>
<b>Chapter 5 – Data &amp; Methods</b> .....	<b>55</b>
<b>5.1 Existing data</b> .....	<b>55</b>
5.1.1 Rainfall data .....	55
5.1.2 Surface water data.....	57
5.1.3 Groundwater level data.....	60
5.1.4 Hydrogeological data for model input .....	63
<b>5.2 Data from fieldwork</b> .....	<b>63</b>
5.2.1 Groundwater level data.....	63
5.2.2 Pumping test.....	66
5.2.3 Infiltration data.....	68
<b>5.3 Data analysis</b> .....	<b>70</b>
5.3.1 Trend identification .....	70
5.3.2 Groundwater level changes .....	71
5.3.3 Surface-groundwater interactions .....	71
<b>5.4 Hydrogeological modelling</b> .....	<b>72</b>
5.4.1 Model geology .....	72
5.4.2 Parameters .....	73
5.4.3 Boundary conditions .....	73
5.4.4 Calibration and validation.....	74
<b>5.5 Research Synopsis</b> .....	<b>75</b>
<b>Chapter 6 – Results</b> .....	<b>77</b>
<b>6.1 Trend identification</b> .....	<b>77</b>
6.1.1 Rainfall .....	77

6.1.2 River Flow/Stage.....	78
6.1.3 Groundwater Levels.....	79
<b>6.2 Groundwater Level Changes.....</b>	<b>96</b>
<b>6.3 Pumping Test.....</b>	<b>103</b>
<b>6.4 Concurrent river flow gaugings.....</b>	<b>106</b>
<b>6.5 Infiltration characteristics.....</b>	<b>109</b>
6.5.1 Site 1.....	110
6.5.2 Site 2.....	111
<b>6.6 Evaluation of MAR potential.....</b>	<b>113</b>
<b>6.7 Hydrogeological modelling.....</b>	<b>114</b>
6.3.1 Changes in hydraulic head.....	114
6.3.2 Changes in groundwater flow.....	117
6.3.3 Changes in Darcy Velocity.....	119
<b>6.7 Summary.....</b>	<b>121</b>
<b>Chapter 7 – Discussion.....</b>	<b>123</b>
<b>7.1 Groundwater resources.....</b>	<b>123</b>
7.1.1 Rainfall.....	123
7.1.2 Waipaoa River flow and stage.....	124
7.1.3 Shallow aquifers.....	124
7.1.4 Deep aquifers.....	124
7.1.5 Groundwater abstractions.....	127
7.2 Groundwater level changes.....	128
<b>7.3 Hydraulic connections.....</b>	<b>132</b>
<b>7.4 Surface-groundwater connections.....</b>	<b>132</b>
<b>7.5 Evaluation of MAR potential of identified sites.....</b>	<b>133</b>
<b>7.6 Hydrogeological modelling.....</b>	<b>135</b>
7.6.1 Inundation at the ground surface.....	135
7.6.2 Changes in hydraulic head & Darcy velocity.....	135
7.6.2 Limitations.....	136
<b>Chapter 8 – Conclusions &amp; Recommendations.....</b>	<b>138</b>
<b>References.....</b>	<b>140</b>
<b>Appendices.....</b>	<b>146</b>

# List of Figures

---

Figure 2.1. Conceptual diagram showing the location of the vadose (unsaturated) zone, capillary fringe, water table, and saturated zone beneath the ground surface (Sourced from Alley et al., 1999). .....	6
Figure 2.2. (A) Conceptual diagram of a groundwater system containing an unconfined aquifer. (B) Conceptual diagram of a groundwater system containing both an unconfined aquifer and a confined aquifer.....	9
Figure 2.3. Surface-groundwater interactions. A) Groundwater discharge to surface water. B) Groundwater recharge from surface water. C) Groundwater recharge via surface water discharge to the vadose zone. D) Stream bank storage. This may or may not discharge to groundwater (adapted from Winter et al., 1998). .....	11
Figure 2.4. Groundwater flow paths from recharge areas to discharge areas (Heath, 1983). .....	14
Figure 2.5. Location of Roys Hill within the Heretaunga Plains in the Hawke's Bay region. ....	21
Figure 3.1. The Poverty Bay flats area.....	25
Figure 3.2. Conceptual cross-section of the Poverty Bay flats groundwater (Sourced from Taylor, 1994). .....	28
Figure 3.3. Approximate extent of the Te Hapara Sands, Shallow Fluvial Deposits and the Waipaoa Gravel aquifers (Adpated from Barber, 1993). .....	29
Figure 3.4. Approximate extent of the Makauri Gravel and Matokitoki Gravel aquifers (Adpated from Barber, 1993). .....	30
Figure 3.5. Poverty Bay flats showing possible recharge zones between the Waipaoa Rover and Waipaoa Gravel aquifer and the Waipaoa and Makauri Gravel aquifers (Adapted from Barber, 1993 and White et al. 2014). .....	35
Figure 4.1. (A) Infiltration basin with deep groundwater levels. (B) Infiltration basin with shallow groundwater levels. $D_w$ indicates the depth to the water table. Arrows indicate the direction in which groundwater is flowing from the infiltration basin (Adapted from Bouwer, 1999). .....	50
Figure 4.2. Conceptual diagram of an infiltration basin with a clogging layer (Adapted from Bouwer, 1999). .....	51
Figure 4.3. Location of the two sites identified using the HIGGS Index.....	54
Figure 5.1. Location of the Gisborne Airport where the two weather stations are located. The three river flow and stage monitoring sites (Kanakanaiia Bridge, Kaiteratahi Bridge, and Matawhero Bridge) on the Waipaoa River are also shown.....	56
Figure 5.2. Location of the 10 river flow gauging sites on the Waipaoa River. ....	59

<b>Figure 5.3. Location of the 49 bores for which groundwater levels are obtained monthly across the Poverty Bay flats. ....</b>	<b>61</b>
<b>Figure 5.4. Location of the four sites where groundwater levels are electronically monitored across eight bores.....</b>	<b>62</b>
<b>Figure 5.5. Location of the 10 bores monitored manually between 14/03/2015 and 27/03/2015 when ex-tropical Cyclone Pam hit the Gisborne District. ....</b>	<b>65</b>
<b>Figure 5.6. Location of GPG036 (pumped bore) and GPG064 and GPG062 (observations bores). Inset shows the wider area within which these bores are located. ....</b>	<b>67</b>
<b>Figure 5.7. Summary of the methods used to identify whether an infiltration basin could be successfully used as a MAR technique to artificially recharge the Makauri Gravel aquifer beneath the Poverty Bay flats.....</b>	<b>76</b>
<b>Figure 6.1. Annual rainfall as recorded at the Gisborne Airport weather station between 1982 and 2014. ....</b>	<b>78</b>
<b>Figure 6.2. Mean monthly Waipaoa River flow and stage at Kanakanaia Bridge between January 1982 and December 2014.....</b>	<b>79</b>
<b>Figure 6.3. Groundwater trends across the 49 bores monitored monthly by the GDC. Identified trends are significant at the 95% confidence level. ....</b>	<b>81</b>
<b>Figure 6.4. Monthly groundwater levels within the Te Hapara Sands from January 1982 to December 2014. ....</b>	<b>83</b>
<b>Figure 6.5. Monthly groundwater levels within the Shallow Fluvial Deposits at GPI007 from February 1995 to December 2014.....</b>	<b>84</b>
<b>Figure 6.6. Groundwater levels during the months of March (M) and September (S) within the Shallow Fluvial Deposits at GPI007 between 1995 and 2014.....</b>	<b>84</b>
<b>Figure 6.7. Monthly groundwater levels within the Waipaoa Gravel aquifer from November 1982 to December 2014. ....</b>	<b>86</b>
<b>Figure 6.8. Monthly groundwater levels within the Makauri Gravel aquifer from May 1982 to December 2014. ....</b>	<b>89</b>
<b>Figure 6.9. Groundwater levels during the months of March in the Makauri Gravel aquifer from 1983 to 2014. ....</b>	<b>90</b>
<b>Figure 6.10 Monthly groundwater levels within the Matokitoki Gravel aquifer from January 1982 to December 2014, as monitored by the GDC.....</b>	<b>94</b>
<b>Figure 6.11. Groundwater levels during the months of March in the Matokitoki Gravel aquifer from 1982 to 2014. ....</b>	<b>95</b>
<b>Figure 6.12. Groundwater levels in the Te Hapara Sands (GPB099) and atmospheric pressure from the 14<sup>th</sup> March 2015 to the 27<sup>th</sup> March 2015.....</b>	<b>97</b>
<b>Figure 6.13. Groundwater levels in the Shallow Fluvial Deposits (GPG051, GPH005, GPH046, and GPH047) and atmospheric pressure from the 14<sup>th</sup> March 2015 to the 27<sup>th</sup> March 2015. ....</b>	<b>98</b>

<b>Figure 6.14. Groundwater levels in the Waipaoa Gravel aquifer (GPE032, GPG013, GPG059, GPH022, and GPI023) and atmospheric pressure from the 14<sup>th</sup> March 2015 to the 27<sup>th</sup> March 2015. ....</b>	<b>100</b>
<b>Figure 6.15. Groundwater levels in the Makauri Gravel aquifer (GPB101, GPB102, GPE002, GPE041, GPG060, GPG088, GPH008, and GPH044) and atmospheric pressure from the 14<sup>th</sup> March 2015 to the 27<sup>th</sup> March 2015. ....</b>	<b>102</b>
<b>Figure 6.16. (A) Groundwater levels (adjusted for barometric effects) at GPG064 and barometric pressure during the 24 pumping test undertaken at GPG036. (B) Groundwater levels (adjusted for barometric effects) at GPG064 and barometric pressure in the 24 hours following cessation of pumping at GPG036 .....</b>	<b>104</b>
<b>Figure 6.17. (A) Groundwater levels (adjusted for barometric effects) at GPG062 and barometric pressure during the 24 pumping test undertaken at GPG036. (B) Groundwater levels (adjusted for barometric effects) at GPG062 and barometric pressure in the 24 hours following cessation of pumping at GPG036. ....</b>	<b>106</b>
<b>Figure 6.18. Concurrent Waipaoa River flow gaugings. Each line represents gaugings across a particular day. (A) Waipaoa River flow as monitored at four gauging sites. (B) Waipaoa River flow gains/losses between the four gauging sites in (A). (C) Waipaoa River flow as monitored at seven gauging sites. (D) Waipaoa River flow gains/losses between the seven gauging sites in (C). (E) Waipaoa River flow as monitored at ten gauging sites. (F) Waipaoa River flow gains/losses between the seven gauging sites in (E). ....</b>	<b>109</b>
<b>Figure 6.19. (A) Soil types present in Hole 2 at Site 1 to a depth of 500 mm. (B) Soil types present in Hole 4 at Site 1 to a depth of 500 mm. The soils found within these two holes were typical of Site 1. ....</b>	<b>110</b>
<b>Figure 6.20. Soil types present at Site 2 to a depth of 500 mm beneath the ground surface (photo was taken approximately 18 hours after infiltrometer test was stopped and water is still present at the site).....</b>	<b>112</b>
<b>Figure 6.21. (A) Hydraulic heads as modelled under the baseline. (B) Hydraulic heads as modelled in Scenario 9.....</b>	<b>117</b>
<b>Figure 6.22. (A) Groundwater flow paths as modelled under the baseline. (B) Groundwater flow paths as modelled in Scenario 9. Black circles within (B) highlight areas where groundwater flow differs from (A).....</b>	<b>119</b>
<b>Figure 7.1. Groundwater trends across the 29 bores monitored within the Makauri Gravel aquifer by the GDC. Identified trends are significant at the 95% level. ..</b>	<b>126</b>

# List of Tables

---

Table 2.1. Representative values for hydraulic conductivity over different materials (Heath, 1983; Schwartz and Zhang, 2003).....	13
Table 3.1. Comparison of groundwater allocations within the Poverty Bay flats between 1992 and 2015. 1992 groundwater allocations were obtained from Barber (1993).....	39
Table 3.2. Comparison of annual groundwater allocation (2015) and annual average groundwater abstraction between 2012 and 2015.....	40
Table 4.1. Parameters within the HIGGS Index and their associated weights. ....	43
Table 4.2. Hydraulic connection ranges, ratings, and typical ratings within the HIGGS Index. ....	44
Table 4.3. Impact of the vadose zone ranges, ratings, and typical ratings within the HIGGS Index.....	44
Table 4.4. Groundwater depth ranges and ratings within the HIGGS Index. The range is measured in metres and is the depth to groundwater beneath the ground surface.....	45
Table 4.5. Groundwater flow direction ranges, ratings, and typical ratings within the HIGGS Index.....	45
Table 4.6. Saturated hydraulic conductivity ranges and ratings within the HIGGS Index. ....	45
Table 5.1. Latitude/longitude, altitude, and start and end dates for which rainfall data was obtained from the Gisborne Airport. All rainfall data was obtained from Cliflo ( <a href="http://cliflo.niwa.co.nz/">http://cliflo.niwa.co.nz/</a> ). ....	57
Table 5.2. Locations where river flow and river stage data is collected on the Waipaoa River. 'Monitoring period' indicates the periods for which river flow and stage data was obtained for this research. 'MSL (m)' shows the height of each monitoring site relative to mean sea level. ....	57
Table 5.3. The 10 river flow gaugings sites on the Waipaoa River, when they were first gauged and the number of gaugings at each site.....	58
Table 5.4. Estimates of water-entry values (adapted from Bouwer, 1999).....	70
Table 5.5. Parameters of the hydrogeological model. Parameter values were chosen based upon an analysis of bore log data.....	73
Table 6.1. Mann-Kendall trend test following Helsel and Hirsch (2002) on annual rainfall at the Gisborne airport weather station.....	78
Table 6.2. Seasonally adjusted Mann-Kendall trend test following Helsel and Hirsch (2002) on Waipaoa River flow and stage. "Seasons" used in this analysis are:	

January – March, April – June, July – September, and October – December following White et al. (2012).....	79
Table 6.3. Seasonally adjusted Mann-Kendall trend test following Helsel and Hirsch (2002) on groundwater levels in the Te Hapara Sands. “Seasons” used in this analysis are: January – March, April – June, July – September, and October – December following White et al. (2012). .....	82
Table 6.4. Seasonally adjusted Mann-Kendall trend test following Helsel and Hirsch (2002) on groundwater levels in the Te Hapara Sands. “Seasons” used in this analysis are: January – March, April – June, July – September, and October – December following White et al. (2012). .....	83
Table 6.5. Seasonally adjusted Mann-Kendall trend test following Helsel and Hirsch (2002) on groundwater levels in the Waipaoa Gravel aquifer. “Seasons” used in this analysis are: January – March, April – June, July – September, and October – December following White et al. (2012). .....	85
Table 6.6. Seasonally adjusted Mann-Kendall trend test following Helsel and Hirsch (2002) on groundwater levels in the Makauri Gravel aquifer. “Seasons” used in this analysis are: January – March, April – June, July – September, and October – December following White et al. (2012). .....	88
Table 6.7. Mann-Kendall trend test following Helsel and Hirsch (2002) on groundwater levels in the Makauri Gravel aquifer during the month of March...	91
Table 6.8. Mann-Kendall trend test following Helsel and Hirsch (2002) on groundwater levels in the Makauri Gravel aquifer during the month of September. ....	92
Table 6.9. Seasonally adjusted Mann-Kendall trend test following Helsel and Hirsch (2002) on groundwater levels in the Matokitoki Gravel aquifer. “Seasons” used in this analysis are: January – March, April – June, July – September, and October – December following White et al. (2012). .....	94
Table 6.10. Mann-Kendall trend test following Helsel and Hirsch (2002) on groundwater levels in the Matokitoki Gravel aquifer during the month of March. ....	95
Table 6.11. Mann-Kendall trend test following Helsel and Hirsch (2002) on groundwater levels in the Matokitoki Gravel aquifer during the month of September. ....	96
Table 6.12. The 10 river flow gaugings sites on the Waipaoa River, when they were first gauged and the number of gaugings at each site. ....	107
Table 6.13. Infiltration rate ( $i_n$ ), downward flow rate ( $i_w$ ), depth of wetting ( $L$ ), and hydraulic conductivity ( $K_s$ ) at Site 1, as calculated using the methods described in Chapter 5 following Bouwer (1999). *All variables were calculated based upon	

their respective infiltrometer tests which lasted in duration from 49 to 137 min. .....	111
<b>Table 6.14. Infiltration rate (<i>in</i>), downward flow rate (<i>iw</i>), depth of wetting (<i>L</i>), and hydraulic conductivity (<i>Ks</i>) at Site 2, as calculated using the methods described in Chapter 5 following Bouwer (1999). All variables were calculated based upon the incomplete infiltrometer test at Site which lasted 60 min.....</b>	<b>113</b>
<b>Table 6.15. MAR potential for the two sites identified for MAR using an infiltration basin using the HIGGS Index. ....</b>	<b>114</b>
<b>Table 6.16. Infiltration rates across the nine MAR scenarios. Inundations at the ground surface denotes scenarios that are predicted to create surface flooding issues as a result of increases in groundwater levels .....</b>	<b>115</b>
<b>Table 6.17. Hydraulic heads as modelled under the baseline (i.e., current conditions), predicted hydraulic heads under Scenario 9, and the difference between hydraulic heads under the baseline and Scenario 9. ....</b>	<b>116</b>
<b>Table 6.18. Darcy velocity for the baseline and Scenario 9 at the observation bores.</b>	<b>120</b>

# Chapter 1 – Introduction

---

## 1.1. Groundwater in New Zealand

Groundwater is the most abundant form of water found in New Zealand accounting for approximately 80% of total water volume (Toebe, 1972). Previous efforts at estimating total groundwater volumes in New Zealand have highlighted that it is difficult to accurately quantify. Toebe (1972) estimated that the total volume of groundwater in New Zealand was  $1.7 \times 10^{12} \text{ m}^3$ . Thirty years later, White and Reeves (2002) estimated that the total volume of groundwater in New Zealand was between  $612 \times 10^9$  to  $619 \times 10^9 \text{ m}^3$ , less than 50% of Toebe (1972) original estimate. Despite difficulties in accurately quantifying volumes, groundwater is an important resource. It is used for many different purposes including; agriculture and horticulture, industry, private and public water supply, and for recreational activities (e.g., geothermal hot pools) (White, 2001; Reid & Scarsbrook, 2009). As such, groundwater contributes to the economic, environmental, health and social well-being of New Zealand.

Analysis of water use in New Zealand in 2000 showed that despite groundwater being the most abundant form of water it only accounted for 29.5% of allocated water resources (Robb, 2000). However, it is anticipated that groundwater resources will be further exploited as available surface water resources trend towards being fully allocated (Fenemor and Robb, 2001; Fenwick et al., 2004). This is already being observed in some regions (Gordon, 2001; Fenwick et al., 2004), and in at least one instance has resulted in unsustainable rates of groundwater abstractions (White et al., 2012). As the use of groundwater in New Zealand intensifies, the need to manage groundwater becomes more important to ensure its long-term sustainability.

## 1.2. Groundwater Management

In New Zealand, regional councils and unitary authorities are responsible for groundwater management under the Resource Management Act (RMA) (New Zealand Government, 1991). Under the RMA councils are required to sustainably manage groundwater resources. Sustainable management is defined as:

*“managing the use, development, and protection of natural and physical resources in a way, or at a rate, which enables people and communities to provide for their social, economic, and cultural well-being and for their health and safety while –*

- (a) sustaining the potential of natural and physical resources (excluding minerals) to meet the reasonably foreseeable needs of future generations; and*
- (b) safeguarding the life-supporting capacity of air, water, soil, and ecosystems; and*
- (c) avoiding, remedying, or mitigating any adverse effects of activities on the environment”* (New Zealand Government, 1991, s. 5(2)).

When groundwater resources are deemed to be not managed sustainably a regional council or unitary authority have a range of options available. For example, in Canterbury when discussing groundwater management issues Sinclair Knight Merz (2010) list four possible management strategies, which are applicable to all regions in New Zealand:

- (1) Do nothing – current groundwater management regime continues as it is;
- (2) Increase hydrogeological understanding of groundwater system whilst maintaining current groundwater management regime – involves increased level of hydrogeological investigations to give groundwater managers greater certainty surrounding groundwater allocations;

- (3) Introduce a new resource management regime in conjunction with (2) – involves utilising findings of hydrogeological investigations to change the way groundwater is managed;
- (4) Augment existing groundwater resources with storage schemes – involves developing methods to store water to enhance existing water resources. This method can involve surface storage (e.g., dams) or sub-surface storage (e.g., managed aquifer recharge).

The Gisborne District Council (GDC) is an example of a council in New Zealand that is examining its groundwater management regime in order to address groundwater sustainability issues within the Poverty Bay flats.

### **1.3. The Poverty Bay flats**

The Poverty Bay flats groundwater system is located within the Gisborne District in New Zealand and is an example of groundwater management becoming particularly important. Within the Poverty Bay flats, groundwater use has intensified over the last 35 years as a result of an increase in irrigated horticulture (Gordon, 2001; Golder Associates, 2014). The intensive use of groundwater has resulted in statistically significant declines in groundwater elevations in multiple aquifers (White et al., 2012). The observed decline in groundwater elevations is likely due to groundwater abstractions, meaning abstraction rates are unsustainable (White et al., 2012). The economic value of groundwater abstractions between 2009 and 2013 was estimated to be \$6.6 million annually (Golder Associates, 2014).

Any limits on future groundwater abstractions due to the unsustainable nature of current practices could constrain economic growth within the Gisborne District, particularly in relation to the horticulture industry, and contribute to degraded environmental outcomes (Golder Associates, 2014). As such, the Gisborne District Council (GDC) is investigating its groundwater management options to ensure that groundwater resources will be managed sustainably in the future. In particular, the GDC is investigating whether managed aquifer recharge (MAR), which is defined

by Dillon et al. (2009, p. 2) as “*the purposeful recharge of water to aquifers for subsequent recovery or environmental benefit*”, can be used as a groundwater management technique to reverse the trend of decreasing groundwater elevations.

## **1.4. Research Objective**

The objective of this research is to identify whether an infiltration basin (a method of MAR) may be successfully used to artificially recharge the Makauri Gravel aquifer beneath the Poverty Bay flats. Supplementary work will also be undertaken to characterise the current state of groundwater resources within the Poverty Bay flats, identify interactions surface-groundwater resources, and examine hydraulic connections between aquifers. The research objective will be achieved by:

- Collating and analysing all available information on the surface and groundwater systems within the Poverty Bay flats;
- Use the “HIGGS Index”, a ranking system, to identify sites that may be suitable for MAR using an infiltration basin; and
- Undertaking fieldwork and hydrogeological modelling to draw conclusions about whether MAR using an infiltration basin will likely be successful or not at the sites identified using the HIGGS Index.

## **1.5. Thesis Structure**

The objective of this research is outlined in the present chapter. Chapter 2 provides a theoretical review of groundwater, groundwater processes, and MAR, including two case studies of different MAR schemes. Chapter 3 builds on the brief introduction given within this chapter by describing the hydrogeology of the Poverty Bay flats in depth. Chapter 4 introduces the “HIGGS Index” as a method used to evaluate the MAR potential of the identified sites. The methods and data used within this research are described in Chapter 5. Results are presented in Chapter 6 and discussed in Chapter 7. A summary of the main findings of this research is provided by way of conclusion (Chapter 8) along with suggestions for future research.

## Chapter 2 – Theoretical Review

---

### 2.1. Introduction

This chapter provides a review of the key theoretical components of this research to aid the investigation of MAR in the Poverty Bay flats. Section 2.2 defines groundwater and outlines some of the processes which affect groundwater movement. Section 2.3 outlines groundwater management in New Zealand with a particular focus on management regimes when groundwater resources are deemed to not be managed sustainably. Section 2.4 defines MAR, examines different MAR methods, and provides a New Zealand case study.

### 2.2. Groundwater

#### 2.2.1 Groundwater & aquifer properties

Water can be found almost anywhere beneath the ground surface. However, not all water found beneath the ground surface is classified as groundwater (Alley et al., 1999). Groundwater is defined as “*subsurface water that occurs beneath the water table in soil and geologic formations that are fully saturated*” (Freeze and Cherry, 1979, p. 2). Water found beneath the ground surface but above the water table is referred to as soil water.

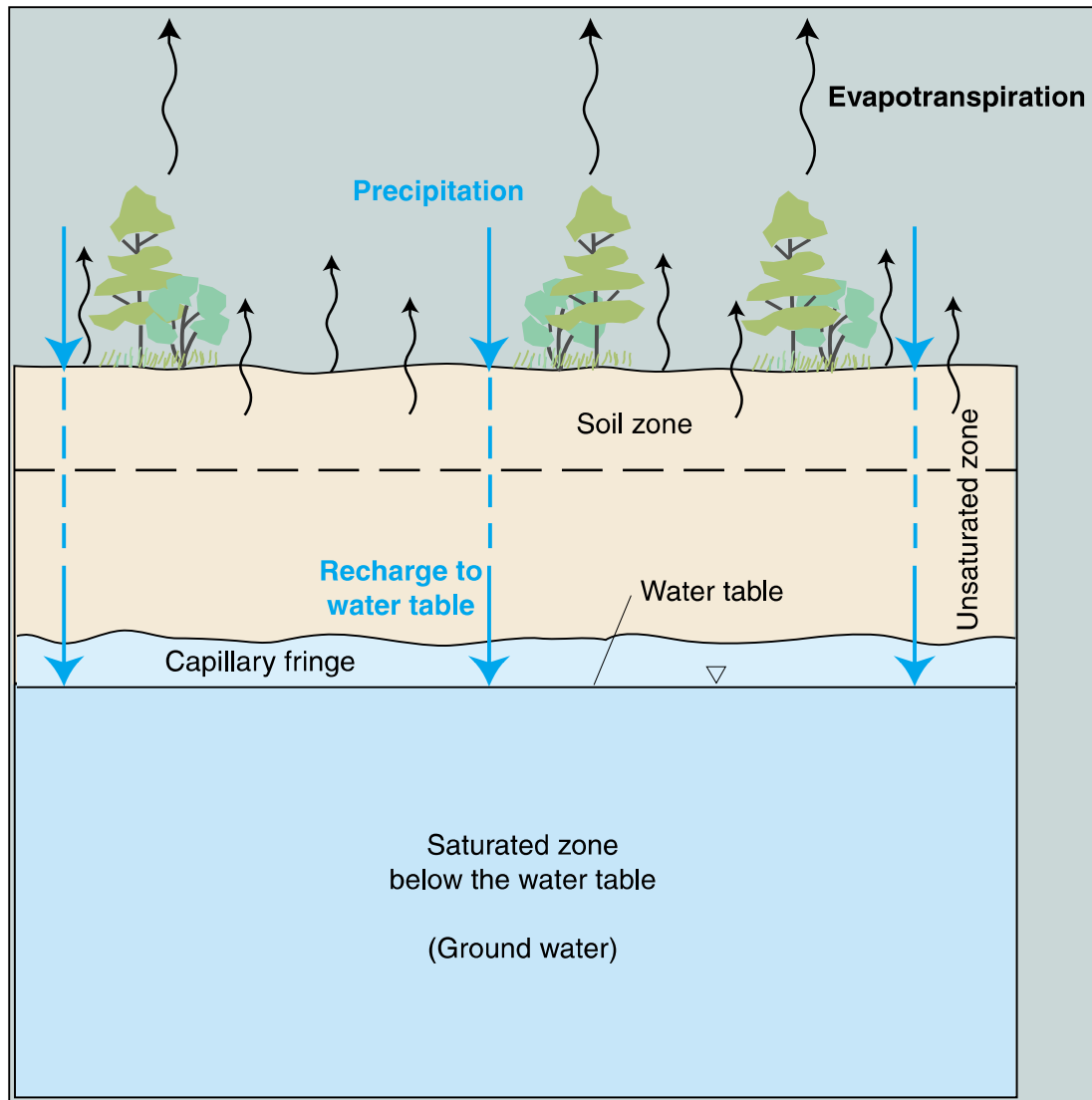


Figure 2.1. Conceptual diagram showing the location of the vadose (unsaturated) zone, capillary fringe, water table, and saturated zone beneath the ground surface (Sourced from Alley et al., 1999).

Aquifers are saturated geological units that are sufficiently permeable for groundwater to be extracted from bores at usable quantities (Freeze and Cherry, 1979; Schwartz and Zhang, 2003). Aquifers can be found in a range of different sediments. They are commonly located in unconsolidated sand and gravel deposits but can also be found in permeable sedimentary rocks such as sandstone and limestone (Bouwer, 1978). The amount of water that can be abstracted from an aquifer over a given time period is dependent on two properties: the transmissivity and storativity an aquifer (Schwartz and Zhang, 2003). Transmissivity describes the ease with which groundwater can move through an aquifer (Schwartz and Zhang, 2003). Explicitly,

transmissivity is the rate at which water of a prevailing kinematic viscosity is transmitted through an aquifer (Heath, 1983; Schwartz and Zhang, 2003). Transmissivity is calculated using the following equation:

$$T = Kb \quad 2.1$$

where  $T$  is the transmissivity,  $K$  is the hydraulic conductivity (see Section 2.23), and  $b$  is the aquifer thickness.

The storativity of an aquifer is the volume of water that is released from an aquifer or taken into storage, per unit surface area of the aquifer, per unit change in head (Schwartz and Zhang, 2003). Storativity values in confined aquifers range  $10^{-3}$  to  $10^{-5}$  (Schwartz and Zhang, 2003). Storativity is calculated using the following equation:

$$S = \frac{\text{volume of water (m}^3\text{)}}{(\text{unit area})(\text{unit head change})} \quad 2.2$$

A related measure to storativity is specific storage which is the volume of water that is released from an aquifer or taken into storage per unit surface area. Specific storage is calculated using the following equation:

$$S_s = \frac{\text{volume of water}}{(\text{unit area})(\text{unit aquifer thickness})(\text{unit head change})} \quad 2.3$$

where  $S_s$  is the specific storage of an aquifer. Specific storage of an aquifer is related to storativity by the following equation:

$$S = S_s B \quad 2.4$$

There are three different types of aquifers: unconfined, confined, and semi-confined. Unconfined aquifers are found at the water table and are often referred to as water table aquifers (Figure 2.2A) (Freeze and Cherry, 1979; Schwartz and Zhang, 2003). The absence of an overlying confining layer at the upper boundary of an unconfined aquifer means the vertical movement of

groundwater is unrestricted (Bouwer, 1978; Heath, 1983). Confined aquifers have confining layers at its upper and lower boundaries which restrict the vertical movement of groundwater (Figure 2.2B) (Schwartz and Zhang, 2003). A semi-confined aquifer contains characteristics of both an unconfined and confined aquifer. In certain areas the vertical movement of groundwater will be restricted due to the presence of a confining layer while in other areas the vertical movement of groundwater will not be restricted due to the absence of a confining layer. Semi-confined aquifers are also known as leaky aquifers (Todd and Mays, 2004).

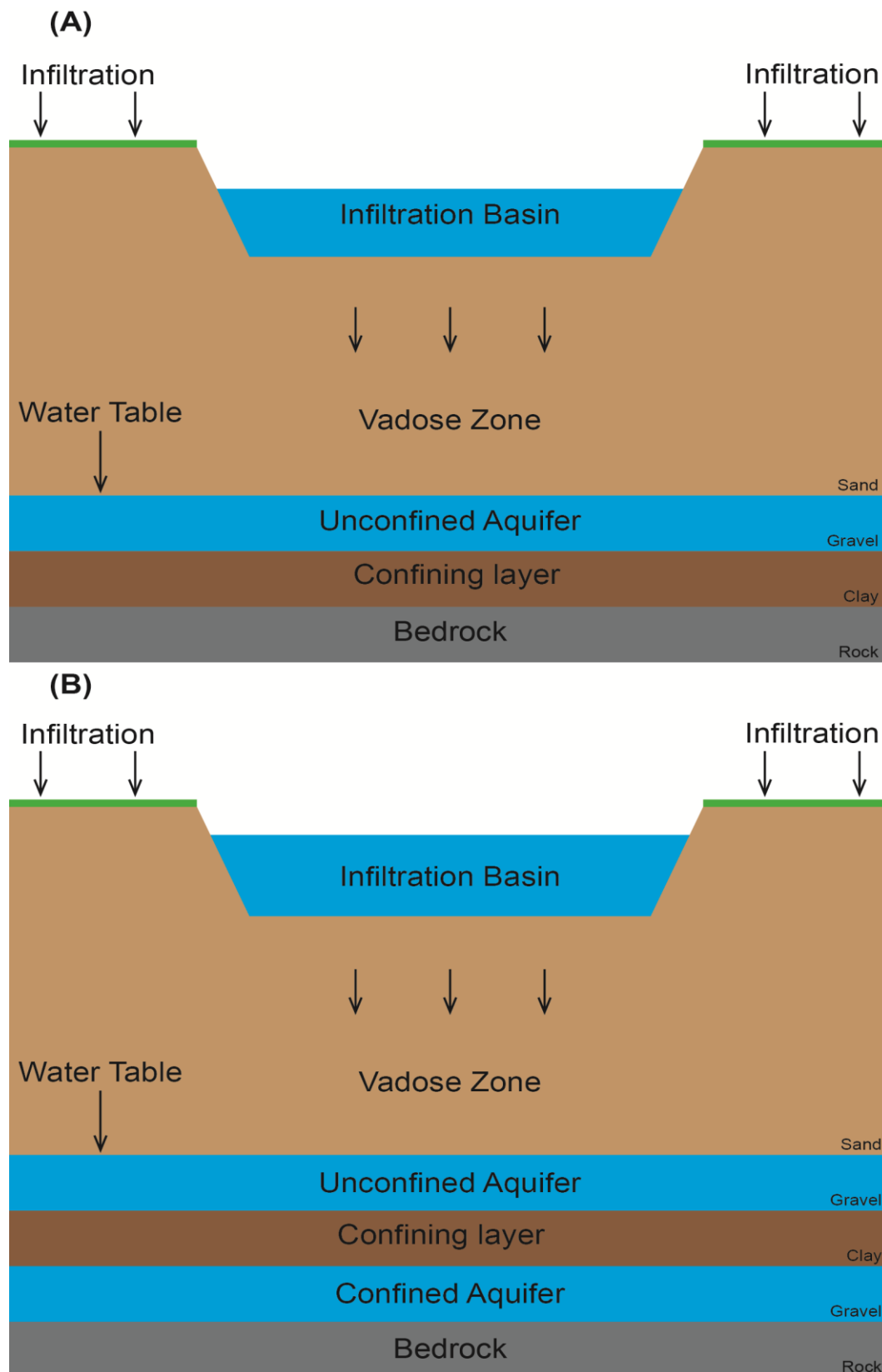


Figure 2.2. (A) Conceptual diagram of a groundwater system containing an unconfined aquifer. (B) Conceptual diagram of a groundwater system containing both an unconfined aquifer and a confined aquifer.

## **2.2.2 Groundwater recharge & discharge**

Groundwater recharge occurs when water enters the saturated zone at the water table (Freeze and Cherry, 1979; Schwartz and Zhang, 2003). It can be defined as an area where groundwater flow is directed away from the water table (Freeze and Cherry, 1979). It occurs via two processes; infiltration due to a rainfall event or via exchange with surface water bodies (e.g., rivers, lakes, and wetlands) discharging to the water table (Freeze and Cherry, 1979).

Infiltration is the process by which water enters the vadose zone from the ground surface (Freeze and Cherry, 1979). Water movement within the vadose zone is controlled by gravitational and capillary forces (Heath, 1983). In the vadose zone the voids between soil particles contain both air and water, thus the soils within this zone are unsaturated and the fluid pressure is less than atmospheric pressure (Freeze and Cherry, 1979; Schwartz and Zhang, 2003). As the water content of the vadose zone increases, the air content decreases, meaning that the fluid pressures become more negative to overcome atmospheric pressure. Water is then drawn down to the capillary fringe as capillary forces are overcome by the additional weight of water. The capillary fringe extends from the vadose zone down to the water table (Figure 2.1). In the capillary fringe the voids between soil particles are saturated but the fluid pressure is less than atmospheric pressure (Freeze and Cherry, 1979). When the capillary fringe can no longer hold the water to soil particles, the water drains down to the water table becoming groundwater (Freeze and Cherry, 1979).

Groundwater can also be recharged by and discharged to surface water bodies including rivers, lakes and wetlands (Figure 2.3) (Freeze and Cherry, 1979; Winter et al., 1998). Groundwater discharge to surface water bodies occurs when the water table is above the surface water level (Figure 2.3A). Therefore, the water table has a greater elevation than the surface water, thus groundwater recharges the surface water body (Winter et al., 1998). This is commonly known as a gaining reach within a river. Conversely, when the elevation of the water table is less than that of a surface water body,

groundwater is recharged by the surface water body (Figure 2.3B; Figure 2.3C) (Winter et al., 1998). This is commonly known as a losing reach within a river. Stream bank storage occurs within rivers and is shown in Figure 2.3D. It occurs when there is a sudden increase in river stage and surface water is stored within the banks of the river. If the elevation of the water table is greater than the surface water will be stored in the river banks. Therefore, surface water is not discharged to groundwater. Instead, over time (days or weeks) the surface water returns to the river (Winter et al., 1998). However, Daniel et al. (1970) note that if the water table elevation is lower than that of the river, over time the stored water will be discharged to groundwater.

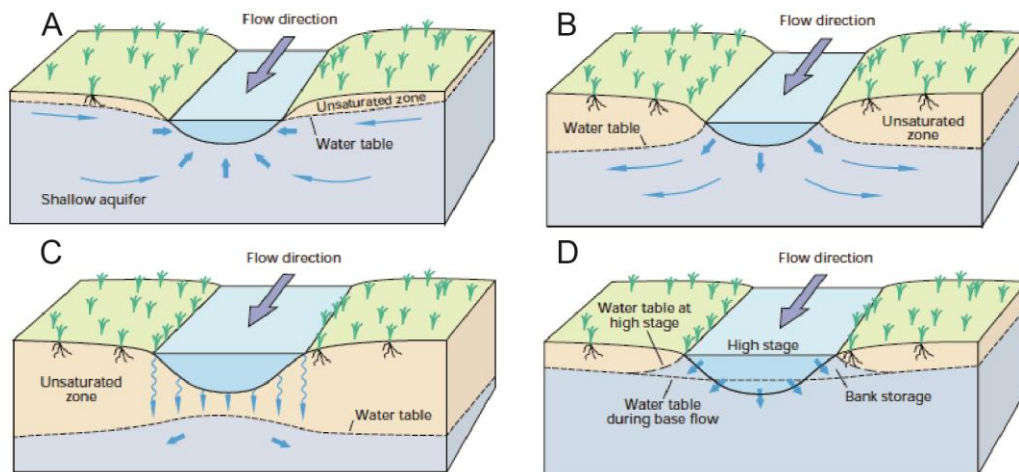


Figure 2.3. Surface-groundwater interactions. A) Groundwater discharge to surface water. B) Groundwater recharge from surface water. C) Groundwater recharge via surface water discharge to the vadose zone. D) Stream bank storage. This may or may not discharge to groundwater (adapted from Winter et al., 1998).

Knowledge of natural groundwater recharge and discharge rates are important as estimates of safe yields. Safe yield is the rate at which groundwater can be abstracted from an aquifer without depleting the resource (Bouwer, 2000).

### 2.2.3 Groundwater flow

Groundwater flow is governed by hydraulic principles and continuously occurs within groundwater systems (Todd and Mays, 2004). Darcy's law, an empirical law on groundwater flow, was formulated by Henry Darcy in 1856 and can be

used to examine groundwater flow (Freeze and Chery, 1979). Darcy's velocity describes fluid flow through a porous medium (Schwartz and Zhang, 2003).

Darcy's law can be used to calculate the specific velocity of groundwater flow within a porous medium at a particular point. The velocity is calculated using the following equation:

$$q = KA \frac{dh}{dl} \quad 2.5$$

where  $q$  is the velocity,  $K$  is the hydraulic conductivity,  $dh$  is the change in hydraulic head, and  $dl$  is the length of groundwater flow.

Hydraulic conductivity ( $K$ ) describes the ease at which groundwater flows in a porous medium (Schwartz and Zhang, 2003). Hydraulic conductivity is calculated using the following equation:

$$K = k \frac{\rho g}{\mu} \quad 2.6$$

where  $k$  is the intrinsic permeability which is a function of the size of the openings through which the fluid moves (Schwartz and Zhang, 2003),  $\rho$  is the density of water,  $g$  is the gravitational acceleration, and  $\mu$  is the viscosity of the fluid.

Hydraulic conductivities are greatest in materials with high permeability like sand and gravel and lowest in materials with low permeability like clay (Schwartz and Zhang, 2003). Hydraulic conductivities for different materials are given in Table 2.1.

Table 2.1. Representative values for hydraulic conductivity over different materials (Heath, 1983; Schwartz and Zhang, 2003).

<b>Material</b>	<b>Hydraulic conductivity (m/s)</b>
Gravel	$3 \times 10^{-4} - 3 \times 10^{-2}$
Coarse sand	$9 \times 10^{-7} - 6 \times 10^{-3}$
Medium sand	$9 \times 10^{-7} - 5 \times 10^{-4}$
Fine sand	$2 \times 10^{-7} - 2 \times 10^{-4}$
Silt	$1 \times 10^{-9} - 4.7 \times 10^{-9}$
Clay	$1 \times 10^{-11} - 4.7 \times 10^{-9}$
Limestone/dolomite	$1 \times 10^{-9} - 6 \times 10^{-6}$
Sandstone/siltstone	$1 \times 10^{-12} - 1.4 \times 10^{-8}$
Unfractured metamorphic/igneous rocks	$3 \times 10^{-14} - 2 \times 10^{-10}$

As outlined earlier, calculation of groundwater velocities using Darcy's law requires the use of hydraulic head data over two points, which can be calculated to identify the hydraulic gradient. The hydraulic gradient defines the direction of groundwater flow (Heath, 1983; Freeze and Cherry, 1979; Schwartz and Zhang, 2003). Once the hydraulic gradient is known equipotential lines can be obtained which describe groundwater elevations across a groundwater system. Equipotential lines can be used to draw groundwater flow nets, as shown in Figure 2.4. Groundwater flow nets can be used to analyse groundwater flow within a groundwater system.

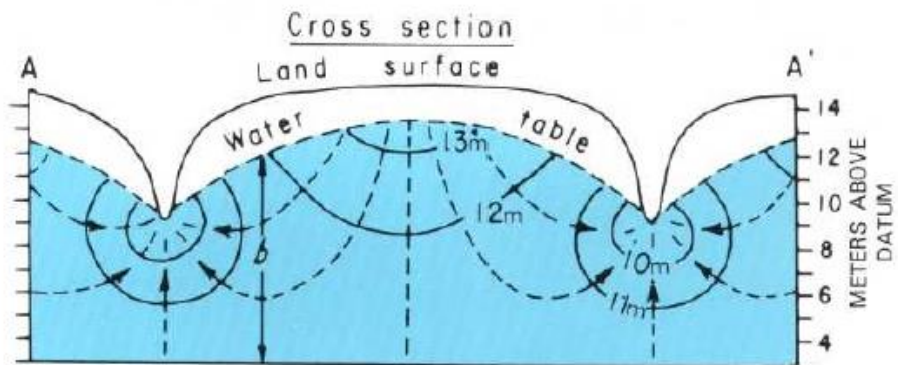
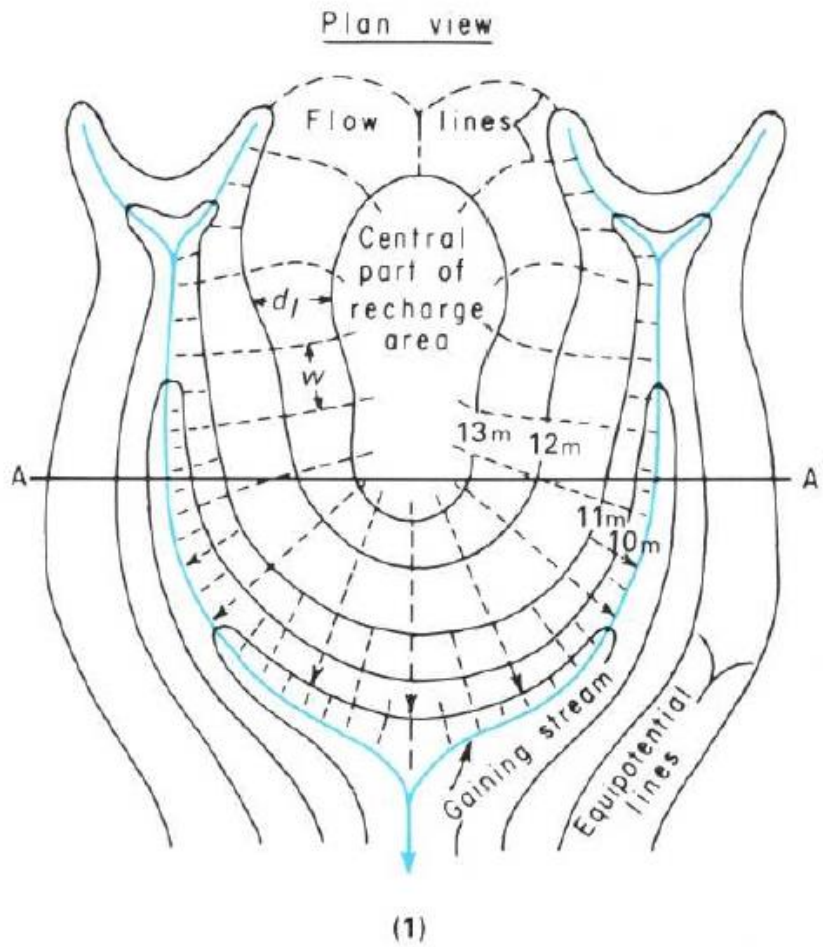


Figure 2.4. Groundwater flow paths from recharge areas to discharge areas (Heath, 1983).

The groundwater principles discussed in Section 6.2 can be used to identify characteristics about a groundwater system. As such, these principles can be used to contribute to groundwater management.

## 2.3 Groundwater management in New Zealand

Groundwater management in New Zealand has evolved over time as outlined by Weeber et al. (2001). Currently, groundwater management is the responsibility of regional councils and unitary authorities (hereafter referred to as councils) under the RMA. The RMA requires that groundwater resources are managed sustainably, which is defined in Chapter 1. Under the RMA councils must develop plans and rules which guide groundwater resource management (Weeber et al., 2001).

Groundwater use has increased over time in New Zealand (e.g., Sinclair Knight Merz, 2010; White et al., 2012). Therefore, the need to manage groundwater resources has become more important, particularly when unsustainable groundwater management practices have been identified. As outlined in Chapter 1, when groundwater resources are deemed to be not managed sustainably a council has a range of options available (Sinclair Knight Merz, 2010). Possible management strategies which are applicable to all regions in New Zealand include:

- (5) Do nothing – current groundwater management regime continues as it is;
- (6) Increase hydrogeological understanding of groundwater system whilst maintaining current groundwater management regime –involves increased level of hydrogeological investigations to give groundwater managers greater certainty surrounding groundwater allocations;
- (7) Introduce a new resource management regime in conjunction with (2) – involves utilising findings of hydrogeological investigations to change the way groundwater is managed;
- (8) Augment existing groundwater resources with storage schemes – involves developing methods to store water to enhance existing water resources. This method can involve surface storage (e.g., dams) or sub-surface storage (e.g., managed aquifer recharge).

Councils should evaluate the benefits and costs of all four possible groundwater management options. Doing this would allow a council to reach conclusions about the best groundwater management regime for that particular groundwater system.

One particular groundwater management technique that is relatively uncommon in New Zealand is MAR. However, over the last five years some councils (e.g., Golder Associates, 2013; Golder Associates, 2104A; Golder Associates, 2014B) have begun investigating whether MAR can be used to address their respective groundwater management issues. MAR is discussed below.

## **2.4 Managed aquifer recharge**

Anthropogenic activities effect groundwater recharge. In particular, the anthropogenic activities that affect groundwater recharge can be broken into three categories; unintentional, unmanaged, and MAR (Dillon et al., 2009). Unintentional aquifer recharge relates to anthropogenic activities which result in an inadvertent increase in groundwater recharge (Dillon et al., 2009). This includes activities such as irrigation or clearance of vegetation which inadvertently increases the amount of groundwater recharge occurring in a particular location. Unmanaged aquifer recharge relates to anthropogenic activities that directly lead to an increase in groundwater recharge without the specific intention of increasing recharge (Dillon et al., 2009). This includes wastewater disposal fields, sumps, and stormwater drainage wells. The third category is MAR. As outlined in Chapter 1, Dillon et al. (2013, p. 2) defines MAR as *“the purposeful recharge of water to aquifers for subsequent recovery or environmental benefit.”* MAR is distinct from unintentional aquifer recharge and unmanaged aquifer recharge in that it is both intentional and purposeful.

MAR schemes were first utilised in Europe in the early 19<sup>th</sup> century followed by the United States towards the end of the 19<sup>th</sup> century (Todd and Mays, 2004). As groundwater use the number of operational MAR schemes has increased. For example, Germany, the Netherlands, and Sweden all utilise

MAR to meet water demands (Todd and Mays, 2004). As a groundwater management technique MAR can be used to reverse declines in groundwater levels, reserve saline intrusion or land subsidence, capture and store seasonal water surpluses, increase the reliability of supply for groundwater users, and provide environmental benefits (Dillon, 2005; Sinclair Knight Merz, 2010). MAR has three major benefits compared with other forms of water storage. First, economically MAR can be more cost effective (Dillon et al., 2009; Dillon et al., 2010). Second, the amount of land required is generally less than other forms of water storage (Dillon, 2010). Third, compared with dams, the environmental impact of MAR schemes is negligible (Golder Associates, 2013).

When assessing the possibility of using MAR as a groundwater management technique Dillon et al. (2009) state that there are five different criteria that must First, there must be sufficient demand for recharged water. Second, there must be adequate source of water available to recharge the groundwater system. Third, there must be a suitable target aquifer. Fourth, there must be sufficient space to capture and treat the water before recharge. Finally, groundwater managers must be capable of designing, constructing, and operating a MAR scheme.

Perhaps the most important point with regard to MAR is that it should not be viewed as a stand-alone groundwater management tool (Dillon, 2005). Instead, it should be part of a package of wider measures that groundwater managers use to ensure that groundwater use is sustainable.

### **2.4.1 Managed aquifer recharge methods**

There are a number of different types of MAR, each of which has their own characteristics, as outlined by Dillon et al. (2009):

- Aquifer storage and recovery (ASR): *“injection of water into a well for storage and recovery from the same well.”* (p. 3).
- Aquifer storage, transfer and recovery (ASTR): *“involves injecting water into a well for storage, and recovery from a different well. This is used*

*to achieve additional water treatment in the aquifer by extending residence time in the aquifer beyond that of a single well (p. 3).*

- *Infiltration basins: “involve diverting surface water into off-stream basins and channels that allow water to soak through an unsaturated zone to the underlying unconfined aquifer” (p. 3).*
- *Infiltration galleries: “buried trenches (containing polythene cells or slotted pipes) in permeable soils that allow infiltration through the unsaturated zone to an unconfined aquifer” (p. 4).*
- *Soil aquifer treatment (SAT): “treated sewage effluent is intermittently infiltrated through infiltration ponds to facilitate nutrient and pathogen removal in passage through the unsaturated zone for recovery by wells after residence in the unconfined aquifer” (p. 4).*
- *Percolation tanks of recharge weirs: “dams built in ephemeral streams detain water which infiltrates through the bed to enhance storage in unconfined aquifers and is extracted down-valley” (p. 4).*
- *Rainwater harvesting for aquifer storage: “roof runoff is diverted into a well, sump or caisson filled with sand or gravel and allowed to percolate to the water-table where it is collected by pumping from a well” (p. 4).*
- *Recharge releases: “dams on ephemeral streams are used to detain flood water and uses may include slow release of water into the streambed downstream to match the capacity for infiltration into underlying aquifers, thereby significantly enhance recharge” (p. 4).*
- *Dry wells: “typically shallow wells where water tables are very deep, allowing infiltration of very high quality water to the unconfined aquifer at depth” (p. 4).*
- *Bank infiltration: “extraction of groundwater from a well or caisson near or under a river or lake to induce infiltration from the surface water body thereby improving and making more consistent the quality of water recovered” (p. 4).*
- *Dune filtration: “infiltration of water from ponds constructed in dunes and extraction from wells or ponds at lower elevation for water quality improvement and to balance supply and demand” (p. 4).*

- Underground dams: *“In ephemeral streams where basement highs constrict flows, a trench is constructed across the streambed, keyed to the basement and backfilled with low permeability material to help retain flood flows in saturated alluvium for stock and domestic use”* (p. 4).
- Sand dams: *“built in ephemeral stream beds in arid areas on low permeability lithology, these trap sediment when flow occurs, and following successive floods the sand dam is raised to create and “aquifer” which can be tapped by wells in dry seasons”* (p. 4).

The MAR method selected to help manage groundwater resources depends entirely on local conditions (Bouwer, 1999). Sinclair Knight Merz (2010) note that the selection of the appropriate MAR method should be based upon seven variables: the lithological profile of the area being investigated, the confinement status of the target aquifer, hydrogeological characteristics of the groundwater system, geomorphological characteristics of the land, source water quality, cost of the land, and investigation costs.

### **2.4.2 Infiltration basins**

Infiltration basins are the most common form of surface infiltration systems (Sinclair Knight Merz, 2010). They are typically constructed by excavating into the underlying soils or building a raised berm to contain the recharge water in one spot (e.g., Figure 2.2) (Bouwer, 1999; Sinclair Knight Merz, 2010). Infiltration basins are a passive form of MAR in that it relies on natural groundwater recharge principles to recharge the target aquifer as opposed to methods that require the use of pumps and/or wells. The major advantage of an infiltration basin is that it is a simple low cost groundwater management tool compared with other forms of MAR (Todd and Mays, 2004; Sinclair Knight Merz, 2010).

Typical infiltration rates within infiltration basins range from 0.3 to 3 m/day (Bouwer, 1999). However, clogging layers can prevent these infiltration rates from being achieved as described by Bouwer (1999). Clogging is caused by an accumulation of sediments at the bottom of the infiltration basin. These

clogging layers can reduce the infiltration rate within an infiltration basin. As such, pre-sedimentation ponds should be installed where clogging may be an issue to remove sediments from the infiltrated water prior to infiltration (Bouwer, 1999).

Examples of MAR schemes that have utilised infiltration basins include the Weber River Basin Aquifer Storage and Recovery Project (Utah, United States), the New River Agua Fria Underground Storage Project (Arizona, United States), Roys Hill artificial recharge scheme (Hawke's Bay, New Zealand).

### **2.4.3. Case Study – Roys Hill artificial recharge scheme**

Roys Hill is located within the Heretaunga Plains in Hawke's Bay on the east coast of the North Island (Figure 2.5). Groundwater from the Heretaunga Plains groundwater system is used for agricultural, domestic, and industrial purposes (Grant, 1972; White and Brown; 1997). In the 1960s and 70s groundwater use began to increase and it was noted that this would likely continue (Grant, 1972). In the summer of 1982/83 declining groundwater levels were observed (Gordon, 2009). In response to these declines the Hawke's Bay Catchment and Regional Water Board (HBCRWB), the predecessor to the Hawke's Bay Regional Council (HBRC), began investigation alternative groundwater management regimes. Specifically, the HBCRWB investigated the possibility of establishing a MAR scheme at Roys Hill (Gordon, 2009). A number of monitoring bores were installed to examine the potential of the recharge scheme. Initial trials resulted in increased groundwater levels in the monitoring bores and led to the conclusion that natural recharge could be supplemented by as much as 20% (Brooks, 1999).

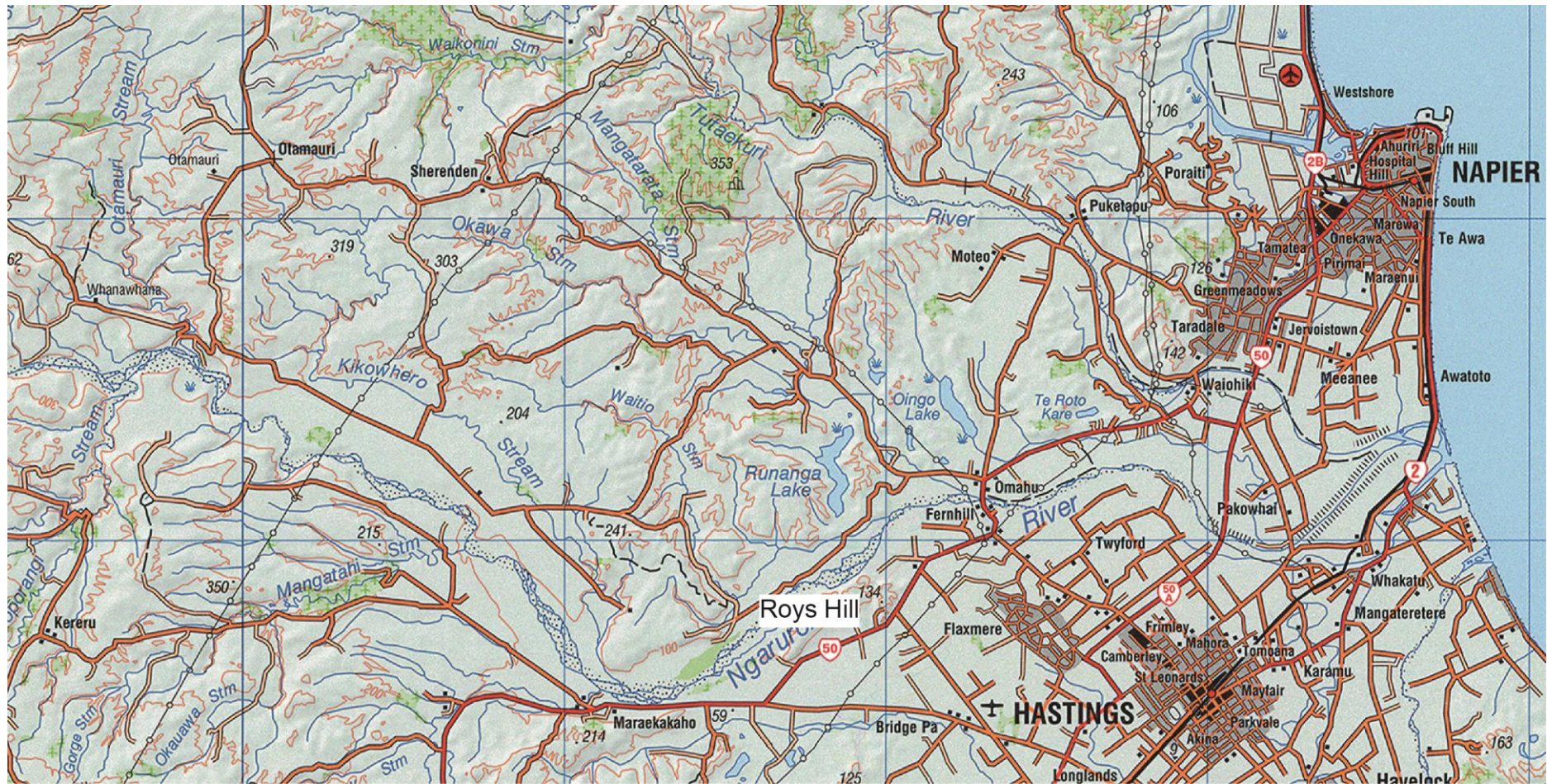


Figure 2.5. Location of Roys Hill within the Heretaunga Plains in the Hawke's Bay region.

In 1988 the Roys Hill artificial recharge scheme was officially commissioned by the HBCRWB (Gordon, 2009). The specific aim of this recharge scheme was to augment the natural groundwater recharge to arrest declines in groundwater levels with the Heretaunga Plains groundwater system (White and Brown; 1997; Gordon, 2009). At the commencement of the recharge scheme river water from the Ngaruroro River was diverted to four infiltration basins at a rate of approximately 1000 L/s over three months of the year (Brooks, 1999). Each infiltration was 50 m in length, 20 m wide, and 2 m deep (Brooks, 1999). To increase the time for which water was diverted to these infiltration basins and to deal with sedimentation issues the river diversion was converted to a trench system diverting shallow groundwater to the infiltration basin at a rate of 400 L/s (Brooks, 1999). In total it was estimated that the diversion system transported between 10,000,000 to 13,000,000 m<sup>3</sup>/year to the infiltration basins (Brooks, 1999).

The first review of the recharge scheme was undertaken by White and Brown (1997). This review concluded that groundwater levels in numerous monitoring bores since 1995 have increased and that this is likely due to the artificial recharge scheme. Groundwater level rises ranged from 0.6 to 5.6 m (White and Brown, 1997). However, subsequent analyses indicated that the rise in groundwater levels is a result of groundwater mounding rather than recharge (Brooks, 1999; Gordon, 2009). There was also confusion surrounding the amount of artificial recharge that leaked back into the Ngaruroro River. Gordon (2009) concluded that further monitoring bores would have been beneficial to ascertain leakage rates from the infiltration basin back into the Ngaruroro River. This highlights that it is essential that monitoring bores are installed in appropriate locations to ascertain the effects of a recharge scheme on nearby surface water bodies.

After operating the recharge scheme for almost 20 years the HBRC did not have a clear understanding of the its benefits. As such, in 2007 the HBRC decommissioned the scheme due to the uncertainty of the benefits it provided (Gordon, 2009). Again, this highlights that careful consideration

should be given to the set-up of monitoring bores so that decision makers can be certain about the effects of such schemes on groundwater levels and the wider hydrogeological environment.

## Chapter 3 – The Poverty Bay Flats

---

### 3.1 Introduction

The Poverty Bay flats are located within the Gisborne District on the east coast of the North Island of New Zealand. Specifically, the Poverty Bay flats are located at the southern end of the Gisborne District on the flood plain of the Waipaoa River (Figure 3.1). The Poverty Bay flats cover an area of 185 km<sup>2</sup> which is the largest area of flat land within the Gisborne District (GDC, 2002). Frequent droughts mean that water is an important resource for irrigation purposes during the summer months (Gordon, 2001). The Waipaoa River is the lone major surface water resource within the Poverty Bay flats (Figure 3.1). Use of the Waipaoa River for irrigation purposes is limited due to low flows during the summer months, poor water quality and limited irrigation infrastructure (Gordon, 2001). These environmental and physical constraints mean groundwater is an important economic resource due to its ability to meet irrigation demands across the Poverty Bay flats (Gordon, 2001).

This chapter presents an in depth analysis of the Poverty Bay flats groundwater system. Section 2.2 provides a detailed description of the geology of the Poverty Bay flats. Section 2.3 examines the characteristics of the aquifers within the groundwater system. Section 2.4 analyses land use changes within the Poverty Bay flats since the 1980s. Section 2.5 describes the current state of groundwater resources.

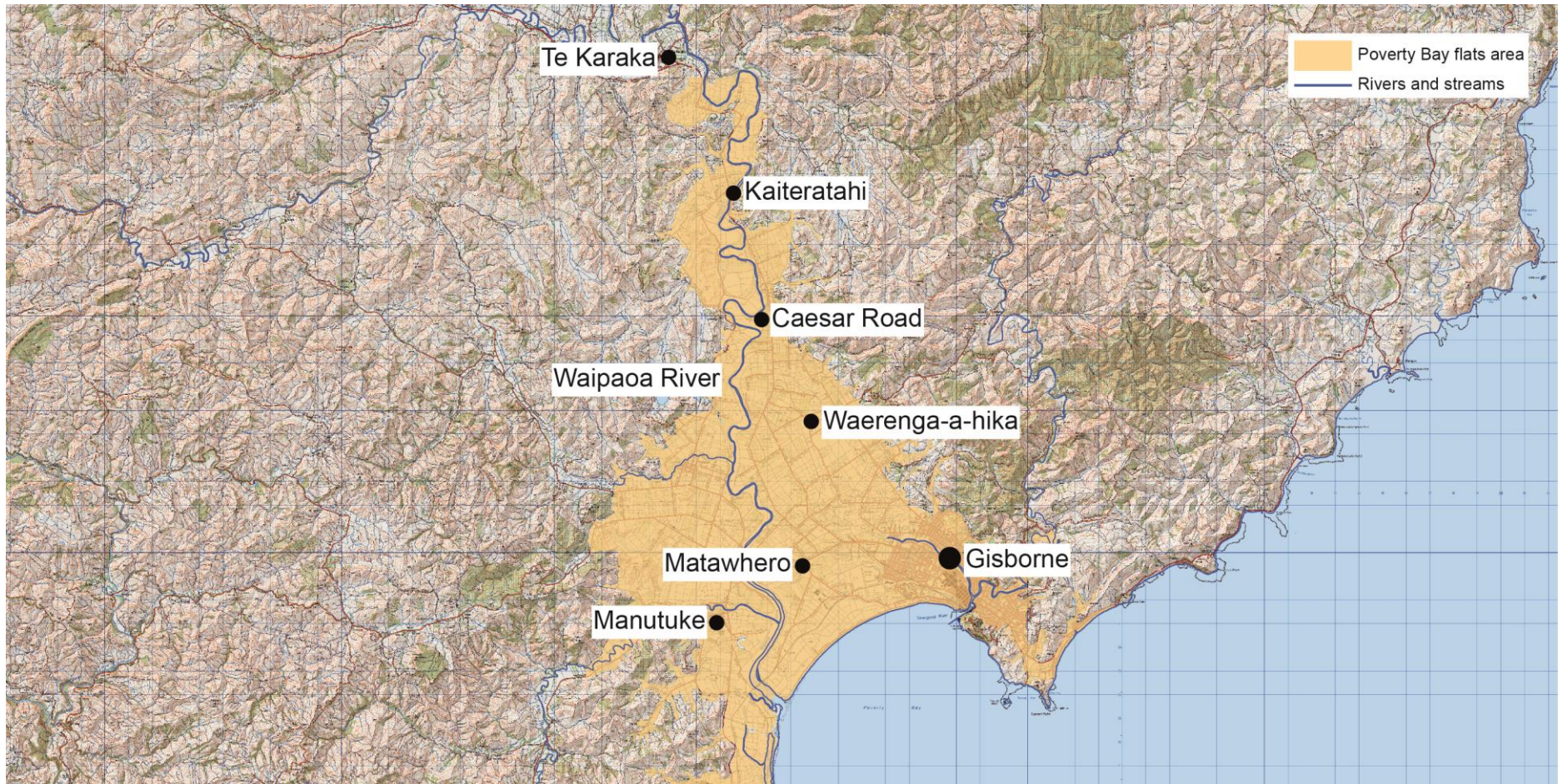


Figure 3.1. The Poverty Bay flats area.

## 3.2 Geology

A detailed description of the geology of the Poverty Bay flats is given by Brown and Elmsly (1987). Their description of the geology is outlined below. Basement rock can be found at depths of between 50 and 200 m below mean sea level (msl) and is made up of tertiary mudstone, sandstone and siltstone. Quaternary terrestrial and marine sediments have been deposited on top of the basement rock on the flood plain of the Waipaoa River in response to sea level changes which have been driven by climatic changes.

During glacial periods deposition of terrestrial gravels, sands and silts was driven by the Waipaoa and Waimata Rivers. During interglacial periods rivers reworked the terrestrial sediments which were overlain by lagoonal and estuarine clays, silts, sands and gravels. The last global glacial period occurred between 70,000 to 14,000 years ago. During this period the sea level was approximately 30 km east of the present coastline. Consequently, the valley and flood plain of the Waipaoa River was filled with alluvium sandstone and siltstone and soft mudstone.

The climate began warming about 14,000 years ago. As a consequence sea level began to rise and forest regeneration occurred within the Waipaoa River catchment reducing erosion. At this time the Waipaoa River was downcutting and reworking the alluvium sediments previously deposited within the floodplain and valley. Uplift in the northeastern area of the Waipaoa River catchment occurred as a result of tectonic activity.

About 10,000 years ago the sea level was at the present day coastline. The Waipaoa River was building a delta in response to changes its length. Initially, fluvial silt was the dominant lithology deposited during this period. This was followed by the deposition of gravels as a result of downcutting of the Waipaoa River into gravel deposits.

The sea level was slightly higher than the present day 6000 years ago. This resulted in marine transgression which led to swamp, estuarine, lagoonal and

beach deposits over the Waipaoa River deposits. During the following 6000 years the Poverty Bay coast prograded as silt deposits filled swamps, lagoons and estuaries. Further tectonic activity resulted uplift and subsequent downcutting of the prograded silt deposits. Gravel alluvium deposits within the Waipaoa River catchment were sporadically reworked during this period resulting in gravel channels within the fluvial silt, marine silt and sand deposits.

Volcanic ash present in the Waipaoa River catchment is a result of volcanic activity in the North Island. The volcanic ash is interbedded with the alluvial deposits and at the coast is concentrated in thick layers due to river deposition. Currently, the Poverty Bay flats consist of an alluvial plain extending approximately 20 km inland and rising to an altitude of 30 m above mean sea level above mean sea level. At the coast there are beach backed sand dunes and sand beach ridges enclosed around estuaries and lagoons.

### **3.3 Groundwater system**

The Poverty Bay flats groundwater system is complex comprising five different aquifers. The five aquifers are; Te Hapara Sands, Shallow Fluvial Deposits, Waipaoa Gravel aquifer, Makauri Gravel aquifer and Matokitoki Gravel aquifer. These aquifers vary in size, thickness and depth (Figure 3.2, Figure 3.3, and Figure 3.4). Recharge to the groundwater system is from rainfall and river-derived water (Barber, 1993; White et al., 2012). Furthermore, the groundwater system is 'leaky', meaning groundwater is readily exchanged between aquifers (Barber, 1993; White et al., 2012). Detailed descriptions of each aquifer are given below.

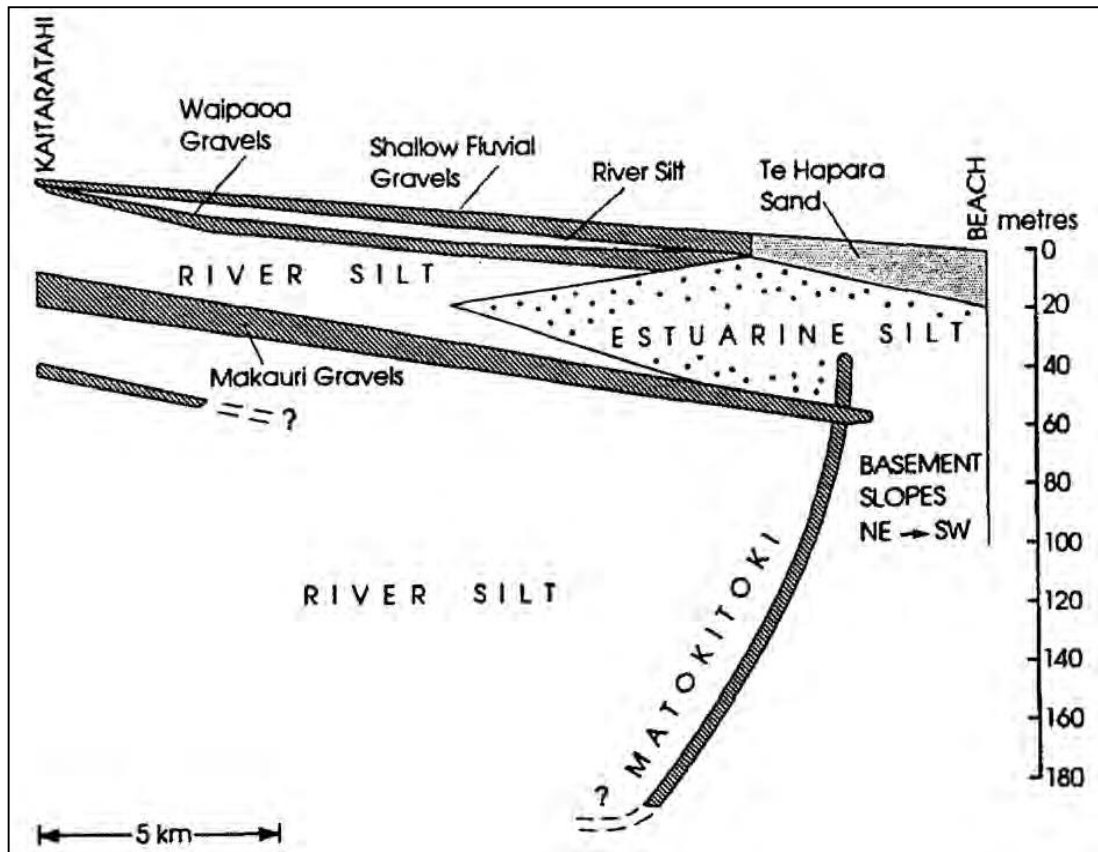


Figure 3.2. Conceptual cross-section of the Poverty Bay flats groundwater (Sourced from Taylor, 1994).

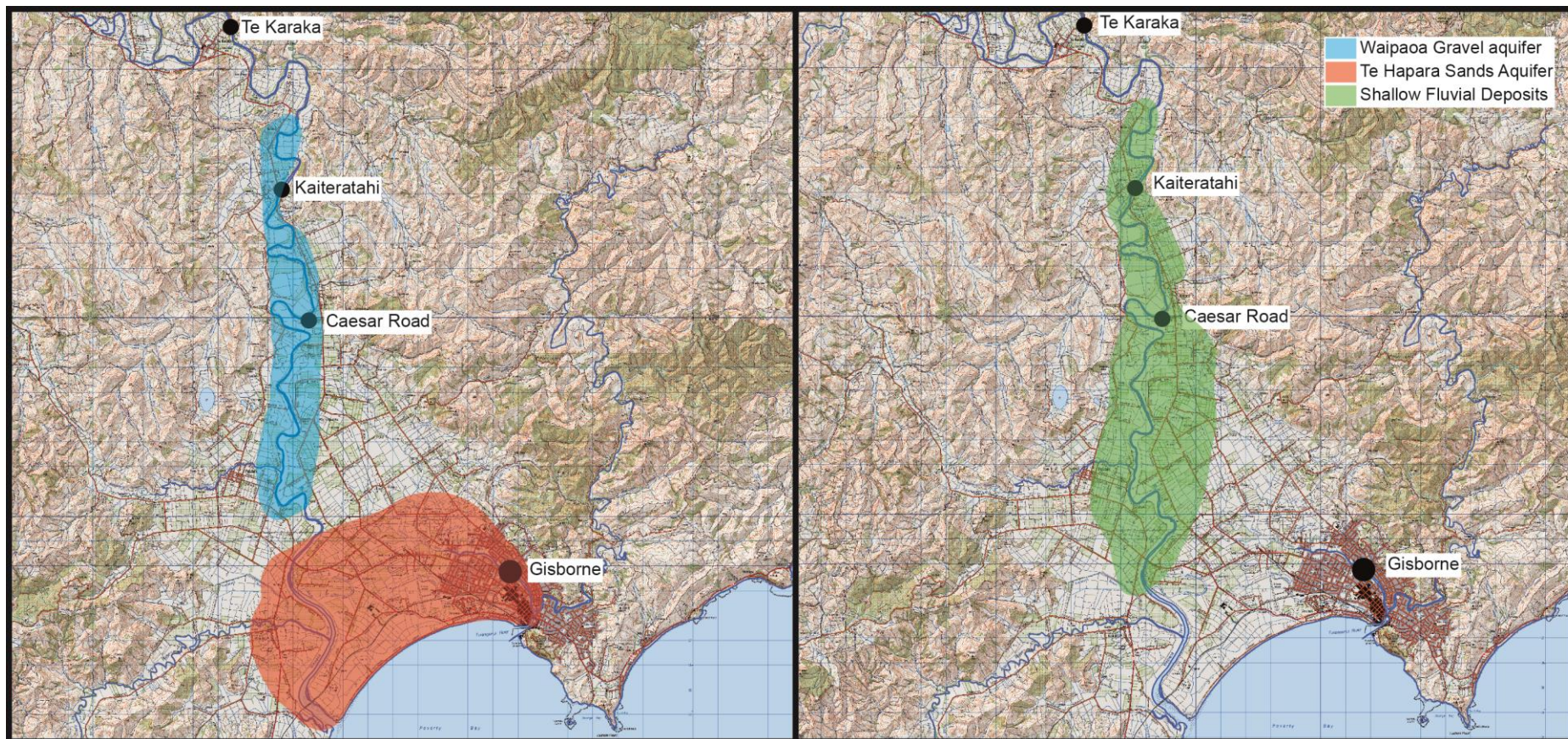


Figure 3.3. Approximate extent of the Te Hapara Sands, Shallow Fluvial Deposits and the Waipaoa Gravel aquifers (Adpated from Barber, 1993).

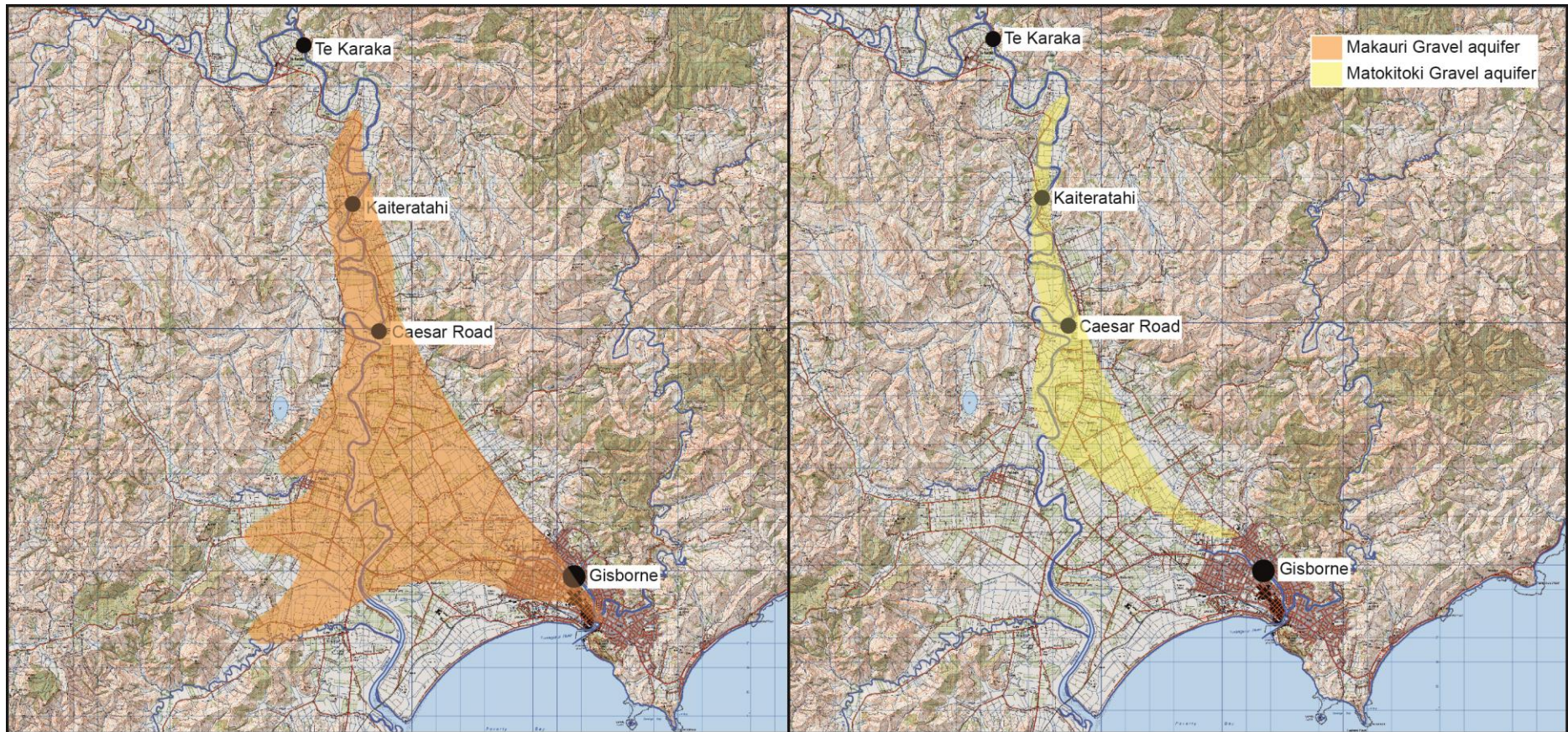


Figure 3.4. Approximate extent of the Makauri Gravel and Matokitoki Gravel aquifers (Adpated from Barber, 1993).

### 3.3.1 Te Hapara Sands

The Te Hapara Sands were formed as a result of coastal progradation over the last 4000 years and the resultant infilling of lagoons and formation of sand dunes (Brown and Elmsly, 1987). The aquifer extends from the coastline to 5 km inland and is up to 20 m thick (Figure 3.2). The aquifer is semi-confined (Gordon, 2001). The permeability of the aquifer decreases towards the southwest due to increasing silt content (i.e., inland towards the Waipaoa River) (Barber, 1993).

Water quality within the Te Hapara Sands is variable (Brown and Elmsly, 1987; Barber, 1993; Taylor, 1994). It is not considered to be potable and is instead used for irrigation purposes (GDC, 2005). The following parameters were assessed; total iron (Fe), conductivity, chloride (Cl) and nitrate nitrogen (NO<sub>3</sub>-N). Median Fe values (0.4 mg/L) suggest an oxidised environment (White et al., 2012). Median conductivity (720 µS/cm) and Cl concentrations (29 mg/L) are low, though they do increase towards the coast (Barber, 1993). The aquifer is susceptible to pollution in areas where permeability is high from agricultural, horticultural, domestic and industrial activities (Barber, 1993). However, low NO<sub>3</sub>-N concentrations (median of 0.1 mg/L) indicate that the anthropogenic impact on groundwater quality is limited (White et al., 2012).

The Te Hapara Sands is recharged from multiple sources. Isotopic analysis indicates the aquifer is recharged by river-derived water and rainfall (Taylor, 1994). River-derived recharge is greatest in close proximity to the Waipaoa River (Taylor, 1994). Furthermore, Barber (1993) stated that the Waipaoa Gravel aquifer and the Shallow Fluvial Deposits also contribute recharge to the Te Hapara Sands. The mean transmissivity of the aquifer is 145 m<sup>2</sup>/day (Barber, 1993). Storage coefficients vary across the aquifer from 2.5×10<sup>-5</sup> within confined areas to 4×10<sup>-2</sup> in semi-confined to unconfined areas (Barber, 1993).

### **3.3.2 Shallow Fluvial Deposits**

The Shallow Fluvial Deposits are formed by pumice sand layers and gravel and coarse sand found within old channels of the Waipaoa River (Barber, 1993; Gordon, 2001). The aquifer borders the Te Hapara Sands and extends inland north of Kaiteratahi (Figure 3.3). The aquifer can be found from the ground surface to depths of 20 m (Barber, 1993). Depending on the depth of the deposits, either a shallow water table aquifer or a semi-confined aquifer is formed. (Brown and Elmsly, 1987; Barber, 1983).

Water quality within the Shallow Fluvial Deposits is variable, with quality deteriorating towards the coast, except for old river channels, which contain good quality groundwater (Brown and Elmsly, 1987; Barber, 1993). Water in this aquifer is suitable for irrigation purposes (Taylor, 1994). The median Fe concentration (1.08 mg/L) suggests an oxidized environment (White et al., 2012). Median conductivity (801  $\mu\text{S}/\text{cm}$ ) and Cl concentrations (28 mg/L) are similar to the Te Hapara Sands. Low  $\text{NO}_3\text{-N}$  concentrations (median of 0.0 mg/L) indicate that the anthropogenic impact on groundwater quality is limited (White et al., 2012).

The Shallow Fluvial Deposits is recharged via river-derived water and rainfall (Barber, 1993; Taylor, 1994). Groundwater levels fluctuate according to wet and dry periods (Barber, 1993). Water samples taken from this aquifer contained tritium indicating that it is of recent origin (Taylor, 1994). Transmissivities within the Shallow Fluvial Deposits in close proximity to the Waipaoa River (e.g., Matawhero) are in the order of 1,100  $\text{m}^2/\text{day}$ , with a storage coefficient of  $5 \times 10^{-3}$ . Further away from the Waipaoa River (e.g., Waerenga-a-hika) transmissivities range from 250-500  $\text{m}^2/\text{day}$  and storage coefficients range from  $2 \times 10^{-3}$  to  $3 \times 10^{-4}$  (Figure 3.1; Figure 3.3) (Barber, 1993).

### **3.3.3 Waipaoa Gravel Aquifer**

The Waipaoa Gravel aquifer extends inland from the Te Hapara Sands to Kaiteratahi (Figure 3.2). The Waipaoa Gravel aquifer was formed during the early phase of coastal progradation when rivers within the Poverty Bay flats

were adjusting to changes in sea level during the post-glacial phase and tectonic uplift (Brown and Elmsly, 1987; Barber, 1993). Adjusting to changes in sea level and tectonic uplift led to the formation of terrace, fan and channel deposits, which extend from Te Karaka, within the Waipaoa River valley, to Waerenga-a-hika (Brown and Elmsly, 1987; Barber, 1993). The channel deposits were restricted to the middle of the Poverty Bay flats, which were adjacent to the present course of the Waipaoa River. (Brown and Elmsly, 1987; Barber, 1993). The Waipaoa Gravel aquifer can be found at depths of 10 to 30 m (Brown and Elmsly, 1987; Barber, 1993).

Water quality within the Waipaoa Gravel aquifer is similar to that of the Waipaoa River (Gordon, 2001). The median Fe concentration (1.08 mg/L) suggests an oxidised environment (White et al., 2012). One bore located north of Caesar Road exhibited higher Fe concentrations (18.7 mg/L) relative to the other monitored bores, which is indicative of localised reduced conditions (White et al., 2012). Median conductivity (801  $\mu$ S/cm) and Cl concentrations (28 mg/L) are similar to the Te Hapara Sands. Previous work found that Fe, conductivity, and Cl concentrations increase to the southwest (Barber, 1993). Low NO<sub>3</sub>-N concentrations (0.0 mg/L) indicate that the anthropogenic impact on groundwater quality is limited (White et al., 2012). Compared with the Te Hapara Sands and the Shallow Fluvial Deposits, the Waipaoa Gravel aquifer is less susceptible to contamination from nutrients and pathogens and other land-use contaminants as it protected by confining layers (Gordon, 2001).

The Waipaoa Gravel aquifer is recharged by the Waipaoa River in its upper reaches as changes in groundwater levels respond to changes in river stage (Barber, 1993). In particular, Taylor (1994) identified a connection between the Waipaoa River and the Waipaoa Gravel aquifer north of Kaiteratahi. Tritium concentrations varied within the aquifer but indicated that recharge had occurred within the last 25 years (Taylor, 1994). Around Kaiteratahi and Caesar Road hydraulic heads in the Waipaoa Gravel aquifer are greater than the Makauri Gravel aquifer. This indicates that the Waipaoa Gravel aquifer is discharging water to the Makauri Gravel aquifer in this area (Figure 3.5)

(Barber, 1993). Furthermore, the water quality of at least one bore in the Waipaoa Gravel aquifer in the Kaiteratahi area is similar to that of the Makauri Gravel aquifer (White et al., 2012), which again indicates that there is a degree of hydraulic connection between these two aquifers. Transmissivities within the Waipaoa Gravel aquifer are variable. Bores in close proximity to the river have transmissivities between 500 and 900 m<sup>2</sup>/day and storage coefficients of 10<sup>-3</sup> whereas bores further away from the river have transmissivities between 180 and 400 m<sup>2</sup>/day (Barber, 1993).

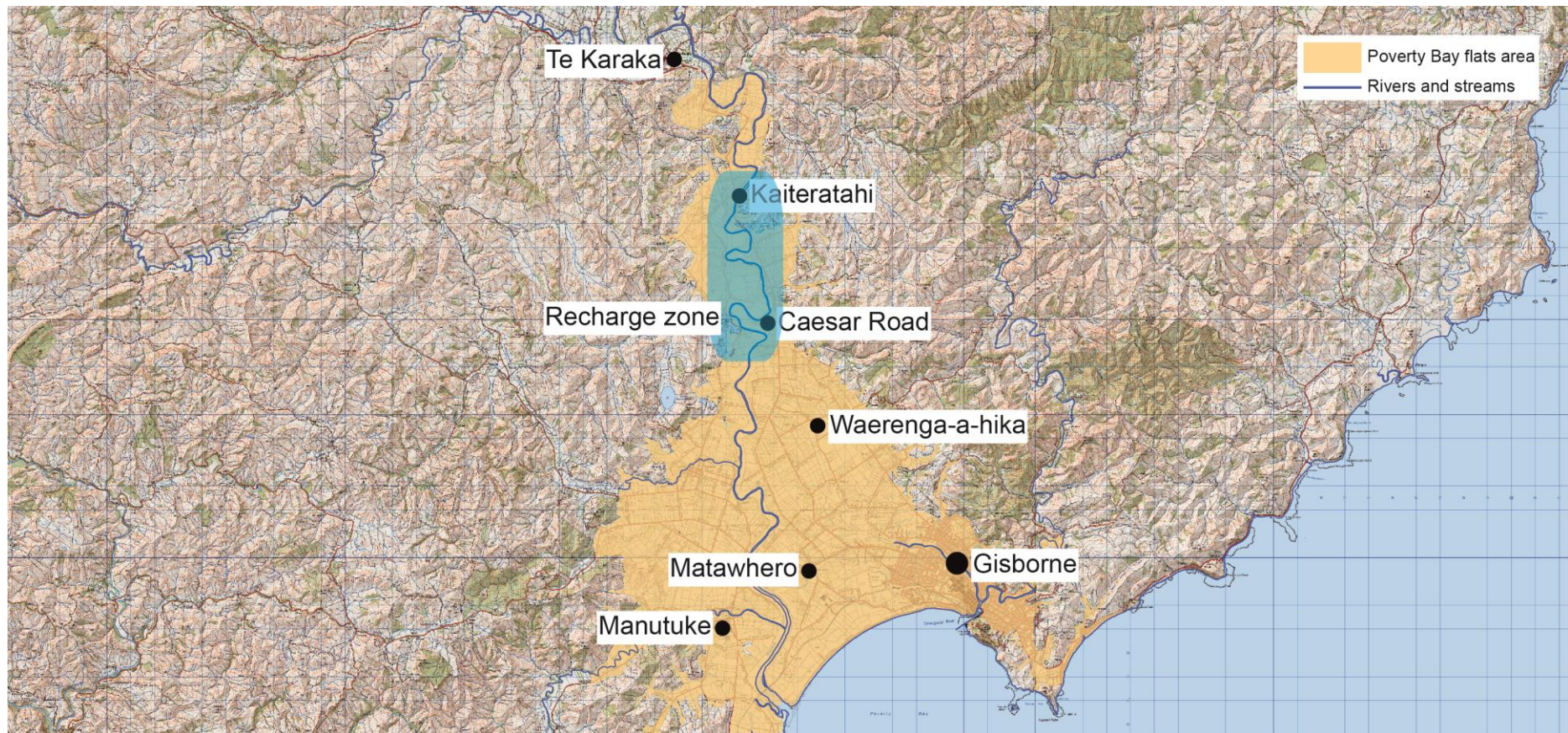


Figure 3.5. Poverty Bay flats showing possible recharge zones between the Waipaoa River and Waipaoa Gravel aquifer and the Waipaoa and Makauri Gravel aquifers (Adapted from Barber, 1993 and White et al. 2014).

### 3.3.4 Makauri Gravel Aquifer

The Makauri Gravel aquifer is the most extensive aquifer beneath the Poverty Bay flats (Figure 3.4). Radiocarbon dating identified that the Makauri gravels were deposited by the Waipaoa River between 9000 and 7000 years ago (Brown, 1984). As shown in Figure 2, the Makauri Gravel aquifer dips from northeast to southwest, which is likely due to tectonic uplift (Taylor, 1994). The Makauri Gravel aquifer is confined to semi-confined aquifer formed by gravel and sand deposits at varying depths. Shallow layers are between 45 and 80 m below the ground surface and deeper layers are between 100 and 130 m below the ground surface (Barber, 1993).

It has been noted that the Makauri Gravel aquifer thins towards the coast (Barber, 1993). At Kaiteratahi the gravel deposits are 7 m thick whereas at Matawhero the gravel deposits are 3 m thick (Barber, 1993). A geological investigation of the Makauri Gravel aquifer concluded that the aquifer has no outlet to the sea (Brown, 1984). However, while the Makauri gravels thin towards the coast evidence of Makauri gravels may have been found in bores near the coast (White et al., 2012). Further studies are needed to confirm whether the Makauri Gravel aquifer has an outlet to the sea.

Groundwater quality in the Makauri Gravel aquifer is generally poor (Brown and Elmsly, 1987; Barber, 1993). In the southern and western regions of the aquifer poor water quality is attributed to long residence times (Barber, 1993). The median Fe concentration (6.73 mg/L) indicates reducing conditions (White et al., 2012). The median conductivity concentration (1250  $\mu\text{S/cm}$ ) indicates evolved groundwater (White et al., 2012). However, the long residence times contradict the findings of Taylor (1994) who estimated that maximum residence times were between 100 and 200 years. The median Cl concentration (53 mg/L) is greater than the overlying shallower aquifers. Low  $\text{NO}_3\text{-N}$  concentrations (median of 0.0 mg/L) indicate that the anthropogenic impact on groundwater quality is limited (White et al., 2012). Like the Waipaoa Gravel aquifer, the depth of this aquifer means it is less susceptible to anthropogenic contamination as it is protected by confining layers. During the pumping season it has been

noted that the quality of the irrigation water deteriorates, which has been attributed to the abstraction rate exceeding the recharge rate (Barber, 1993).

It is likely Makauri Gravel aquifer is recharged in a number of different areas (Barber, 1993; Taylor, 1994; White et al., 2012). Barber (1993) suggests the aquifer is recharged from four different sources; from the hills to the northeast of the Poverty Bay flats, leakage from the Waipaoa River during summer, leakage from the Waipaoa Gravel aquifer and flow through the deep aquifers around Caesar Road. White et al. (2012) states that the aquifer is recharged by the Waipaoa River, and possibly by rainfall upstream of Kaiteratahi in the Waipaoa River Valley. Taylor (1994) stated that it is possible that the aquifer receives water from eastern areas of the Poverty Bay flats. Transmissivities within the Makauri Gravel aquifer range from 1000 to 2,500 m<sup>2</sup>/day and storage coefficients range from  $1 \times 10^{-4}$  to  $2 \times 10^{-4}$  (Gordon, 2001). Transmissivities are greatest in the middle of this aquifer around Caesar Road (Barber, 1993).

### **3.3.5 Matokitoki Gravel Aquifer**

According to Brown and Elmsly (1987), the Matokitoki Gravel aquifer is the remnants of early Quaternary terrestrial and marine deposits that survived erosion and were subsequently buried by younger deposits. The aquifer is confined and ranges in depth from 34 to 135 m (Barber, 1993). It is shallowest at Gisborne and increases in depth towards Kaiteratahi (Figure 3.2). The exact extent of the Matokitoki Gravel aquifer is unknown but it is estimated to extend from Gisborne to north of Kaiteratahi (Figure 3.4).

Groundwater quality within the Matokitoki Gravel aquifer is variable (Barber, 1993). It is not suitable for domestic or industrial use without prior treatment (Barber, 1993). The median Fe concentration (11.6 mg/L) indicates reduced conditions (White et al., 2012). However, Fe concentrations are variable indicating that there are varying degrees of reducing conditions within this aquifer (White et al., 2012). The median conductivity concentration (2555 µS/cm) indicates evolved groundwater

(White et al., 2012). Unlike the Makauri Gravel aquifer, this is consistent with the findings of Taylor (1994) who estimated that the groundwater residence time was approximately 4,300 years. The median Cl concentration (336 mg/L) is significantly greater than the median Cl concentration within the Makauri Gravel aquifer. Prolonged periods of pumping result in raised conductivity and CL concentrations within the aquifer (Barber, 1993). The depth of this aquifer and the fact it is confined mean that it is not susceptible to anthropogenic contamination (Gordon, 2001). Hence, the low NO<sub>3</sub>-N concentrations (0.00 mg/L).

The Matokitoki Gravel is recharged by the Waipaoa River and the overlying Makauri Gravel aquifer (Gordon, 2001). Given the groundwater residence time is 4,300 years (Taylor, 1994) groundwater flow is very slow in this aquifer. It is likely that this aquifer discharges water vertically to overlying sediments which subsequently recharges streams, rivers and drains (Barber, 1993). The average transmissivity in this aquifer is 380 m<sup>2</sup>/day and storage coefficients range from  $2 \times 10^{-4}$  to  $8 \times 10^{-5}$  (Gordon, 2001)

### **3.4 Land use changes**

Despite comprising only 2.2% of the total land area of the Gisborne District the Poverty Bay flats are an important component of the economy of the Gisborne District due to the intensive use of land (Telfer, 2013). Traditionally, land use was predominantly agriculture (Gordon, 2001). However, by 1987 the amount of land being used for intensive horticulture was increasing (Brown and Elmsly, 1987). It was noted by Brown and Elmsly (1987) that this trend towards intensive horticulture was expected to continue providing sufficient water was available for irrigation. Consequently, groundwater use within the Poverty Bay flats has increased (Gordon, 2001). Intensive horticulture resulted in a mixture of horticultural crops grown within the Poverty Bay flats by the mid-2000s (GDC, 2007). This is important as different horticultural crops have different water requirements. For example, kiwifruit requires approximately 50 m<sup>3</sup> of water per hectare for optimum production whereas citrus fruits require 25 m<sup>3</sup> per

hectare (Telfer, 2013). With regard to intensive horticulture, Telfer (2013) stated that the single biggest influence on crop type grown were economic forces. Therefore, the crops grown within the Poverty Bay flats will likely change in conjunction with economic forces. It is important to examine how changes in land use have affected groundwater resources within the Poverty Bay flats.

### 3.5 Groundwater resources

Economically, the availability of groundwater resources in the Poverty Bay flats is important given it is a major source of irrigation water (Gordon, 2001). Since the 1980s and 1990s groundwater use within the Poverty Bay flats has increased markedly as a result of the land use changes discussed in Section 2.4. This is shown in Table 3.1 which compares groundwater allocations in 1992 and 2015.

Table 3.1. Comparison of groundwater allocations within the Poverty Bay flats between 1992 and 2015. 1992 groundwater allocations were obtained from Barber (1993).

Aquifer	Annual allocation m <sup>3</sup> /day (1992)	Annual allocation m <sup>3</sup> (2015)
Te Hapara Sands, Shallow Fluvial Deposits, and Waipaoa Gravel aquifer	19,904	2,967,166
Makauri Gravel aquifer	25,353	8,019,723
Matokitoki Gravel aquifer	6,840	2,388,600

The Makauri Gravel aquifer is the most productive aquifer within the Poverty Bay flats groundwater system. It accounts for 60% of all allocated groundwater within the Poverty Bay flats (Table 3.1). There is a large discrepancy between the amount of groundwater allocated compared with annual average groundwater abstractions (Table 3.2). In the shallow aquifers (Te Hapara Sands, Shallow fluvial Deposits, and the Waipaoa Gravel aquifer) 8% of the annual groundwater allocation is abstracted. In Makauri and Matokitoki Gravel aquifers 16% and 3% of the annual groundwater allocation within each aquifer is abstracted, respectively. Overall, the Makauri Gravel aquifer accounts for 80% of all abstracted groundwater between 2012 and 2015.

Table 3.2. Comparison of annual groundwater allocation (2015) and annual average groundwater abstraction between 2012 and 2015.

Aquifer	Annual allocation m <sup>3</sup> (2015)	Annual average groundwater abstraction m <sup>3</sup> (2012-2015)	% of allocation abstracted
Te Hapara Sands, Shallow Fluvial Deposits, and Waipaoa Gravel aquifer	2,967,166	255,413	8
Makauri Gravel aquifer	8,019,723	1,274,979	16
Matokitoki Gravel aquifer	2,388,600	59,842	3

It is noted that the discrepancy between allocated groundwater and actual groundwater abstractions means that groundwater use could increase substantially as it stands. This highlights the need to identify the current state of groundwater resources within the Poverty Bay flats, particularly within the Makauri Gravel aquifer, which accounts for the majority of groundwater abstractions.

In the early 1990s when groundwater use within the Poverty Bay flats was increasing the GDC produced a report examining the groundwater system (Barber, 1993). This report identified that groundwater levels within the Makauri Gravel aquifer were declining. The report noted that groundwater management would be important to sustain the economic value of the resource. It appears that no action was undertaken to address the observed declines. A report by the GDC in 2007 briefly discussed groundwater level trends (GDC, 2007). It concluded that prior to 1997 groundwater levels in the Makauri Gravel aquifer were declining but that the situation has been reversed due to wetter climatic conditions.

In 2012, the state of groundwater resources within the Poverty Bay flats was re-evaluated (White et al., 2012). A total of 25 bores over five aquifers were analysed (the report assumed that bores within the Waipaoa Gravel aquifer were representative of the Shallow Fluvial Deposits). The report found that current groundwater abstraction rates from Te Hapara Sands, Shallow Fluvial Deposits, and Waipaoa Gravel aquifers were sustainable as groundwater levels were either stable or increasing at statistically significant rates ranging between 0.01 and 0.06 m/yr. Conversely,

groundwater levels were found to be declining at statistically significant rates in the Makauri Gravel and Matokitoki Gravel aquifers. Declines ranged from -0.02 to 0.10 m/yr in the Makauri Gravel aquifer and from -0.02 to -0.07 m/yr in the Matokitoki Gravel aquifer. No statistically significant trends were observed in rainfall data (from the Gisborne Airport weather station) or Waipaoa River flow (at Kanakanaia Bridge). Therefore, White et al. (2012) concluded that observed groundwater level declines in the Makauri and Matokitoki Gravel aquifers were probably due to groundwater abstractions.

To arrest these observed declines in groundwater levels in the Makauri and Matokitoki Gravel aquifers the GDC has been investigating alternative groundwater management regimes. Specifically, the GDC has been investigating, in conjunction with Golder Associates, whether MAR can be used as a tool to reverse groundwater level declines (Golder Associates, 2014A; Golder Associates, 2014B). This research has stemmed from the work undertaken by GDC and Golder Associates. As outlined in Chapter 1, this research investigates whether an infiltration basin may be successfully used as a MAR technique to artificially recharge the Makauri Gravel aquifer beneath the Poverty Bay flats. Supplementary work will also be undertaken to characterise the current state of groundwater resources within the Poverty Bay flats, identify interactions surface-groundwater resources, and examine hydraulic connections between aquifers.

## Chapter 4 – The HIGGS Index

Site selection is an important process when assessing the MAR potential for a given area, as discussed in Chapter 2. To identify sites that may be used for MAR using an infiltration basin the HIGGS Index was developed during the course of this research. It was developed using the premise that the MAR potential of a site using an infiltration basin could be evaluated by obtaining a limited number of hydrogeological parameters for a given location. A total of five hydrogeological parameters were included within the HIGGS Index. These parameters were included within the HIGGS Index by the author of this research due to the effect that each parameter could potentially have on the likelihood of an infiltration successfully reaching an aquifer. The parameters are:

- H – Hydraulic connection;
- I – Impact of the vadose zone;
- G – Groundwater depth;
- G – Groundwater flow direction;
- S – Saturated hydraulic conductivity.

These parameters are the assigned weights and ratings. The weights and ratings provide information about how a parameter will affect the infiltration basin at a site. The HIGGS Index uses a numerical approach to evaluate the MAR potential of a given location using the following equation:

$$MAR_p = H_W H_R \times I_W I_R \times Gd_W Gd_R \times G_W G_R \times S_W S_R \quad 4.1$$

where  $MAR_p$  is the MAR potential for a given site,  $H_W H_R$  is the weight and rating for hydraulic connection,  $I_W I_R$  is the weight and rating for impact of the vadose zone,  $Gd_W Gd_R$  is the weight and rating of groundwater depth,  $G_W G_R$  is the weight and rating for groundwater flow direction, and  $S_W S_R$  is the weight and rating for saturated hydraulic conductivity.

Once the MAR potential for multiple sites has been calculated the investigator can identify where MAR using an infiltration basin will most likely be successful.

This chapter provides an in depth discussion of the HIGGS Index. Section 4.1 discusses the weights used within the HIGGS Index. Section 4.2 describes the ranges used within the HIGGS Index. Section 4.3 discusses the ratings used within the HIGGS Index. Section 4.4 provides a detailed discussion of the parameters within the HIGGS Index. Assumptions of the HIGGS Index are presented in Section 4.5. The sites analysed using the HIGGS Index during the course of this research are presented in Section 4.6.

## 4.1 Weights

Weights in the HIGGS Index range from two to five (Table 4.1). Weights numerically describe the importance of each parameter to the likelihood of an infiltration basin successfully recharging the target aquifer. The process of assigning weights to each parameter was undertaken by the author of this research after a comprehensive review of the relevant literature. Saturated hydraulic conductivity was assigned a weight of 5 indicating that the author believes it is the most important parameter within the HIGGS Index when it comes to evaluating the MAR potential of a given site. Groundwater flow direction was assigned a weight of 2 indicating that the author believes it is the least important parameter within the HIGGS Index when it comes to evaluating the MAR potential of a given site. The weights assigned to each parameter are constant and cannot be changed regardless of the hydrogeological setting.

Table 4.1. Parameters within the HIGGS Index and their associated weights.

Parameter	Weight
Hydraulic connection (H)	4
Impact of the vadose zone (I)	4
Groundwater depth (G)	3
Groundwater flow direction (G)	2
Saturated hydraulic conductivity (S)	5

## 4.2 Ranges

Ranges were assigned to each parameter by the author of this research. The ranges reflect the variability that each parameter may have in different hydrogeological settings and are given in descriptive or numeric formats (Table 4.2 to Table 4.6). When the range is given in a numeric format the appropriate range is pre-defined. For example, the saturated hydraulic conductivity at a particular location determines the range used for this parameter. When the range is given in a descriptive format the investigator must determine the most appropriate range. For example, when assessing the hydraulic connection the investigator must determine the degree to which the infiltration basin is connected with the underlying target aquifer.

Table 4.2. Hydraulic connection ranges, ratings, and typical ratings within the HIGGS Index.

<b>Hydraulic Connection</b>		
<b>Range</b>	<b>Rating</b>	<b>Typical Rating</b>
No connection	0	0
Weak connection	0.2 – 0.4	0.3
Moderate connection	0.4 – 0.6	0.5
Good connection	0.6 – 0.9	0.7
Strong connection	1.0	1.0

Table 4.3. Impact of the vadose zone ranges, ratings, and typical ratings within the HIGGS Index.

<b>Impact of the vadose zone</b>		
<b>Range</b>	<b>Rating</b>	<b>Typical Rating</b>
Clay/silt	0.1 – 0.4	0.3
Sand and gravel with significant clay and silt	0.4 – 0.6	0.5
Sand and Gravel	0.7 – 1.0	0.9

Table 4.4. Groundwater depth ranges and ratings within the HIGGS Index. The range is measured in metres and is the depth to groundwater beneath the ground surface.

<b>Groundwater depth (m)</b>	
<b>Range</b>	<b>Rating</b>
0.00 – 0.50	0.1
0.51 – 1.00	0.2
1.01 – 2.00	0.3
2.01 – 4.00	0.4
4.01 – 6.00	0.5
6.01 – 8.00	0.6
8.01 – 10.00	0.7
10.01 – 15.00	0.8
15.01 – 20.00	0.9
20.01+	1.0

Table 4.5. Groundwater flow direction ranges, ratings, and typical ratings within the HIGGS Index.

<b>Groundwater flow direction</b>		
<b>Range</b>	<b>Rating</b>	<b>Typical Rating</b>
No confidence	0.1	0.1
Moderate confidence	0.2 – 0.9	0.6
High confidence	1.0	1.0

Table 4.6. Saturated hydraulic conductivity ranges and ratings within the HIGGS Index.

<b>Saturated hydraulic conductivity (m/day)</b>	
<b>Range (m)</b>	<b>Rating</b>
0	0
0.01 – 0.10	0.1
0.11 – 0.25	0.2
0.26 – 0.50	0.3
0.51 – 0.75	0.4
0.76 – 1.00	0.5
1.01 – 1.50	0.6
1.51 – 2.50	0.7
2.51 – 5.00	0.8
5.01 – 10.00	0.9
10.01+	1.0

## **4.3 Ratings**

Ratings within the HIGGS Index are linked to the ranges described in Section 4.2. Ratings within the HIGGS Index vary from 0.0 to 1.0. A rating of 0.0 for a parameter indicates that MAR using an infiltration basin will not be possible at a given site. Conversely, a rating of 1.0 indicates that a parameter is likely to be conducive to MAR using an infiltration basin. The ratings for two parameters (groundwater depth and saturated hydraulic conductivity) have one rating associated with each range. The remaining three parameters (hydraulic connection, impact of the vadose zone media, and groundwater flow direction) have a series of ratings that could be given for each range, reflecting the variable nature of each parameter. A typical rating has been given to provide some guidance, but the investigator must choose the appropriate rating based upon site-specific factors.

Unlike weights, ranges and ratings can be altered if detailed information is known for a given area. For example, should an investigator have detailed information about the sediments present within the vadose zone, the investigator may choose to refine the range and ratings to reflect this information. When the investigator makes changes to the range and/or ratings they must be applied across all sites being evaluated.

## **4.4 Parameters**

### **4.4.1 Hydraulic connection**

When assessing options for MAR, Sinclair Knight Merz (2010) state that semi-confined/confined aquifers are likely to require well injection methods to bypass any existing aquicludes. In spite of this, the HIGGS Index assumes that it is possible for a hydraulic connection to exist between an infiltration basin and a semi-confined/confined aquifer.

The strength of the hydraulic connection between the infiltration basin and the unconfined aquifer is dependent upon the sediments present within the vadose zone. The hydraulic connection between an infiltration basin and a

semi-confined aquifer is somewhat more complex. A semi-confined to confined aquifer by definition is overlain by an aquitard or aquiclude, at least in part, thus preventing or limiting the downwards movement of water (Freeze and Cherry, 1979).

However, it is theoretically possible that a hydraulic connection can exist between an infiltration basin and a semi-confined/confined aquifer. For example, an aquitard overlying an aquifer may provide inflow via leakage (Freeze and Cherry, 1979). Alternately, pathways may exist where shallow aquifers are connected with deeper aquifers in an area. It is this premise that a hydraulic connection can exist between an infiltration basin and a semi-confined to confined aquifer that is utilised within the HIGGS Index. Information such as that gained from groundwater quality tests, bore logs, piezometric surveys and pumping tests can provide information regarding the potential hydraulic connection between an infiltration basin and a semi-confined to confined aquifer. Table 4.2 shows that the hydraulic connection ranges are descriptive. Therefore, the investigator must make a subjective judgement about the potential hydraulic connection between an infiltration basin and the confined aquifer based upon known information.

#### **4.4.2 Impact of the vadose zone**

Impact of the vadose zone media is one of the most important parameters within the HIGGS Index, which is reflected in its weighting. Its importance stems from the effect that sediments within the vadose zone can have on infiltration rates, and thus recharge potential. Recharge potential within the HIGGS Index is defined as the ability of the sediments found within the vadose zone to transmit water from an infiltration basin to an underlying aquifer. As shown in (Figure 2.1), the vadose zone extends from the ground surface down to the capillary fringe. Infiltration rates within the vadose zone are primarily influenced by the porosity of the sediments found within this zone. Porosity is defined as *“the percentage of the total volume of the material that is occupied by pores or interstices”* (Bouwer, 1978, p. 21). Sediments with low porosities impede the vertical movement of water, and therefore have a low recharge potential. Sediments with high

porosities have little impact upon the vertical movement of water, and therefore have a high recharge potential.

Described below, in order of increasing recharge potential, are the various sediments outlined in

Table 4.3 and how they affect recharge.

(1) Clay/silt;

Clay and silt are fine sediments ranging in size from 0 to 2  $\mu\text{m}$  (micrometres) and 2 to 50  $\mu\text{m}$ , respectively (Bouwer, 1978). Both clay and silt act as a barrier to limit the downwards movement of water. Clay/silt ratings range from 0.1 to 0.4, reflecting the fact that the ratio of clay to silts will differ in different geological settings. When assessing the recharge potential of clay/silt layers within the vadose zone it is important to look at the ratio of clay to silt. The higher the clay ratio the lower the recharge potential.

(2) Sand and gravel with significant clay and silt

Sand and gravel, when compared with clay and silt, is a porous medium. Freeze and Cherry (1979) estimate that the porosity of sand and gravel deposits can range from 5 to 50%, depending on the size of the sediments. Sand ranges in size from 50  $\mu\text{m}$  to 2 mm and gravel ranges in size from 0.6 to 7.6 cm (Bouwer, 1978). Due to the size of these sediments, it is possible for the interstices (the empty space between sediments) to be filled with silt or clay. The recharge potential of sand and gravel with significant amounts of clay and silt present is dependent upon the size of the sediments presence and the ratio of sand to gravel and clay to silts, which is reflected in the ratings range. A high rating indicates that there is little clay and silt present within the sand and gravel. A low rating indicates the opposite.

(3) Sand and gravel

Sand and gravel, as mentioned above, is a porous medium. In some instances the interstices will remain void of clay and silt, meaning the porosity will remain high. The ratings range is 0.7 to 1.0. This reflects the fact that the size of the sand and gravel

sediments will determine the recharge potential, with larger sediments being more conducive to recharge.

The investigator can utilise all available information, such as bore logs, geological maps, and soil maps to identify sediments that will likely be conducive to MAR using an infiltration basin. From here, it is likely that the investigator will have to conduct field studies to determine the exact type of soils found within the vadose zone and the impact that these soils will have on infiltration rates.

#### **4.4.3 Groundwater depth**

Within the HIGGS Index groundwater depth refers to distance between the groundwater surface and the water table. Groundwater depth is an important parameter within the HIGGS Index. Its importance is a result of the fact that the depth of the water table can affect infiltration rates. When assessing how the depth to the water table will affect infiltration rates it is important to assess whether a restrictive clogging layer will be present beneath the infiltration basin as this affects how sensitive infiltration rates are to changes in groundwater depth (Bouwer, 1999).

When no clogging layer is present the hydraulic continuity between the infiltration basin and the underlying aquifer is unbroken, and therefore infiltration rates are sensitive to changes in the depth of the water table (Bouwer, 1999). If the depth to water table is sufficient, for example 20 m, then infiltration will predominantly be downward and driven by gravity (Bouwer, 1978; Bouwer, 1999), as shown in Figure 4.1A. In this instance the hydraulic gradient is approximately one (Bouwer, 1999). Conversely, if the depth to the water table is shallow, for example 1 m, then infiltration will predominantly be lateral and controlled by the piezometric slope (Bouwer, 1978; Bouwer, 1999), as shown in Figure 4.1B.

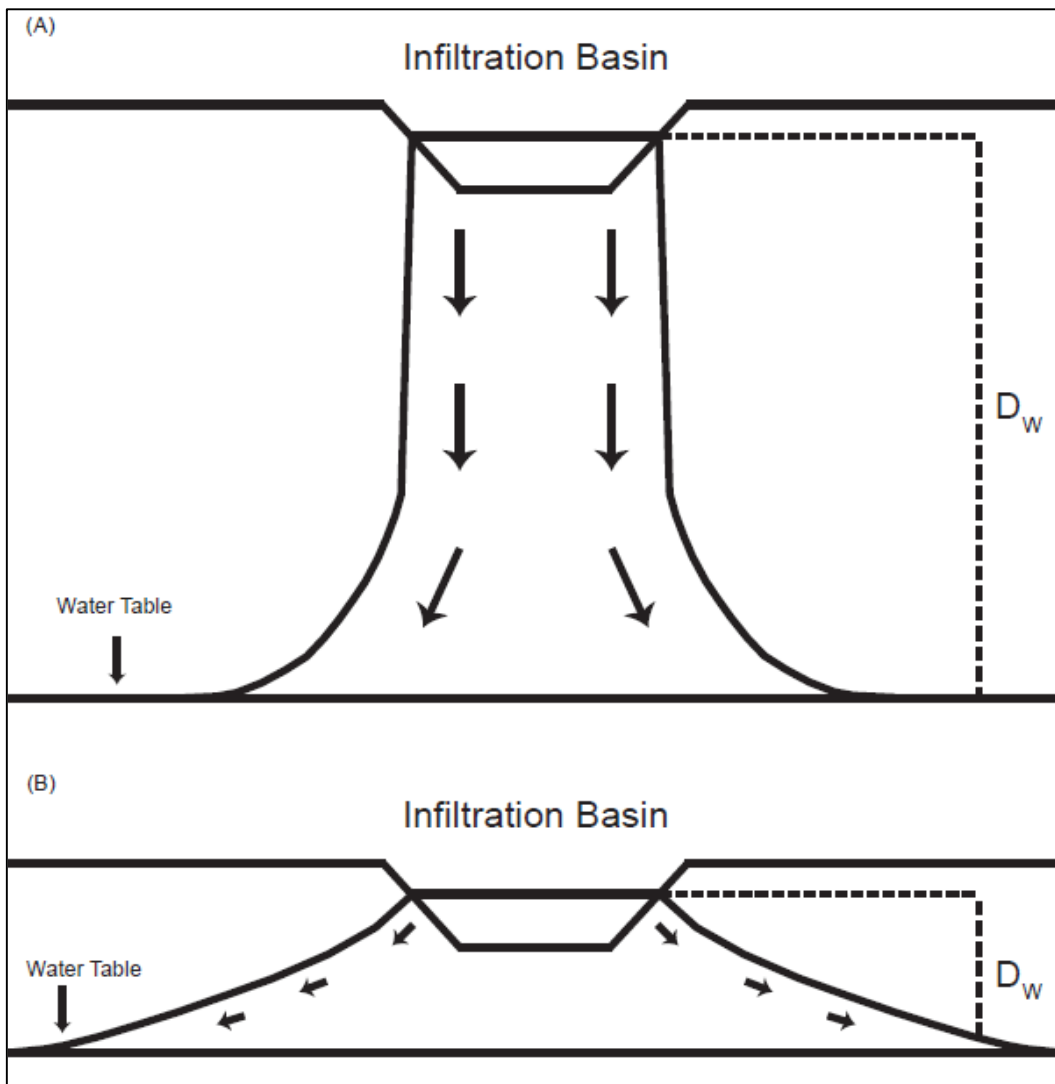


Figure 4.1. (A) Infiltration basin with deep groundwater levels. (B) Infiltration basin with shallow groundwater levels.  $D_w$  indicates the depth to the water table. Arrows indicate the direction in which groundwater is flowing from the infiltration basin (Adapted from Bouwer, 1999).

When a restrictive clogging layer is present infiltration rates are less sensitive to changes in the depth to the water table (Bouwer, 1999). A restrictive clogging layer means that the hydraulic continuity between the infiltration basin and the underlying aquifer is broken and the sediments beneath the clogging layer remain unsaturated (Figure 4.2). In this situation, the clogging layer controls infiltration rates rather than gravity (Bouwer, 1982). The infiltration rate is determined by the hydraulic conductivity and the thickness of the clogging layer (Bouwer, 1990).

The depth at which the water table begins to affect infiltration rates is determined by the capillary fringe, which lies between the vadose zone

and the water table (Figure 2.1). Providing the capillary fringe is below the bottom of the infiltration basin the infiltration rate is independent of the water table (Bouwer, 1982; Bouwer, 1999). As the water table rises infiltration rates remain unaffected until the capillary fringe reaches the bottom of the clogging layer (Bouwer, 1999). When the capillary fringe is at the bottom of the clogging layer the infiltration rate begins to decrease linearly until the infiltration rate is zero, which occurs when the water table rises to meet the water level within the infiltration basin (Bouwer, 1999).

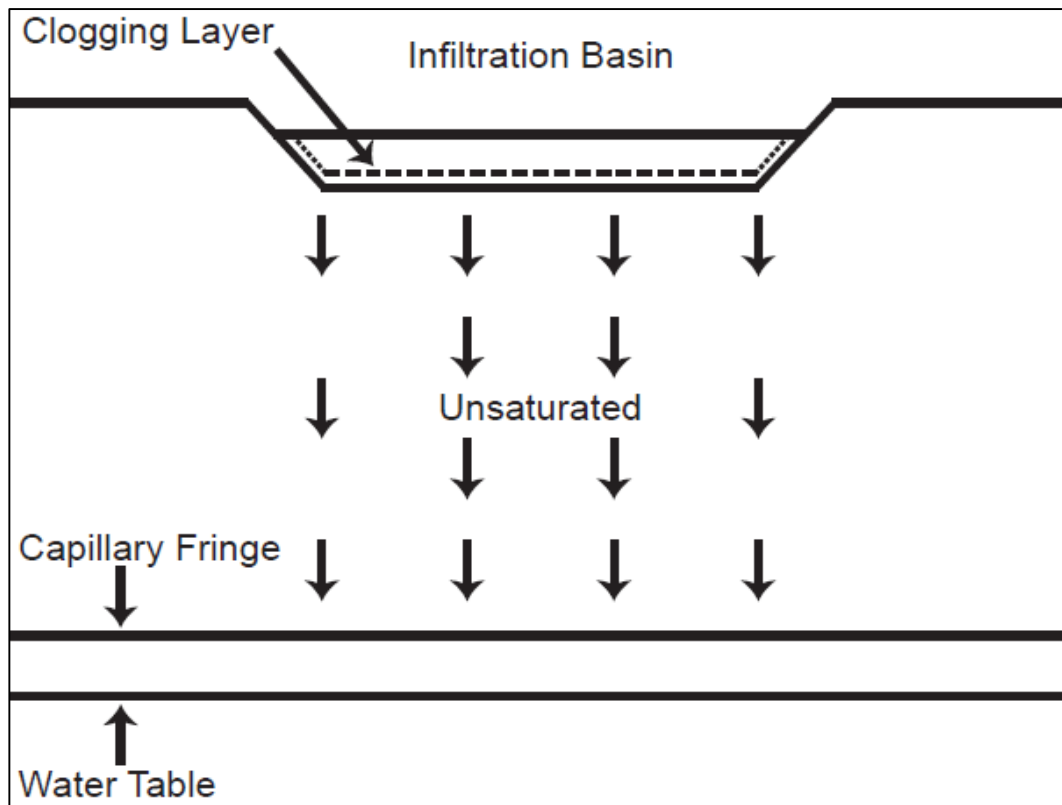


Figure 4.2. Conceptual diagram of an infiltration basin with a clogging layer (Adapted from Bouwer, 1999).

Regardless of whether a restrictive clogging layer is present within an infiltration basin or not, it is important for the investigator to ascertain what the depth to the water table is beneath the infiltration basin so it can be accounted for within the HIGGS Index.

#### 4.4.4 Groundwater flow direction

Groundwater flow direction has the lowest weighting of any parameter within the HIGGS Index (Table 4.1), yet is nonetheless an important parameter. An infiltration basin must be located in an area which will achieve the schemes desired outcomes (assuming all other parameters

are conducive to MAR). For example, an objective of a MAR scheme may be to artificially recharge a specific area of an aquifer. Therefore, an infiltration basin must be located in an area that can utilise groundwater flow to reach the intended area. Table 4.5 shows that the groundwater flow direction ranges are descriptive. Therefore, the investigator must make subjective judgements based upon known information as to whether the water artificially recharged will be transported via groundwater flow to its intended area or not.

#### **4.4.5 Saturated hydraulic conductivity**

Estimating saturated hydraulic conductivity is an important aspect of the HIGGS Index as the amount of water that can be transferred from an infiltration basin to an underlying aquifer over a given period will determine the amount of land required to achieve a MAR schemes objectives (Bouwer, 1999). Heath (1983) lists a number of different factors that affect saturated hydraulic conductivity, including soil porosity, soil permeability, the density and the viscosity of the water, and the strength of the gravitational field. The greater the porosity and permeability of a soil, the greater the saturated hydraulic conductivity. Bore logs and soil maps can be used to obtain information about the porosity and permeability of sediments beneath the infiltration basin, and thus provide initial estimates of saturated hydraulic conductivity to help determine the area of land that will be required for an infiltration basin. However, it is likely that detailed field studies (e.g., infiltrometer tests) will be required to provide accurate estimates of saturated hydraulic conductivity.

### **4.5 Assumptions**

The HIGGS Index is subject to three assumptions. They are:

- 1) Recharge is via an infiltration basin:  
As mentioned Chapter 2, there are a number of different methods that can be used to achieve MAR. However, the HIGGS Index was developed specifically to evaluate MAR potential of a site using an infiltration basin.
- 2) The investigator is attempting to recharge a semi-confined aquifer:

The HIGGS Index was developed with the specific aim of artificially recharging a semi-confined aquifer. The parameters included in the HIGGS Index reflect this aim.

3) Assumes all parameters are readily available:

Given that the investigator would most likely have an understanding of the groundwater system if MAR is being investigated, it is likely that all five parameters are available to the investigator for any given groundwater system. Each parameter is essential to the outcomes of the HIGGS Index when assessing a sites MAR potential.

If any of the above assumptions are not met then the investigator should consider whether it is appropriate to use the HIGGS Index to evaluate the MAR potential across multiple sites.

## **4.6 Site Selection**

The five parameters within the HIGGS Index were analysed via a desktop study to identify sites that may be suitable for MAR using an infiltration basin within the Poverty Bay flats. This desktop study concluded that two sites warranted further investigation. Discussions were held with GDC to identify any possible issues that may arise at each site and negatively affect this research. No issues were identified. Subsequently, landowners were contacted to gain permission to undertake the research on their land. Permission was granted by both landowners.

The identified sites are shown in Figure 4.3. Site 1 is in the northern reaches of the Poverty Bay flats off Lavenham Road and covers an area of 0.62 km<sup>2</sup>. Site 2 is located in the middle reaches of the Poverty Bay flats off Caesar Road and covers an area of 0.01 km<sup>2</sup>. The MAR potential of each site was subsequently evaluated using the HIGGS Index. Results are presented in Chapter 6.

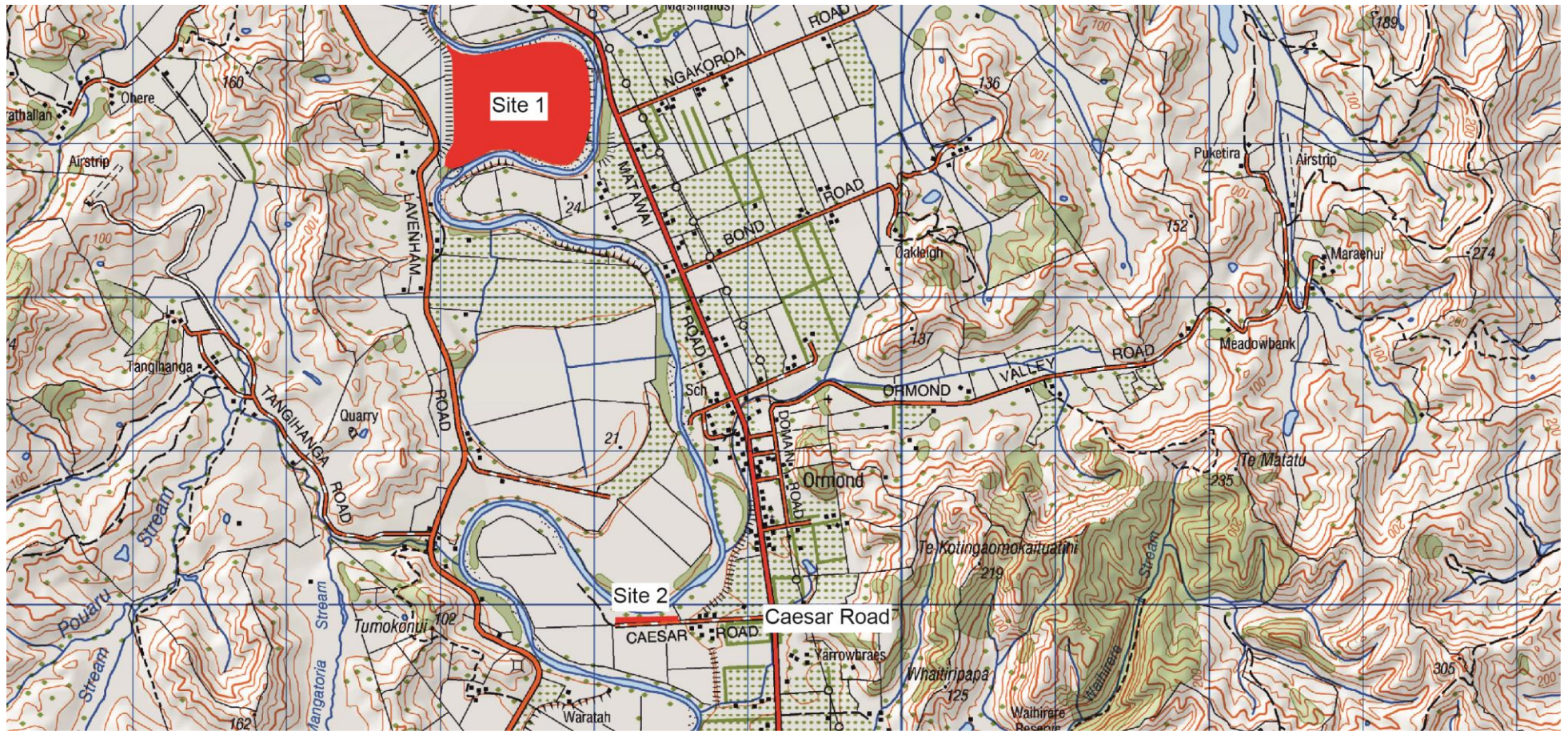


Figure 4.3. Location of the two sites identified using the HIGGS Index.

## Chapter 5 – Data & Methods

---

This chapter outlines the data and methods used within this research. Section 5.1 describes the existing datasets obtained from the National Institute of Water and Atmospheric Research (NIWA) and the GDC. Section 5.2 describes the data collected during the course of this research whilst undertaking fieldwork. Section 5.3 outlines the methods used to analyse the data described in Sections 5.1 and 5.2. Section 5.4 describes the hydrogeological model used to model the Poverty Bay flats groundwater system. Section 5.5 summarises the data and methods used within this research.

### 5.1 Existing data

#### 5.1.1 Rainfall data

Daily rainfall data was obtained for two purposes; to identify whether rainfall exhibited any trends within the Poverty Bay flats and to characterise how groundwater levels change in response to a rainfall event and associated changes in river flow and stage. Rainfall data has been recorded at the Gisborne Airport since 1937 at two different sites by NIWA (Figure 5.1). Rainfall data from Gisborne Aero weather station was obtained between 01/01/1982 and 01/03/1993 and between 13/12/1989 and 05/05/2015 at Gisborne AWS weather station (Table 5.1). Linear regression was undertaken on rainfall data collected between 13/12/1989 and 01/03/1993 at both weather stations. From the resulting equation daily rainfall at Gisborne AWS between 01/01/1982 and 12/12/1989 was estimated to provide one dataset from 01/01/1982 through to 05/05/2015.

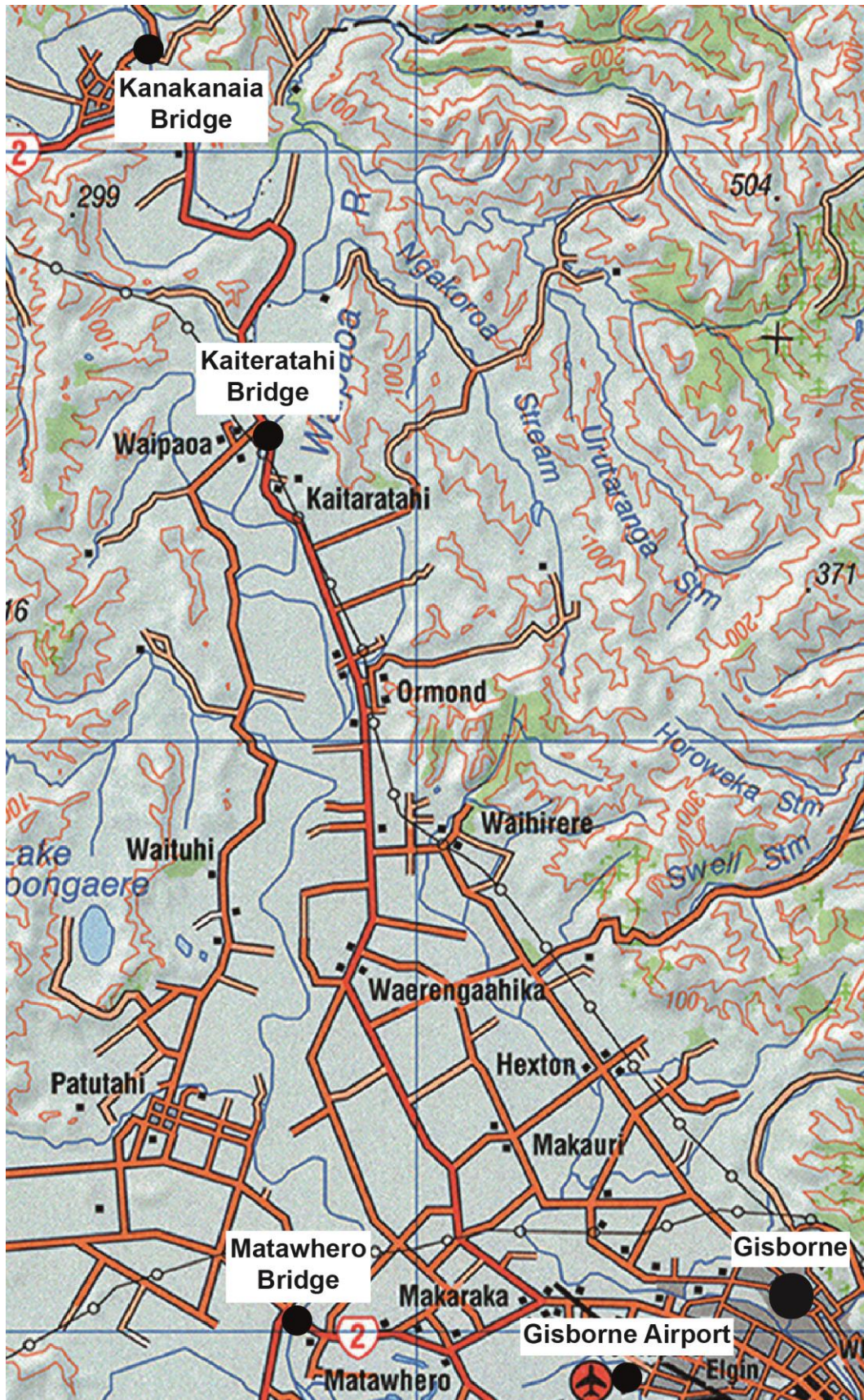


Figure 5.1. Location of the Gisborne Airport where the two weather stations are located. The three river flow and stage monitoring sites (Kanakanaia Bridge, Kaiteratahi Bridge, and Matawhero Bridge) on the Waipaoa River are also shown.

Table 5.1. Latitude/longitude, altitude, and start and end dates for which rainfall data was obtained from the Gisborne Airport. All rainfall data was obtained from Cliflo (<http://cliflo.niwa.co.nz/>).

Weather station	Latitude/Longitude	Altitude (msl)	Start date	End date
Gisborne Aero	-38.661/177.986	4	01/01/1982	01/03/1993
Gisborne AWS	-38.660/177.984	5	13/12/1989	05/05/2015

### 5.1.2 Surface water data

Daily surface water data from the Waipaoa River was obtained from the GDC for two purposes; to identify any trends in Waipaoa River flow and stage data and to characterise how groundwater levels change in response to a rainfall event and associated changes in river flow and stage. River flow and stage data is recorded at three sites on the Waipaoa River; Kanakanaia Bridge, Kaiteratahi Bridge, and Matawhero Bridge (Figure 5.1). The periods for which river flow and stage data were obtained are given in Table 5.2. To record river stage at each monitoring site a staff gauge has been installed against which river stage is measured.

Table 5.2. Locations where river flow and river stage data is collected on the Waipaoa River. 'Monitoring period' indicates the periods for which river flow and stage data was obtained for this research. 'MSL (m)' shows the height of each monitoring site relative to mean sea level.

Location	Monitoring period	MSL (m)
Kanakanaia Bridge	01/01/1982 – 05/05/2014	28.59
Kaiteratahi Bridge	14/08/1989 – 05/05/2014	17.4
Matawhero Bridge	01/01/1982 – 05/05/2014	-0.07

Concurrent river flow gauging data was also obtained from the GDC to identify surface-groundwater interactions between reaches on the Waipaoa River. These gaugings have been undertaken at low flows at irregular intervals since 1993 by the GDC at 10 different sites (Table 5.3; Figure 5.2).

Table 5.3. The 10 river flow gaugings sites on the Waipaoa River, when they were first gauged and the number of gaugings at each site.

Site	First Gauged	Number of surface gaugings
Kanakanaia Bridge	26/02/2013	3
Clarke's	11/11/2010	5
Kaiteratahi Bridge	26/02/2013	3
Whitmore Road	16/11/1993	20
Ford Road	16/11/1993	20
Bruce Road	16/11/1993	20
Brown Road	16/11/1993	20
Ferry Road	26/02/2013	3
Tietjens Road	11/11/2010	5
Bloomfield Road	11/11/2010	5

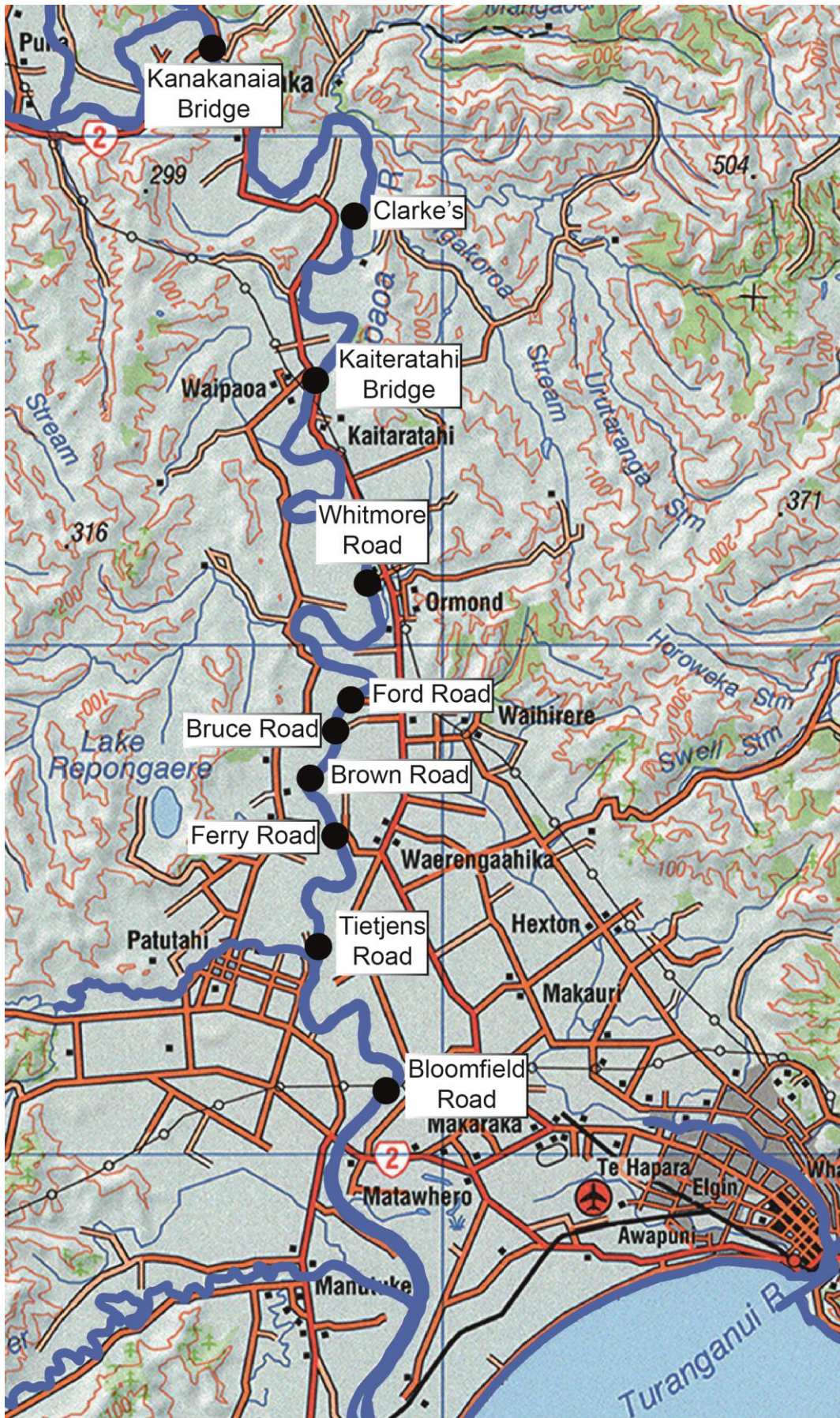


Figure 5.2. Location of the 10 river flow gauging sites on the Waipaoa River.

### **5.1.3 Groundwater level data**

The GDC monitors groundwater levels using two different methods; manual monitoring which occurs once a month and using telemeters which record groundwater levels at 15 minute intervals. Since 1982 groundwater levels have been monitored manually by the GDC. Initially five bores over four aquifers were monitored. Over time the number of bores monitored has increased to 49 over five aquifers (Figure 5.3). Groundwater level data was obtained for the period from when each bore was first monitored, which was between January 1982 and February 1995, through to December 2014 (Appendix A). This data was analysed to identify whether groundwater levels exhibited any trends. Telemeters are used to record groundwater levels in eight bores across the Poverty bay flats in four different locations (Figure 5.4). Groundwater level data recorded using telemeters was obtained on a daily time-step (09:00 am) between 14/03/2015 and 27/03/2015. This data was analysed to characterise how groundwater levels change in response to a rainfall event and associated changes in river flow and stage.

Groundwater levels can be affected by changes in atmospheric pressure (Bouwer, 1978; Freeze and Cherry, 1979). Increases in atmospheric pressure cause declines in groundwater levels and vice versa (Freeze and Cherry, 1979). As such, it is important to correct groundwater level data for atmospheric effects. Hourly atmospheric pressure data from the Gisborne AWS weather station was obtained between 14/03/2015 and 27/03/2015 from Cliflo (<http://cliflo.niwa.co.nz/>). Groundwater level data recorded using telemeters was corrected for atmospheric effects using the methods described in Appendix B. Groundwater level data obtained from the manual monitoring was not corrected for atmospheric effects due to the time between each reading.

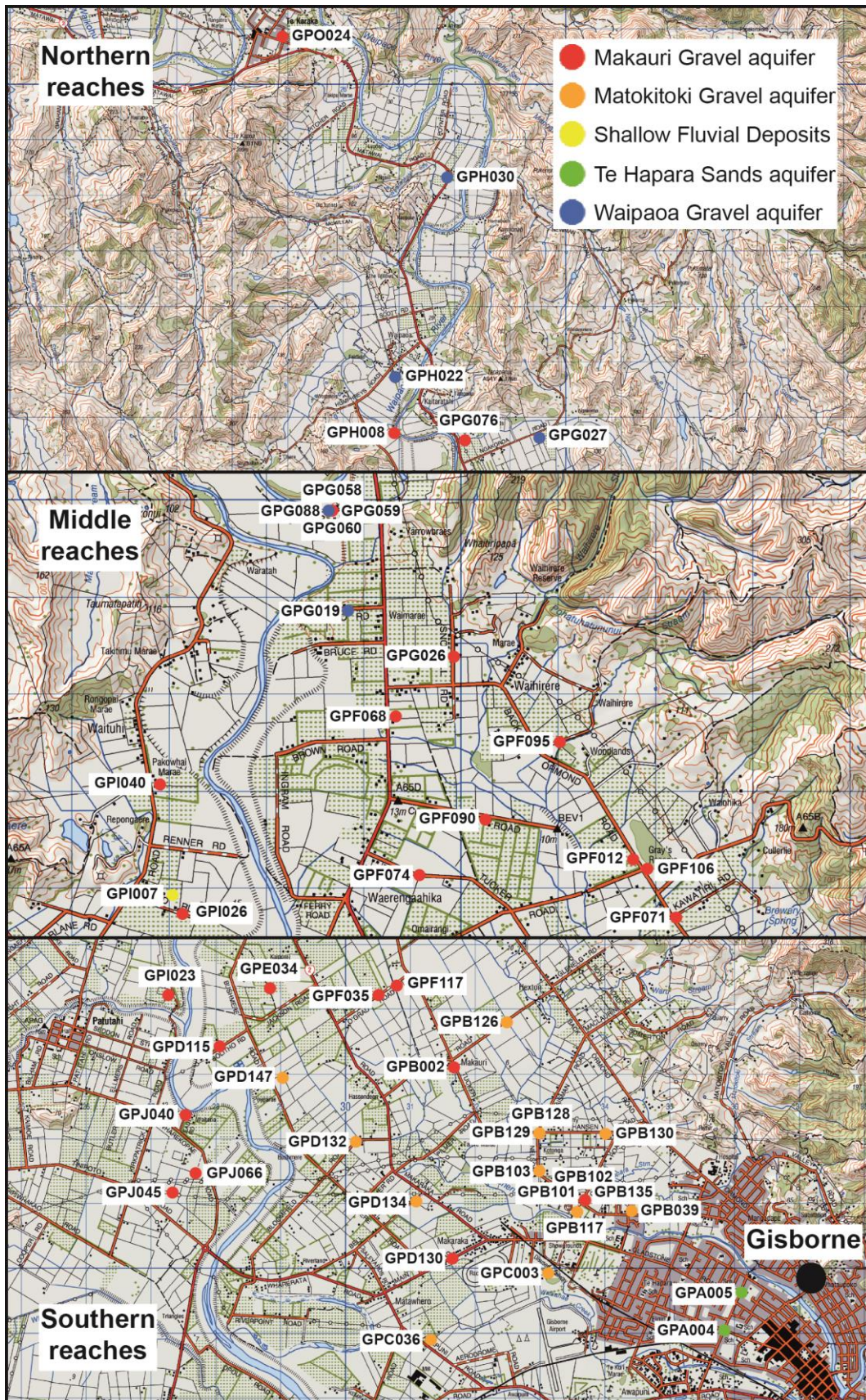


Figure 5.3. Location of the 49 bores for which groundwater levels are obtained monthly across the Poverty Bay flats.

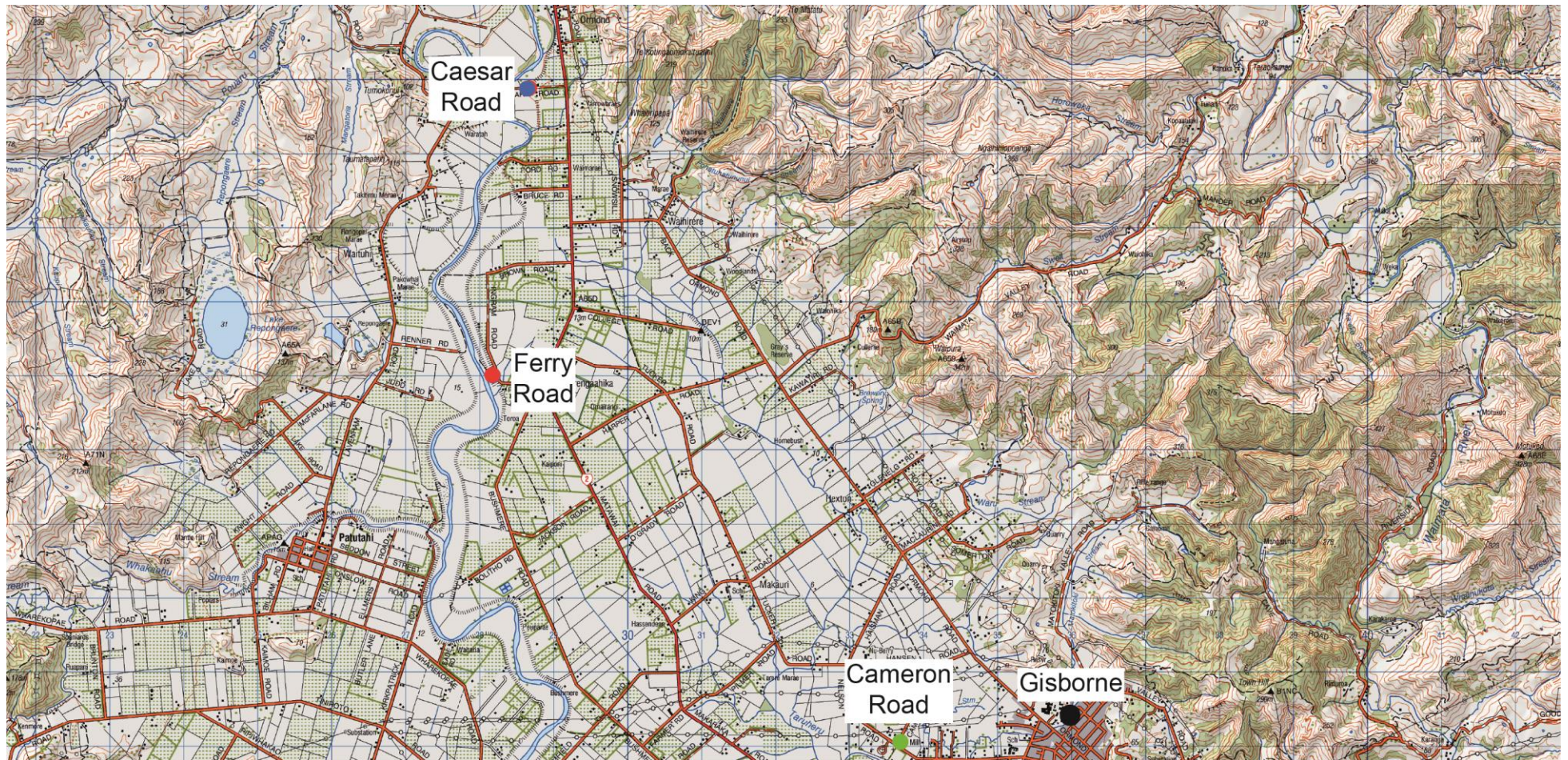


Figure 5.4. Location of the four sites where groundwater levels are electronically monitored across eight bores.

### 5.1.4 Hydrogeological data for model input

Geological and water use data was obtained from the GDC for the specific purpose of developing a hydrogeological model of the Poverty Bay flats groundwater system. Lithological data was obtained from 529 bore logs within the Poverty Bay flats ranging in depth from 0.8 m to 300 m below the ground surface. The data was used to identify geological units beneath the Poverty Bay flats, which were subsequently input into the hydrogeological model. Water use data for the period 2012 to 2015 showed how much water was abstracted from both surface water bodies and aquifers within the Poverty Bay flats over the course of an irrigation season. The data was used to identify groundwater abstraction areas within the hydrogeological model.

## 5.2 Data from fieldwork

### 5.2.1 Groundwater level data

The groundwater level data that was obtained from GDC to characterise how groundwater levels respond to rainfall and changes in river flow and stage from the GDC was limited in its spatial coverage (Figure 5.4). Therefore, further manual monitoring of daily groundwater levels was undertaken in 10 bores between 14/03/2015 and 27/03/2015 to increase the spatial coverage (Figure 5.5). Groundwater level monitoring was undertaken using a Solinst Model 101 P1 Water Level Meter. Unlike the groundwater level data monitored manually in Section 4.1.3 groundwater level data was recorded relative to the ground surface (i.e., metres below the ground surface) and was converted to metres above mean sea level (aMSL) using the following equation:

$$GWL_{msl} = BE - (GWL_{GS} - ToC) \quad 5.1$$

where  $GWL_{msl}$  is the groundwater level relative to mean sea level in m,  $BE$  is the bore elevation relative to mean sea level in m,  $GWL_{GS}$  is the groundwater level relative to the ground surface in m, and  $ToC$  is the distance between the top of the casing and the ground surface in m.

Groundwater levels were then corrected for atmospheric effects using the methods described in Appendix B.

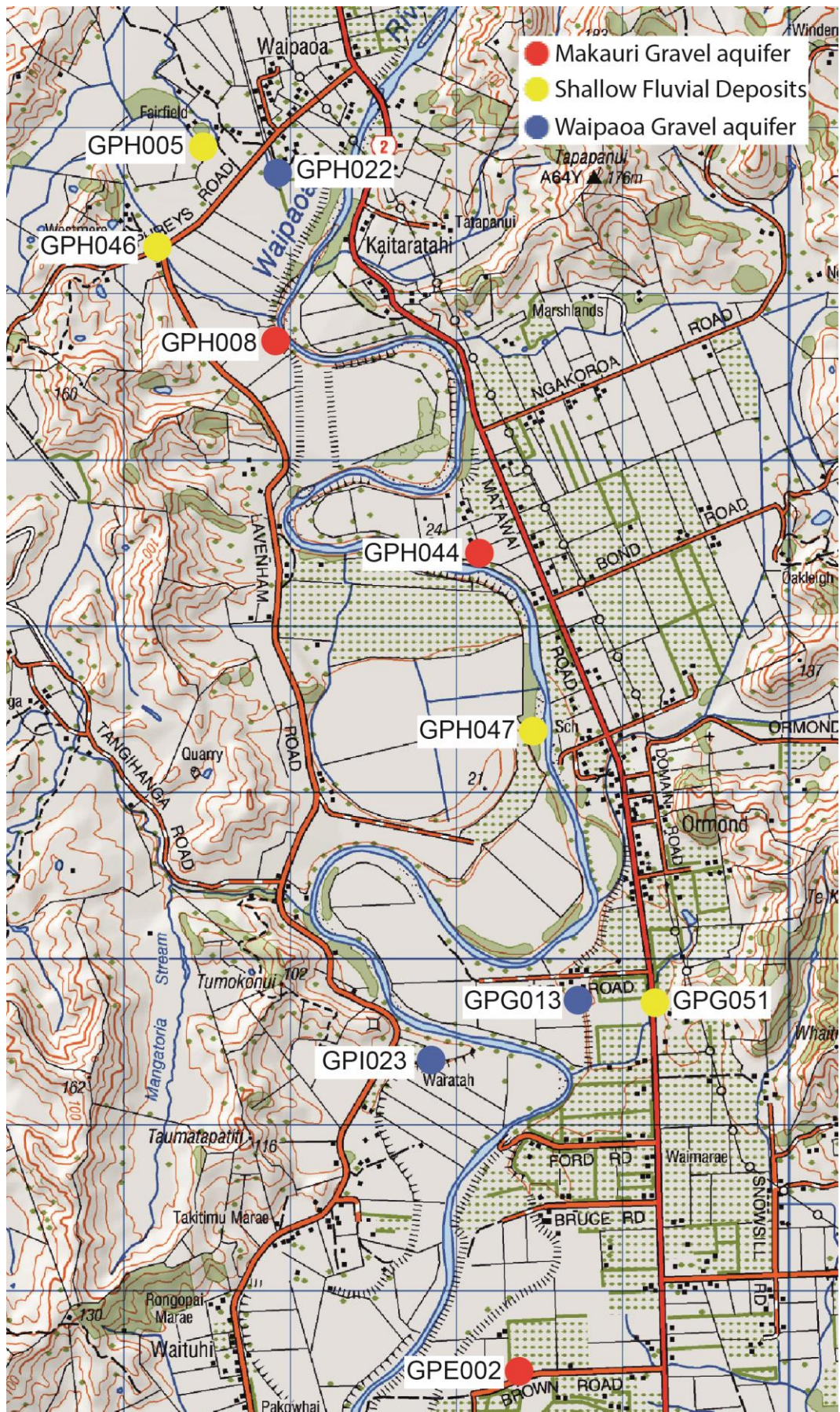


Figure 5.5. Location of the 10 bores monitored manually between 14/03/2015 and 27/03/2015 when ex-tropical Cyclone Pam hit the Gisborne District.

### **5.2.2 Pumping test**

Pumping tests are undertaken to help attain an understanding of aquifer characteristics (Freeze and Cherry, 1979). With regard to this research pumping tests are important as they can help identify whether connections exist between different aquifers. A total of 43 pumping tests have been undertaken within the Poverty Bay flats (Appendix C). An analysis of the spatial distribution of these pumping tests identified that none had been completed within the Makauri Gravel aquifer in the Caesar Road area. To increase the spatial distribution of pumping tests within the Makauri Gravel aquifer a pumping test was undertaken in close proximity to Caesar Road. In the Caesar Road area, GPG036 was the only bore that met the requirements for this pumping test. GPG036 tapped the Makauri gravel aquifer and had nearby bores tapping the overlying Waipaoa Gravel aquifer that could be monitored for any drawdown associated with the pumping test (Figure 5.6).



Figure 5.6. Location of GPG036 (pumped bore) and GPG064 and GPG062 (observations bores). Inset shows the wider area within which these bores are located.

To ensure that the pumping test ran for a sufficient duration the theoretical drawdown at the observation bores was calculated for different time periods using standard equations (Bouwer,1978).

$$u = \frac{r^2 S}{4Tt} \quad 5.2$$

$$s = \frac{QW(u)}{4\pi T} \quad 5.3$$

where  $u$  is a dimensionless value,  $r$  is the distance between the pumped and observation bores in m,  $S$  is the storage coefficient of the pumped aquifer,  $T$  is the transmissivity of the pumped aquifer,  $t$  is the pumping duration in days,  $s$  is the theoretical drawdown at the observation bore within the pumped aquifer,  $Q$  is the pumping rate in m<sup>3</sup>/day,  $W(u)$  is the well function, which is related to  $u$ . Values for  $W(u)$  can be found in Ferris (1962).

From 5.3 it was estimated that a pumping test of 24 hours duration would result in drawdown at the observation bores if a hydraulic connection exists between the Makauri Gravel aquifer and the Waipaoa Gravel aquifer. Beginning at 8:30 am on the 16th of June 2015, GPG036 was pumped for a period of 24 hours at a rate of approximately 110 m<sup>3</sup>/day. The observation bores, GPG062 and GPG064, were monitored for 48 hours beginning at 8:30 am on the 16th of June 2015. Due to the setup of GPG036 monitoring could not be undertaken at this bore. Atmospheric pressure data from the Gisborne AWS weather station was obtained from Cliflo (<http://cliflo.niwa.co.nz/>) for the period when observations bores were monitored so recorded groundwater levels could be corrected for atmospheric effects using the methods described in Appendix B.

### 5.2.3 Infiltration data

Infiltration data was obtained to evaluate the MAR prospects of the two sites identified using the HIGGS Index (Chapter 4). Infiltration data was attained via infiltrometer tests at the two sites identified using the HIGGS Index (discussed in Chapter 4). A detailed description of the testing procedure at each site is given in Appendix D. Following the completion of

the infiltrometer tests the infiltration data was used to calculate the saturated hydraulic conductivity ( $K_s$ ), which is equivalent to the long-term infiltration rate, using the following equations from Bouwer (1999):

$$i_n = \frac{y_n}{t_n} \quad 5.4$$

where  $i_n$  is the infiltration rate,  $y_n$  is the last water level drop, and  $t_n$  is the amount of time it takes for the last water drop to occur.

$$i_w = \frac{i_n \pi r^2}{\pi (r + x)^2} \quad 5.5$$

where  $i_w$  is the downward flow rate,  $r$  is radius of the inner ring, and  $x$  is the lateral divergence. The depth of the wet front ( $L$ ) at the end of the infiltrometer test is then calculated:

$$L = \frac{y_t \pi r^2}{n \pi (r + x)^2} \quad 5.6$$

where  $L$  is the depth of the wet front,  $n$  is the fillable porosity of the soil.  $n$  is estimated based upon soil texture and the initial water content of the soil. Bouwer (1999) states that  $n$  may be 0.3 for dry uniform soils, 0.2 for moist soils, and 0.1 for wet soils. Given that the prevailing soil conditions at both sites were dry  $n$  was assumed to be 0.3. Finally,  $K_s$  was calculated:

$$K_s = \frac{i_w L}{(z + L - h_{we})} \quad 5.7$$

where  $z$  is the mean water level within the inner ring of the infiltrometer during the final drop and  $h_{we}$  is the water-entry value of the soil and is used to estimate the suction at the wet front as it infiltrates downwards.  $h_{we}$  can be estimated using the values given in Table 5.4.

Table 5.4. Estimates of water-entry values (adapted from Bouwer, 1999).

Sediment	Water entry value (cm)
Coarse sands	-5.08
Medium sands	-10.16
Fine sands	-15.24
Loamy sands-sandy loams	-25.4
Loams	-35.56
Structured clays (aggregated)	-35.56
Dispersed clays	-101.6

Once calculated  $K_s$  can be used to draw conclusions about the amount of land required to achieve a given amount of recharge per year, or alternately, whether the long-term infiltration rates are sufficient to justify the use of an infiltration basin.

## 5.3 Data analysis

### 5.3.1 Trend identification

Identifying the presence or absence of trends within environmental data allows the current state of a resource to be evaluated (Helsel and Hirsch, 2002). Knowing the current state of a resource allows good management decisions to be made. Trend analyses were first undertaken within the Poverty Bay flats in 2012 across three variables; rainfall, river flow, and groundwater levels (White et al., 2012). The analyses were undertaken to update the work of White et al. (2012) and provide updated information as to the current state of groundwater resources. Trend tests were undertaken on the following datasets:

- Annual rainfall data (Section 5.1.1);
- Waipaoa River flow and stage data including mean annual, mean monthly, mean seasonal, and mean and minimum summer (i.e., February) datasets (Section 5.1.2).
- Monthly groundwater level data collected manually by the GDC (Section 5.1.3).

All trend analyses were undertaken over the same period; 1982 – 2014, as data exists for all three datasets for this period. Two types of trend tests were used; the Mann-Kendall non-parametric trend test and the seasonally adjusted Mann-Kendall non-parametric trend test. The Mann-Kendall non-parametric trend test was used on data that did not require seasonal effects to be accounted for (e.g., annual rainfall). As outlined by Helsel and Hirsch (2012), seasonal effects can be a source of variation, and therefore must be accounted for. As such, the seasonally adjusted Mann-Kendall non-parametric trend test was used on data that did require seasonal effects to be accounted for. When accounting for seasonal effects the data was broken down into four groups following White et al. (2012). The four “seasons” were; January to March, April to June, July to September, and October to December. Results from the trend tests were then used to identify long-term trends within each variable and the possible causes of these changes.

### **5.3.2 Groundwater level changes**

The relationship between groundwater levels and rainfall and river stage was characterised by undertaking groundwater level monitoring before, during, and after a rainfall event in March 2015 (Sections 5.1.3 and 5.2.1). Groundwater level changes were analysed by examining changes in groundwater levels in each bore throughout the course of the monitoring period. Particular focus was given to the spatial distribution of groundwater level changes within each aquifer and how these changes fit with our current knowledge of the Poverty Bay flats groundwater system. From the analysis inferences were made as to why individual bores and aquifers responded as they did.

### **5.3.3 Surface-groundwater interactions**

The concurrent river flow gaugings from the Waipaoa River discussed in Section 5.1.2 were used to analyse surface-groundwater interactions within the Poverty Bay flats. Gains and losses between reaches were treated as groundwater discharge to the Waipaoa River and groundwater recharge from the Waipaoa River following White et al. (2012). It is noted that the concurrent river flow gaugings used within this research have two

limitations, which was taken into account when analysing this data. First, some tributaries of the Waipaoa River are not gauged meaning the contribution of such tributaries cannot be accounted for (White et al., 2014). Second, limited information is available regarding surface water abstractions when surface gaugings have been undertaken, meaning the impact of surface water abstractions on concurrent river flow gaugings cannot be accounted for.

## **5.4 Hydrogeological modelling**

A hydrogeological model was developed during the course of this research to model the Poverty Bay flats groundwater system. In particular, the hydrogeological model was used to predict whether an infiltration basin may be successfully used as a MAR technique to artificially recharge the Makauri Gravel aquifer. The model was developed using Comsol, which uses the finite element method to solve boundary value problems (Comsol, 2012). The utilised model is a steady state 2-dimensional model covering 10 km of the Poverty Bay flats to a depth of 100 metres below mean sea level (Appendix E).

### **5.4.1 Model geology**

As discussed in Chapter 3 the geology of the Poverty Bay flats is complex. Model geology was specified using bore logs in close proximity to the modelled area. Where no bore log data existed assumptions were made about the underlying geology via spatial extrapolations. To simplify the geological data for modelling purposes, three main layers within the Poverty Bay flats groundwater system were identified: vadose zone, aquifers, and aquitards. The vadose zone extends from the ground surface to the uppermost aquifer and varies in thickness from 0 and 10.05 m. Three aquifers within the Poverty bay flats groundwater system were identified and modelled: the Shallow Fluvial Deposits, the Waipaoa Gravel aquifer, and the Makauri Gravel aquifer. The thickness and depth of these aquifers varies throughout the model. A total of 10 aquitards were incorporated into the model. Like the aquifers, the thickness and depth of the aquitards is variable.

### 5.4.2 Parameters

The hydrogeological model used within this research contains two parameters; hydraulic conductivity and porosity. Porosity is not a required parameter for steady state modelling but provides Darcy flow values. Bore logs were analysed to identify the dominant sediments present within each geological unit. Hydraulic conductivities and porosity values were then estimated based upon the bore log data using representative values from Schwartz and Zhang (2003) (Table 5.5).

Table 5.5. Parameters of the hydrogeological model. Parameter values were chosen based upon an analysis of bore log data.

Layer	Hydraulic conductivity (m/s)	Porosity
Vadose zone	$1 \times 10^{-6}$	0.4
Aquifers	$1 \times 10^{-4}$	0.25
Aquitards	$1 \times 10^{-9}$	0.6

### 5.4.3 Boundary conditions

Boundary conditions describe the state of a particular variable at the boundary of a model (Pinder and Celia, 2006). There are three types of boundary conditions; Dirichlet, Neumann, and Cauchy boundary conditions (Schwartz and Zhang, 2003). Each boundary condition represents the groundwater system using different variables (Schwartz and Zhang, 2003). The Dirichlet and Neumann boundary conditions were applied to the hydrogeological model. Groundwater level data (Sections 5.1.3 and 5.2.1) was used to estimate hydraulic head values at the aquifer boundaries (i.e., Dirichlet boundary condition).

Mass flux boundaries were used internally within the model to represent groundwater abstraction and recharge areas (i.e., an internal Neumann boundary condition). Groundwater abstraction rates were estimated from water use data (Section 5.1.4). Groundwater recharge zones were incorporated within the model based on previous research and were estimated through trial and error (e.g., White et al., 2014). Mass flux

values for the groundwater abstraction and recharges zones were altered throughout the calibration and validation process to reflect model outputs. When running the model under different MAR scenarios an additional mass flux boundary was used to represent inflow to the groundwater system from an infiltration basin.

#### 5.4.4 Calibration and validation

Calibration involves the adjustment of model parameters to achieve a good fit between observed and predicted variables (e.g., hydraulic heads) (Schwartz and Zhang, 2003). Calibration is necessary to provide a quantitative assessment of model performance (Krause et al., 2005). The hydrogeological model used within this research was calibrated manually where internal boundary conditions (groundwater recharge and abstraction areas) and parameters were adjusted during each model run. No changes were made to external boundary conditions. At the conclusion of each run the model performance was evaluated using the goodness of fit index  $V$  (Bardsley, 2013) and the root mean squared error (RMSE).  $V$  is calculated using the following equation:

$$V = r^2 / (2 - E) \quad 5.8$$

where  $r^2$  is the coefficient of determination with regards to the linear regression between the observed and predicted values, and  $E$  is the Nash-Sutcliffe Efficiency (Nash and Sutcliffe, 1970), which is calculated using the following equation:

$$E = 1 - \frac{\sum(O_i - P_i)^2}{\sum(O_i - \bar{O})^2} \quad 5.9$$

where  $O_i - P_i$  are the observed and predicted values, respectively.

$V$  provides a measure of the goodness of fit between 0 and 1 where 1 represents a perfect fit between observed and predicted variables (Bardsley, 2013). The model was calibrated against hydraulic head data from 10 bores. After the final model run during calibration,  $V$  was calculated to be 0.96. The root mean squared error (RMSE) was then

used to calculate the difference in metres between the observed and predicted hydraulic heads. The RMSE was 0.59.

Validation is the process by which the calibrated model is assessed to check that the model is a valid representation of the hydrogeological system being modelled (Schwartz and Zhang, 2003). In this instance, validation was undertaken using hydraulic head data from nine bores not used during the calibration process. During validation  $V$  was calculated to be 0.87 and the RMSE was 0.42. Based upon  $V$  values during calibration and validation the model could be improved slightly. However, given the simplified nature of the model it will be sufficient for purposes of this research; to identify whether an infiltration basin may be successfully used as a MAR technique to artificially recharge the Makauri Gravel aquifer.

## **5.5 Research Synopsis**

A summary of the methods used in this research, as described in this chapter, is presented in Figure 5.7. It highlights the overarching objective of the research and the data that was collected and analysed to achieve the research objective.

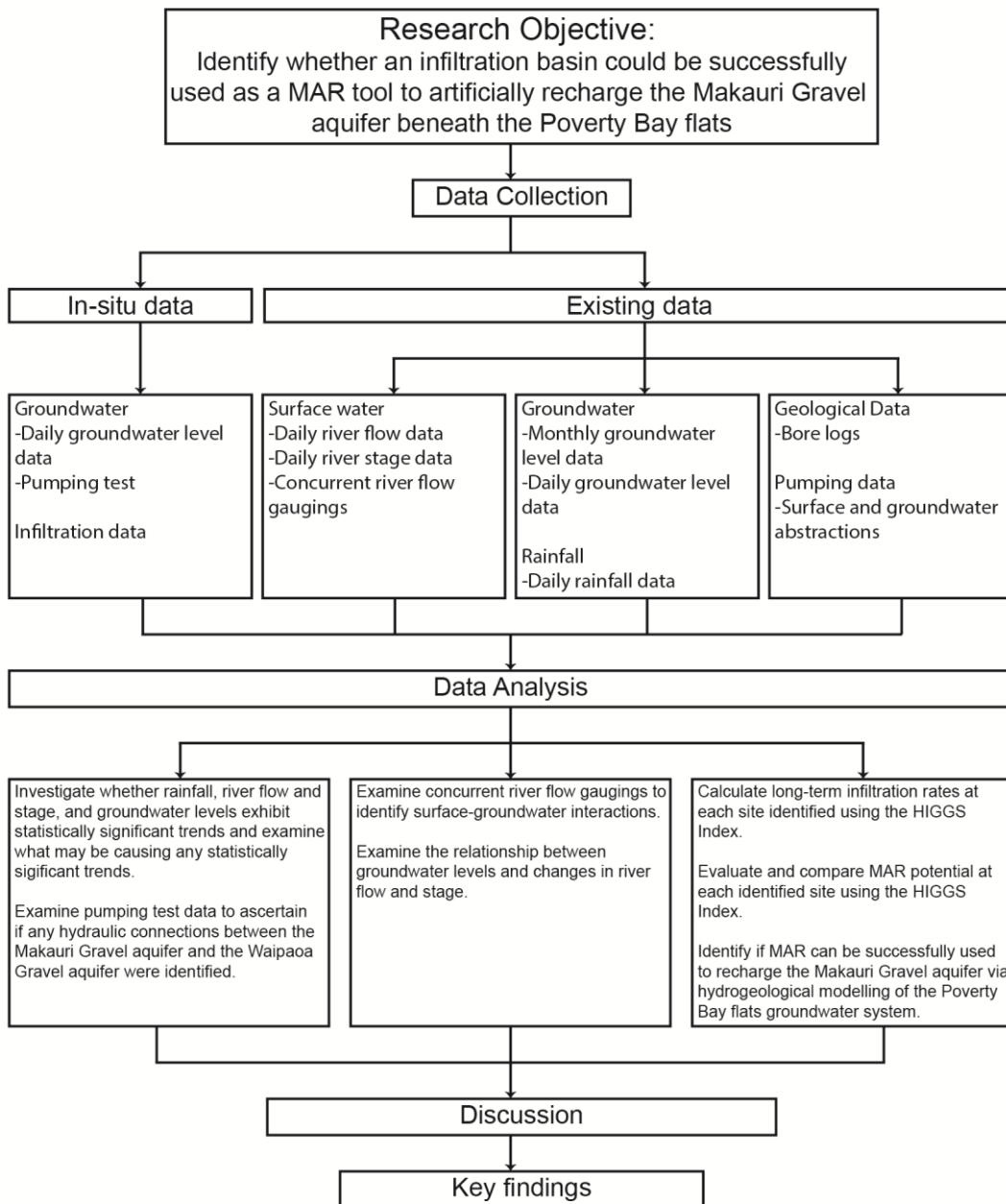


Figure 5.7. Summary of the methods used to identify whether an infiltration basin could be successfully used as a MAR technique to artificially recharge the Makauri Gravel aquifer beneath the Poverty Bay flats.

## Chapter 6 – Results

---

This chapter presents the results of this research over the following seven sections. Firstly, result from trend analyses on rainfall, river and stage, and groundwater within the Poverty Bay flats are presented to identify whether any of these variables exhibited any trends. Section 6.2 describes the changes in groundwater levels as a result of a rainfall event and associated changes in river stage. Section 6.3 presents the results of a pumping test undertaken within the Makauri Gravel aquifer. These results were used to determine if any hydraulic connection exists between the Makauri Gravel aquifer and the overlying Waipaoa Gravel aquifer. Section 6.4 presents an analysis of concurrent Waipaoa River flow gaugings to identify surface-groundwater interactions. Sections 6.5 and 6.6 describe the infiltration characteristics and evaluate the MAR potential at the two sites identified using the HIGGS Index, respectively. Section 6.7 presents the results of the hydrogeological modelling undertaken to ascertain whether an infiltration basin may be used as a MAR technique to artificially recharge the Makauri Gravel aquifer. Section 6.8 concludes with a summary of the key results presented within this chapter.

### 6.1 Trend identification

Identifying trends, if present, can aid our understanding of a particular resource (e.g., groundwater) and help inform management decisions. Therefore, trend analyses were undertaken on rainfall, river flow and stage, and groundwater levels to identify if any trends were exhibited by each variable.

#### 6.1.1 Rainfall

Rainfall on the Poverty Bay flats is recorded at the Gisborne Airport weather station by the National Institute of Water and Atmospheric Research (NIWA) (Figure 5.1). Mean annual rainfall at the Gisborne Airport weather station is 1004.3 mm per year for the period 1982 – 2014 (Table 6.1). The lowest and highest annual rainfall totals during the monitoring period were 638 mm in 1998 and 1324 mm in 2012

(Figure 6.1). A trend test did not identify a statistically significant trend with regards to annual rainfall at the 95% confidence level (Table 6.1).

Table 6.1. Mann-Kendall trend test following Helsel and Hirsch (2002) on annual rainfall at the Gisborne airport weather station.

Location	Period	Mean annual rainfall (mm)	p-value	Trend	Mean Annual Sen slope (m)
Gisborne Airport weather station	1982 – 2014	1004.3	0.245		

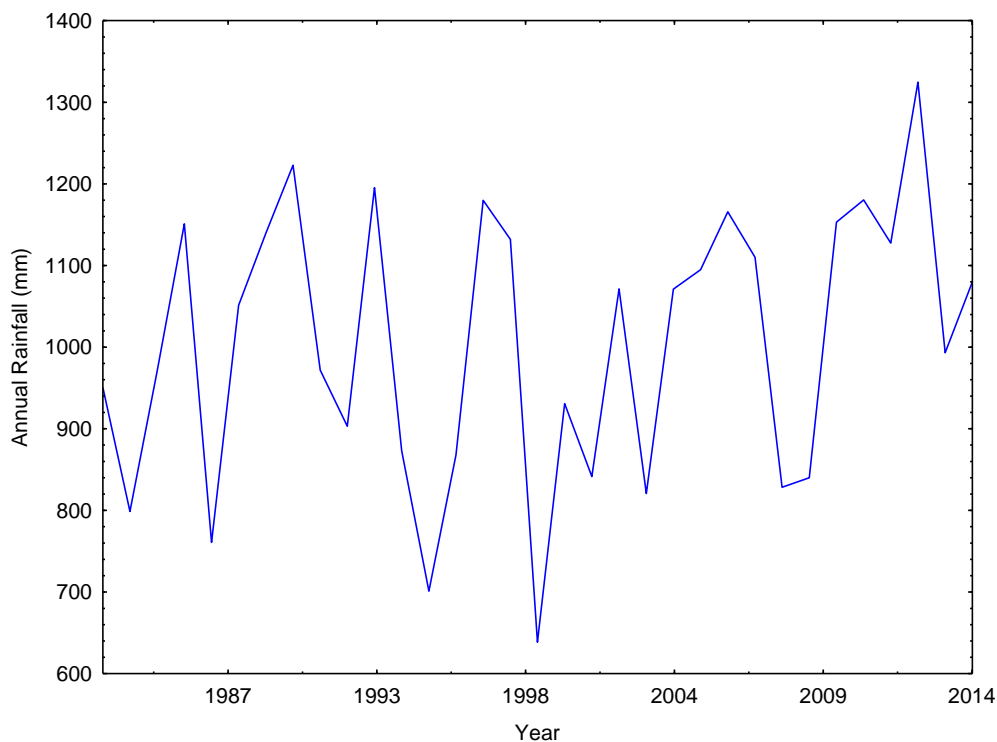


Figure 6.1. Annual rainfall as recorded at the Gisborne Airport weather station between 1982 and 2014.

### 6.1.2 River Flow/Stage

River flow on the Waipaoa River is recorded at three different locations; Kanakanaia Bridge, Kaiteratahi Bridge, and Matawhero Bridge (Figure 5.1). Due to instrumentation error at Kaiteratahi Bridge and tidal effects at Matawhero Bridge a trend analysis was performed only on river flow and stage data at Kanakanaia Bridge. At Kanakanaia Bridge mean monthly river flow is  $35.34 \text{ m}^3 \text{ s}^{-1}$  and mean monthly river stage is 30.283 m above mean sea level (aMSL). Maximum mean monthly river flow was  $372 \text{ m}^3 \text{ s}^{-1}$  in March 1998 and maximum mean monthly river stage was 32.045 m aMSL in September 2013 (Figure 6.2).

Trend analyses on Waipaoa River flow data for the period 1982 – 2014 were undertaken on the following datasets; mean annual, mean monthly, mean seasonal, and mean and minimum summer (i.e., February) data. No statistically significant trends were identified at the 95% confidence level. Mean monthly river stage was also analysed. A trend test indicated that river stage is increasing at a rate of 0.016 m per year (Table 6.2).

Table 6.2. Seasonally adjusted Mann-Kendall trend test following Helsel and Hirsch (2002) on Waipaoa River flow and stage. “Seasons” used in this analysis are: January – March, April – June, July – September, and October – December following White et al. (2012).

Waipaoa River	Period	Mean monthly	p-value	Trend	Mean Annual Sen Slope (m)
River flow	1982 – 2014	35.34 m <sup>3</sup> s <sup>-1</sup>	0.443		
River stage	1982 – 2014	30.28 (msl)	0.000	Increase	0.016

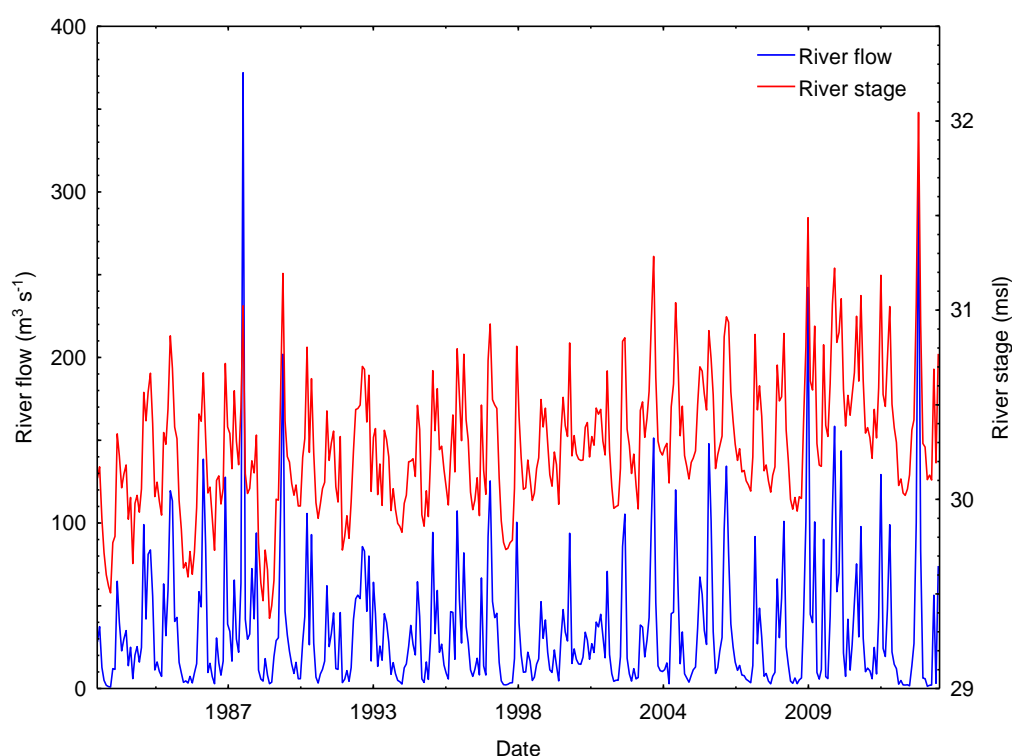


Figure 6.2. Mean monthly Waipaoa River flow and stage at Kanakanaia Bridge between January 1982 and December 2014.

### 6.1.3 Groundwater Levels

Since 1982 groundwater levels have been monitored monthly within the Poverty Bay flats. Initially five bores over four aquifers were monitored. Over time the number of bores monitored monthly has increased to 49

over five aquifers (Figure 6.3). Trend tests were undertaken on all 49 bores to provide updated information as to the current state of groundwater resources within the Poverty Bay flats. Groundwater trends within this section are described by aquifer.

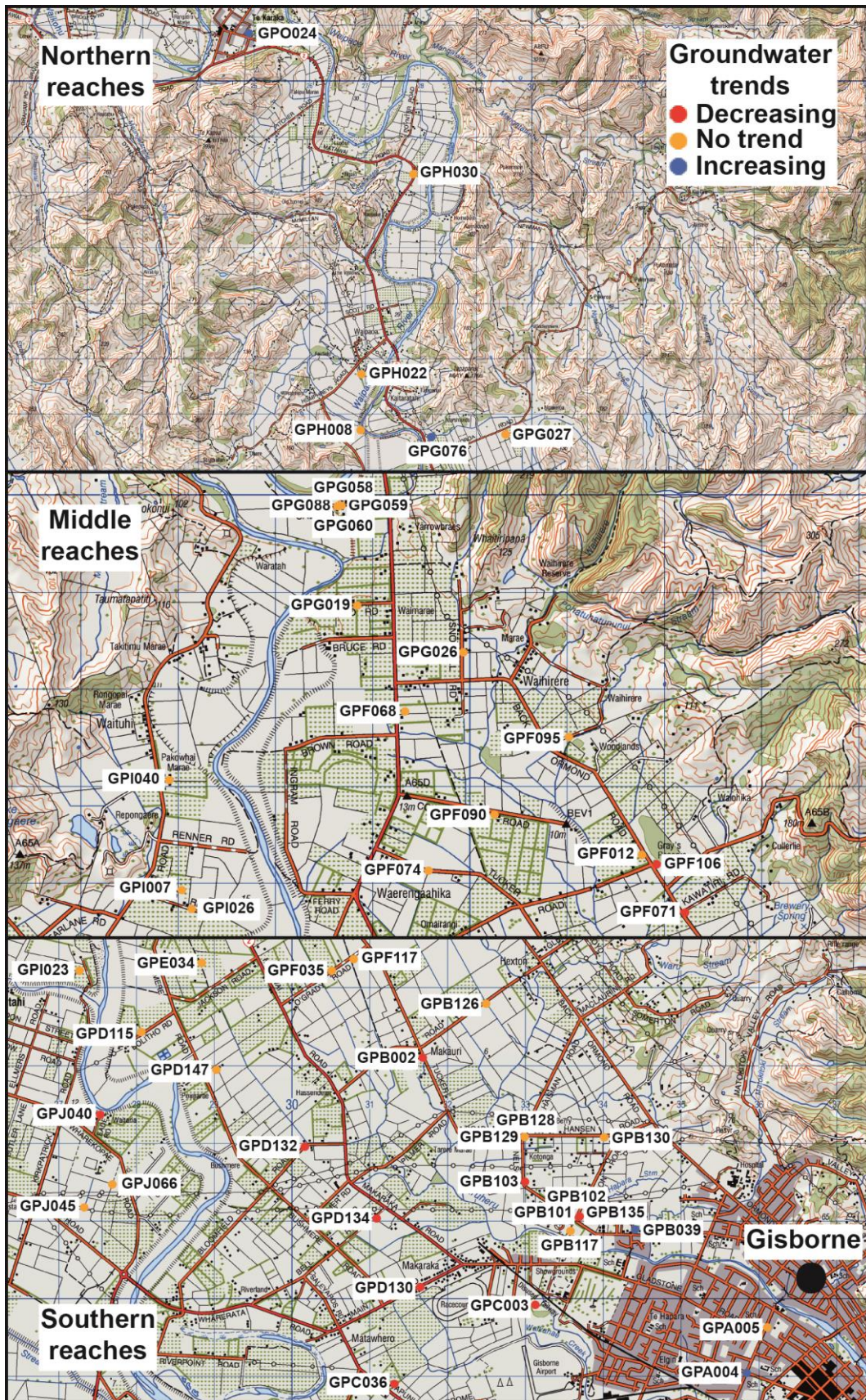


Figure 6.3. Groundwater trends across the 49 bores monitored monthly by the GDC. Identified trends are significant at the 95% confidence level.

## Te Hapara Sands

Median groundwater levels range from 3.34 m aMSL at GPA004 to 4.36 m aMSL at GPA005 (Table 6.3). Since 1983 the seasonal variation in both bores has decreased from 1.5 m to 1 m at GPA004 and from 1.4 m to 0.8 m at GPA005 (Figure 6.4). A trend test indicates that groundwater levels are rising at 0.008 m/yr at GPA004 at a statistically significant rate (Table 6.3). No statistically significant trend was identified at GPA005 (Table 6.3). Trend tests were also undertaken on groundwater data collected during the months of March (summer minimum) and September (winter maximum) to identify what may be inducing changes in groundwater levels. No statistically significant trends were identified during these months for either bore (Appendix F).

Table 6.3. Seasonally adjusted Mann-Kendall trend test following Helsel and Hirsch (2002) on groundwater levels in the Te Hapara Sands. "Seasons" used in this analysis are: January – March, April – June, July – September, and October – December following White et al. (2012).

Bore	Observations	Median groundwater elevation (msl)	p-value	Trend	Median Annual Sen Slope (m)
GPA004	381 observations (Jan 1982 – Sep 2013)	3.34	0.027	Increase	0.008
GPA005	396 observations (Jan 1982 – Dec 2014)	4.37	0.797		

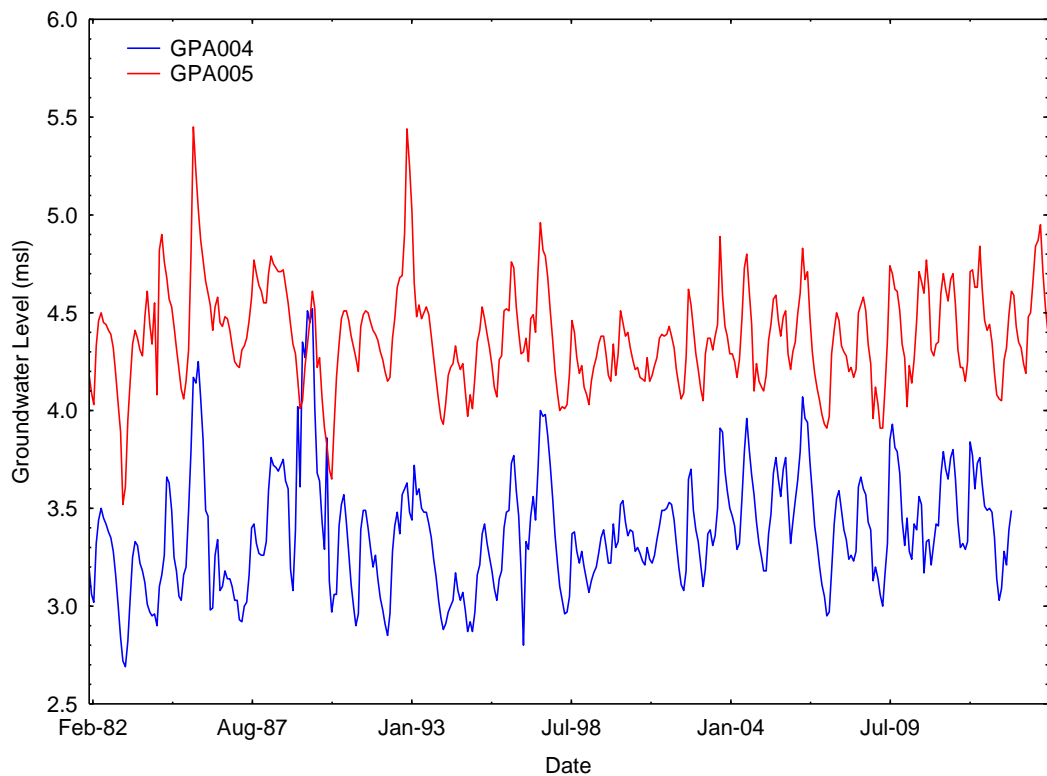


Figure 6.4. Monthly groundwater levels within the Te Hapara Sands from January 1982 to December 2014.

### Shallow Fluvial Deposits

GPI007 is the only bore monitored within the Shallow Fluvial Deposits. The median groundwater level at GPI007 is 6.12 m aMSL (Table 6.4). After a drought groundwater levels take several years to recover (Figure 6.5). The seasonal low at this bore has declined over time (Figure 6.6). No statistically significant trends are present at this bore (Table 6.4; Appendix F).

Table 6.4. Seasonally adjusted Mann-Kendall trend test following Helsel and Hirsch (2002) on groundwater levels in the Te Hapara Sands. “Seasons” used in this analysis are: January – March, April – June, July – September, and October – December following White et al. (2012).

Bore	Observations	Median groundwater elevation (msl)	p-value	Trend	Median Annual Sen slope (m)
GPI007	381 observations (Feb 1995 – Dec 2014)	6.12	0.454		

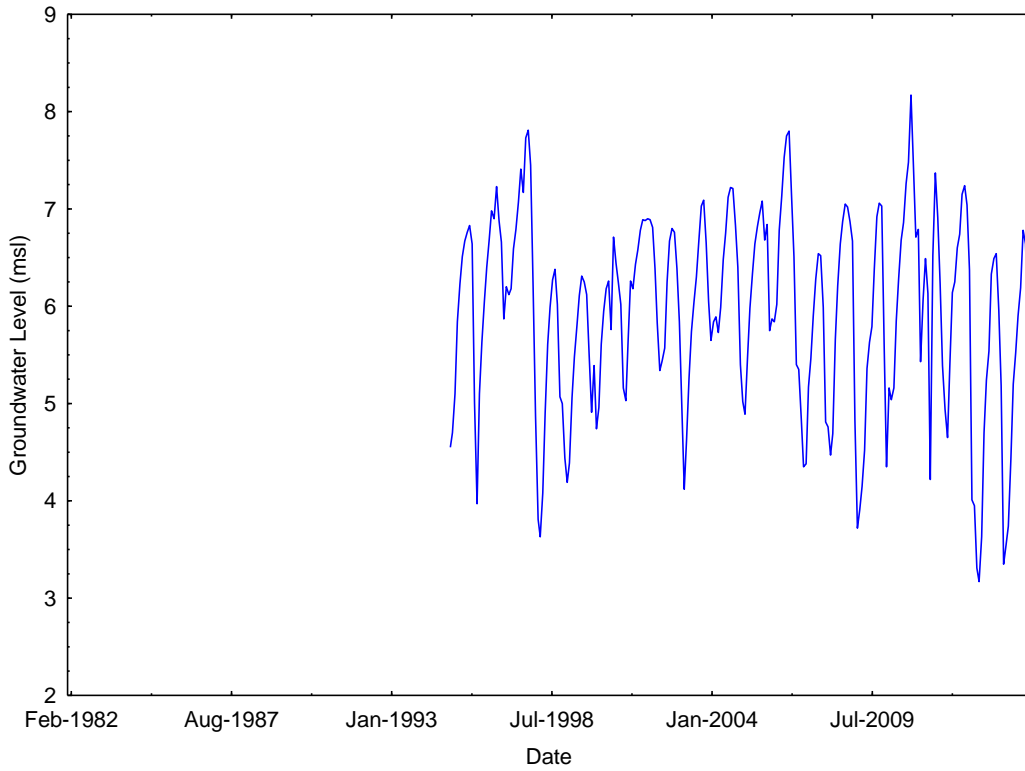


Figure 6.5. Monthly groundwater levels within the Shallow Fluvial Deposits at GPI007 from February 1995 to December 2014.

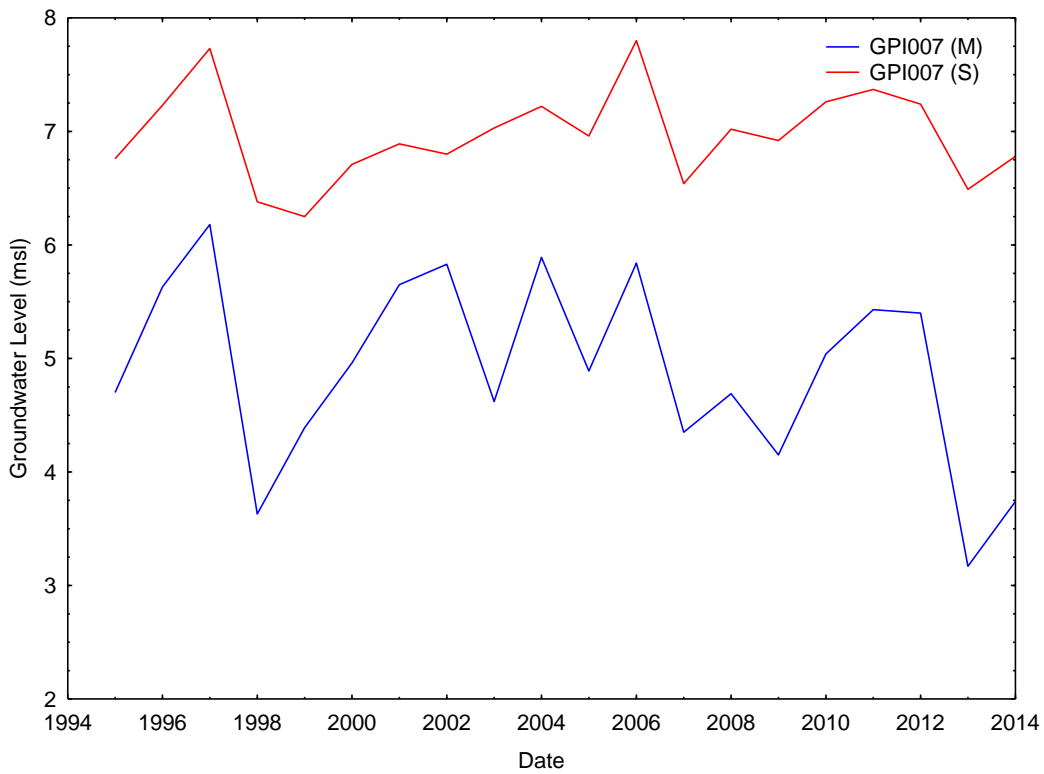


Figure 6.6. Groundwater levels during the months of March (M) and September (S) within the Shallow Fluvial Deposits at GPI007 between 1995 and 2014.

## Waipaoa Gravel aquifer

Median groundwater levels within the Waipaoa Gravel aquifer range from 25.75 m aMSL in the northernmost monitored bore to 9.72 m aMSL in southernmost monitored bore, thus reflecting topography (Table 6.5; Figure 6.3). The spatial gradient of recorded groundwater levels indicate that groundwater flows south southeast towards the coast. Seasonal variation in groundwater levels ranges from 2 m to 5 m, though greater variation is found in the down-gradient bores GPG019 and GPG059 (Figure 6.3; Figure 6.7). After a drought groundwater levels take several years to recover at GPG019, GPG059, and GPG076 (Figure 6.7). No statistically significant trends were present within the monthly data (Table 6.5). GPG076 was the only bore to display a statistically significant trend during March or September; a 0.024 m/yr increase during the month of September (Appendix F).

Table 6.5. Seasonally adjusted Mann-Kendall trend test following Helsel and Hirsch (2002) on groundwater levels in the Waipaoa Gravel aquifer. "Seasons" used in this analysis are: January – March, April – June, July – September, and October – December following White et al. (2012).

Bore	Observations	Median groundwater elevation (msl)	p-value	Trend	Median Annual Sen Slope (m)
GPG019	281 observations (Aug 1991 – Dec 2014)	9.720	0.397		
GPG059	353 observations (Aug 1985 – Dec 2014)	12.880	0.828		
GPG076	240 observations (Jan 1995 – Dec 2014)	14.655	0.187		
GPH022	386 observations (Nov 1982 – Dec 2014)	18.990	0.302		
GPH030	240 observations (Jan 1995 – Dec 2014)	25.750	0.484		

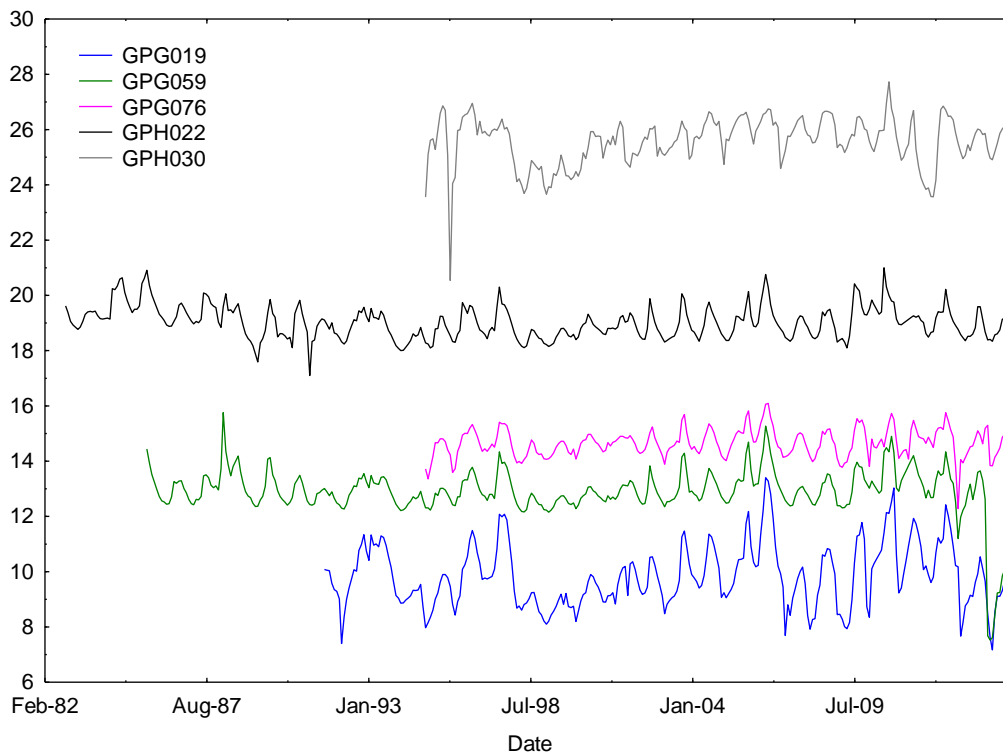


Figure 6.7. Monthly groundwater levels within the Waipaoa Gravel aquifer from November 1982 to December 2014.

### **Makauri Gravel aquifer**

Median groundwater levels within the Makauri Gravel aquifer range from 33.36 m aMSL in the northern reaches of the Poverty Bay flats to 4.94 m aMSL in the southern reaches of the Poverty Bay flats, which reflects topography (Table 6.6; Figure 6.3). The spatial gradient of recorded groundwater levels indicate that groundwater flow south southeast towards the coast, though there is some localised variation. For example, GPF095 and GPI040 are located on either side of the Poverty Bay flats and exhibit high groundwater levels relative to nearby up-gradient bores.

Seasonal variation in groundwater levels is greatest in the middle reaches of the Makauri Gravel aquifer and decreases towards the northern and southern reaches of the aquifer. Furthermore, in some bores the seasonal variation has increased over time and this trend is present throughout the aquifer (Figure 6.8). For example, the seasonal variation at GPB002 has increased from approximately 1 m to 6 m between 1982 and 2009. Like the Shallow Fluvial Deposits and Waipaoa Gravel aquifer, groundwater levels in the Makauri Gravel aquifer take several years to recover from a

drought. Most bores within the Makauri Gravel aquifer show declines in seasonal lows over time (Figure 6.9). The exceptions are GPH008, GPG077, and GPO024. These bores are located in the north reaches of the Poverty Bay flats (Figure 6.3).

Nine of the 29 bores monitored within the Makauri Gravel aquifer exhibited statistically significant trends. GPG077 and GPO024 showed increases of 0.017 and 0.020 m/yr (Table 6.6). As previously mentioned these two bores are located in the north reaches of the Poverty Bay flats (Figure 6.3). GPG077 and GPO024 also exhibit statistically significant increases during the month September but not March (Table 6.7; Table 6.8). The remaining seven bores that exhibit statistically significant trends all show declines in groundwater levels ranging from -0.024 to -0.114 m/yr (Table 6.6). These declines are primarily seen in the southern reaches of the Makauri Gravel aquifer (Figure 6.3).

Of the seven bores that exhibited statistically declines, two exhibited statistically significant decreases during both March (-0.065 to -0.138 m/yr) and September (-0.031 to -0.076 m/yr), and two exhibited statistically significant decreases during March alone (-0.041 to -0.046) (Table 6.7; Table 6.8). Four of the 20 bores that did not exhibit statistically significant trends showed declines during March (-0.025 to -0.156 m/yr) and a further two bores exhibited statistically significant declines during September (-0.038 to -0.044 m/yr) (Table 6.7; Table 6.8).

Overall, results from the trend analyses show that groundwater levels within the Makauri Gravel aquifer are declining.

Table 6.6. Seasonally adjusted Mann-Kendall trend test following Helsel and Hirsch (2002) on groundwater levels in the Makauri Gravel aquifer. “Seasons” used in this analysis are: January – March, April – June, July – September, and October – December following White et al. (2012).

<b>Bore</b>	<b>Observations</b>	<b>Median groundwater elevation (msl)</b>	<b>p-value</b>	<b>Trend</b>	<b>Median Annual Sen slope (m)</b>
GPB002	322 observations (May 1982 – Feb 2009)	6.395	0.000	Decrease	-0.114
GPB101	373 observations (Dec 1983 – Dec 2014)	5.040	0.190		
GPB102	371 observations (Feb 1984 – Dec 2014)	8.840	0.000	Decrease	-0.032
GPB135	281 observations (Aug 1991 – Dec 2014)	4.940	0.020	Decrease	-0.024
GPD115	240 observations (Jan 1995 – Dec 2014)	5.595	0.415		
GPD130	321 observations (Apr 1988 – Dec 2014)	5.460	0.015	Decrease	-0.029
GPE034	237 observations (Jan 1995 – Dec 2014)	5.880	0.278		
GPF012	239 observations (Jan 1995 – Dec 2014)	6.190	0.224		
GPF035	284 observations (Jul 1988 – Dec 2014)	6.010	0.071		
GPF068	232 observations (Jan 1995 – Dec 2014)	6.570	0.344		
GPF071	281 observations (Aug 1991 – Dec 2014)	6.220	0.050	Decrease	-0.037
GPF074	254 observations (Nov 1993 – Dec 2014)	5.480	0.082		
GPF090	239 observations (Feb 1995 – Dec 2014)	6.120	0.639		
GPF095	281 observations (Aug 1991 – Dec 2014)	12.880	0.332		
GPF106	318 observations (Jul 1988 – Dec 2014)	6.245	0.014	Decrease	-0.037
GPF117	240 observations (Nov 1993 – Dec 2014)	6.390	0.268		
GPG026	240 observations (Jan 1995 – Dec 2014)	7.010	0.144		
GPG058	353 observations (Aug 1985 – Dec 2014)	10.400	0.386		
GPG060	353 observations (Aug 1985 – Dec 2014)	10.130	0.061		
GPG077	309 observations (Apr 1989 – Dec 2014)	16.870	0.000	Increase	0.017
GPG088	257 observations (Aug 1993 – Dec 2014)	9.030	0.508		
GPH008	362 observations (Nov 1984 – Dec 2014)	17.380	0.063		
GPI026	362 observations (Aug 1986 – Dec 2014)	6.620	0.361		
GPI032	224 observations (Feb 1995 – Sep 2013)	6.160	0.991		
GPI040	300 observations (Jan 1990 – Dec 2014)	11.660	0.114		
GPJ040	389 observations (Aug 1982 – Dec 2014)	6.400	0.000	Decrease	-0.044
GPJ045	249 observations (Apr 1994 – Dec 2014)	5.670	0.280		
GPJ066	281 observations (Aug 1991 – Dec 2014)	5.610	0.115		
GPO024	240 observations (Jan 1995 – Dec 2014)	33.355	0.030	Increase	0.020

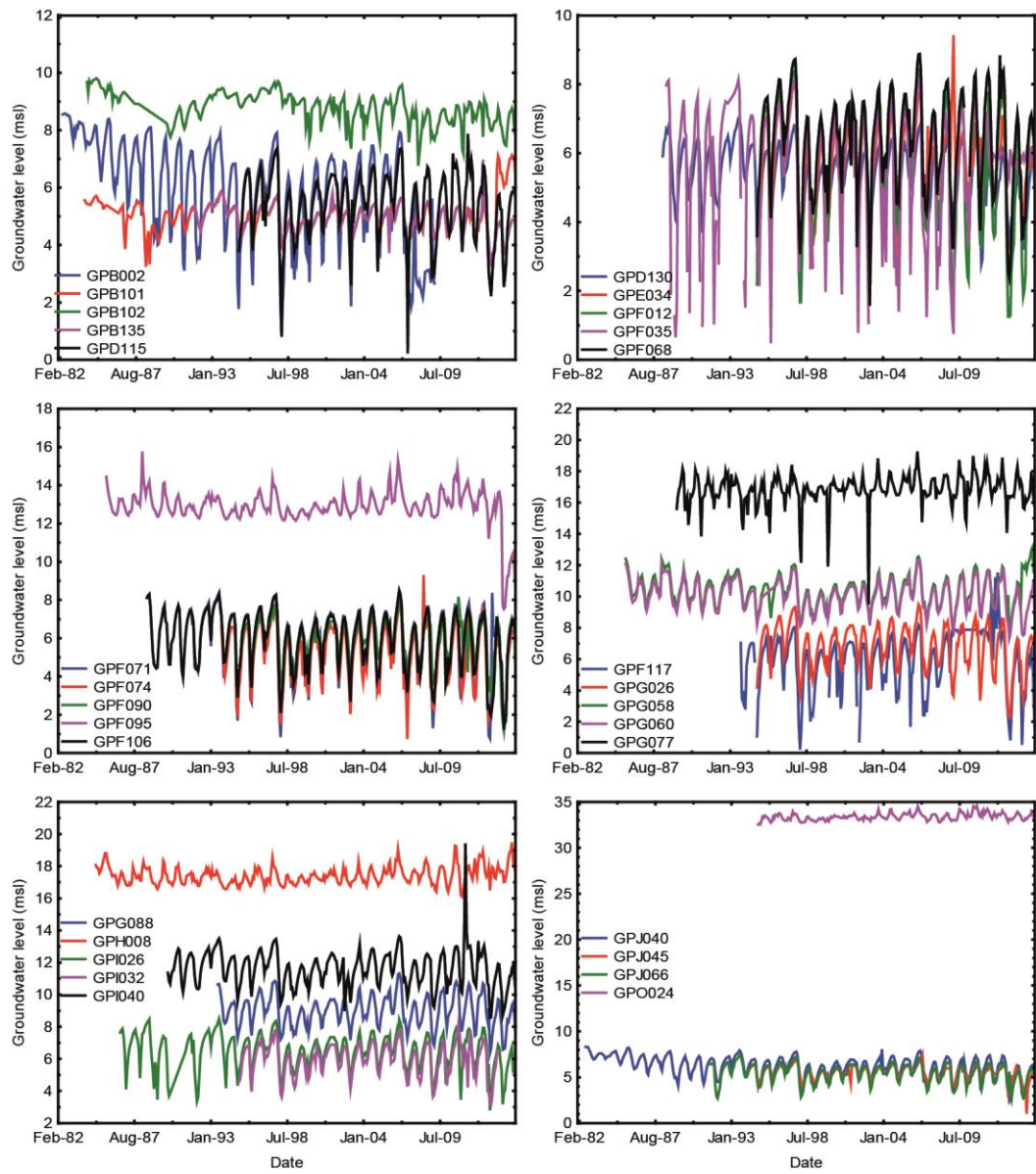


Figure 6.8. Monthly groundwater levels within the Makauri Gravel aquifer from May 1982 to December 2014.

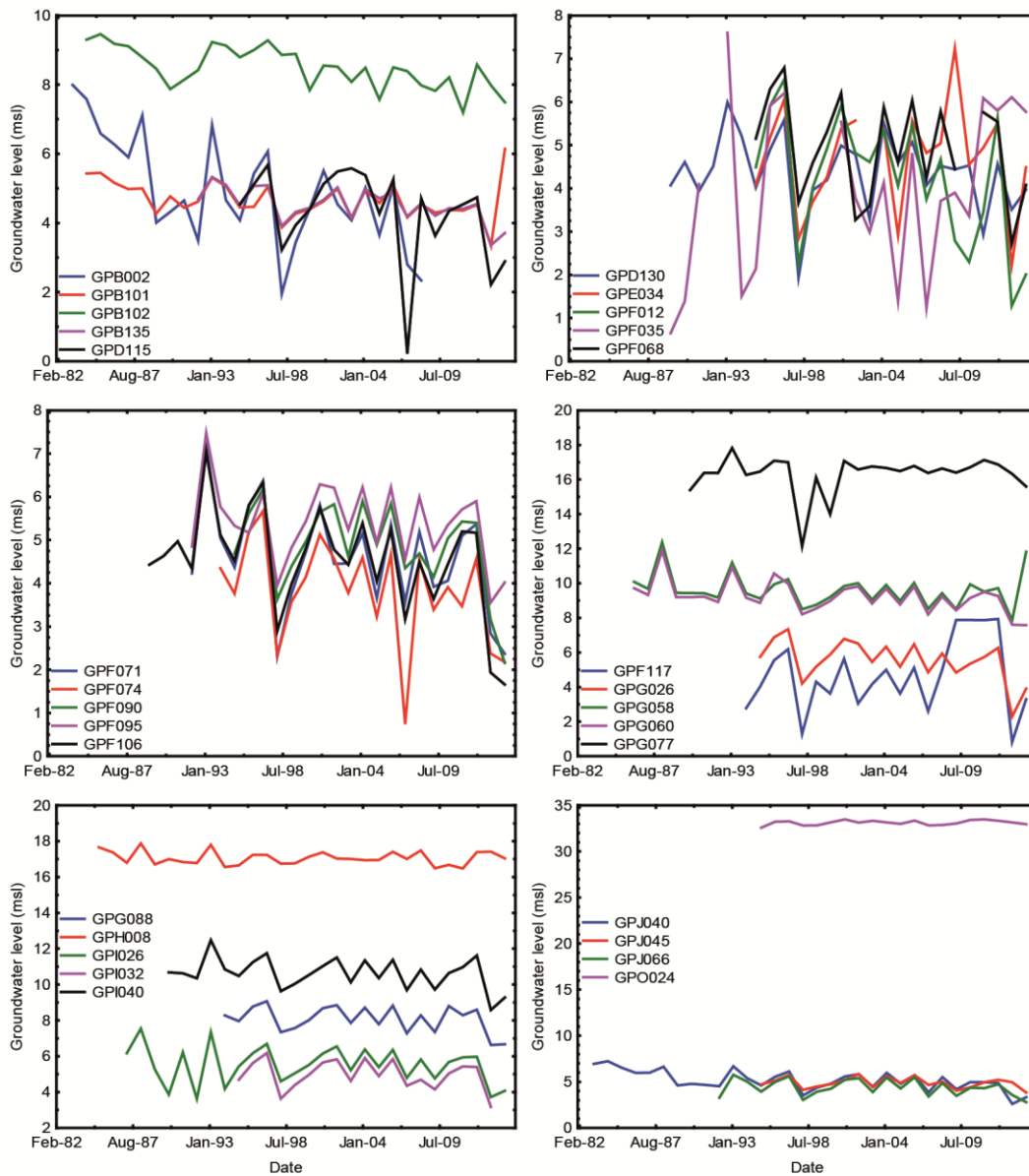


Figure 6.9. Groundwater levels during the months of March in the Makauri Gravel aquifer from 1983 to 2014.

Table 6.7. Mann-Kendall trend test following Helsel and Hirsch (2002) on groundwater levels in the Makauri Gravel aquifer during the month of March.

<b>Bore</b>	<b>Observations</b>	<b>p-value</b>	<b>Trend</b>	<b>Median Annual Sen slope (m)</b>
GPB002	26 observations (1983 – 2008)	0.002	Decrease	-0.138
GPB101	31 observations (1984 – 2014)	0.020	Decrease	-0.025
GPB102	31 observations (1984 – 2014)	0.000	Decrease	-0.046
GPB135	23 observations (1992 – 2014)	0.006	Decrease	-0.041
GPD115	20 observations (1995 – 2014)	0.153		
GPD130	26 observations (1989 – 2014)	0.321		
GPE034	19 observations (1995 – 2014)	0.944		
GPF012	20 observations (1995 – 2014)	0.027	Decrease	-0.156
GPF035	22 observations (1989 – 2014)	0.159		
GPF068	19 observations (1995 – 2014)	0.208		
GPF071	23 observations (1992 – 2014)	0.186		
GPF074	21 observations (1994 – 2014)	0.085		
GPF090	20 observations (1995 – 2014)	0.243		
GPF095	23 observations (1992 – 2014)	0.303		
GPF106	26 observations (1989 – 2014)	0.118		
GPF117	21 observations (1994 – 2014)	0.319		
GPG026	20 observations (1995 – 2014)	0.044	Decrease	-0.087
GPG058	29 observations (1986 – 2014)	0.215		
GPG060	29 observations (1986 – 2014)	0.018	Decrease	-0.046
GPG077	25 observations (1990 – 2014)	0.607		
GPG088	21 observations (1994 – 2014)	0.277		
GPH008	30 observations (1985 – 2014)	0.789		
GPI026	28 observations (1987 – 2014)	0.363		
GPI032	19 observations (1995 – 2013)	0.552		
GPI040	25 observations (1990 – 2014)	0.338		
GPJ040	32 observations (1983 – 2014)	0.002	Decrease	-0.065
GPJ045	20 observations (1995 – 2014)	0.538		
GPJ066	23 observations (1992 – 2014)	0.291		
GPO024	20 observations (1995 – 2014)	0.345		

Table 6.8. Mann-Kendall trend test following Helsel and Hirsch (2002) on groundwater levels in the Makauri Gravel aquifer during the month of September.

Bore	Observations	p-value	Trend	Median Annual Sen slope (m)
GPB002	27 observations (1982 – 2008)	0.000	Decrease	-0.076
GPB101	31 observations (1984 – 2014)	0.671		
GPB102	31 observations (1984 – 2014)	0.125		
GPB135	24 observations (1991 – 2014)	0.297		
GPD115	20 observations (1995 – 2014)	0.795		
GPD130	27 observations (1988 – 2014)	0.079		
GPE034	20 observations (1995 – 2014)	0.030	Decrease	-0.044
GPF012	20 observations (1995 – 2014)	0.603		
GPF035	27 observations (1988 – 2014)	0.037	Decrease	-0.038
GPF068	20 observations (1995 – 2014)	0.496		
GPF071	24 observations (1991 – 2014)	0.728		
GPF074	21 observations (1994 – 2014)	0.487		
GPF090	20 observations (1995 – 2014)	0.144		
GPF095	24 observations (1991 – 2014)	1.000		
GPF106	27 observations (1988 – 2014)	0.067		
GPF117	21 observations (1994 – 2014)	0.432		
GPG026	20 observations (1995 – 2014)	1.000		
GPG058	30 observations (1985 – 2014)	0.580		
GPG060	30 observations (1985 – 2014)	0.789		
GPG077	26 observations (1989 – 2014)	0.006	Increase	0.037
GPG088	22 observations (1993 – 2014)	0.382		
GPH008	30 observations (1985 – 2014)	0.045	Increase	0.021
GPI026	29 observations (1986 – 2014)	0.560		
GPI032	19 observations (1995 – 2013)	0.248		
GPI040	25 observations (1990 – 2014)	0.708		
GPJ040	33 observations (1982 – 2014)	0.004	Decrease	-0.031
GPJ045	21 observations (1994 – 2014)	0.506		
GPJ066	24 observations (1991 – 2014)	0.345		
GPO024	20 observations (1995 – 2014)	0.000	Increase	0.037

### Matokitoki Gravel aquifer

Median groundwater levels within the Matokitoki Gravel aquifer range from 10.51 m aMSL to 4.58 m aMSL ( Table 6.9). Though a significant amount of spatial variation in groundwater levels exists, the spatial gradient indicates that groundwater flows south towards the coast in this aquifer.

The seasonal variation in groundwater levels within the Matokitoki Gravel aquifer is variable ranging from approximately 1 m to 6 m, except for GPB103 which exhibited a seasonal variation of 9.5 m (Figure 6.10). Groundwater levels within the Matokitoki Gravel aquifer take several years to recover from a drought (Figure 6.10). All bores, excluding GPB039, show declines in seasonal lows over time (Figure 6.11).

Seven of the 12 bores monitored within the Matokitoki Gravel aquifer exhibited statistically significant groundwater trends. Groundwater level at GPB039, located in the south-eastern corner of this aquifer, are increasing at a rate of 0.029 m/yr ( Table 6.9). During September groundwater levels are also increasing at a statistically significant rate at GPB039, yet no trend is present during the month of March (Table 6.10; Table 6.11).

Six bores exhibit statistically significant declines in groundwater levels ranging from -0.028 to -0.066 m per year ( Table 6.9). Of these six bores, only GPC003 and GPC036 display statistically significant declines in groundwater levels during the months of March and September (Table 6.10; Table 6.11). GPB103 and GPB128 display declines during March and GPB132 and GPD134 display declines during September (Table 6.10; Table 6.11). Of the five bores that did not exhibit a trends on monthly data, two displayed a statistically significant declines during the month of March (-0.025 to -0.050 m per year), while none of these five bores displayed any trends during September (Table 6.10; Table 6.11). Overall, the trend tests. indicates that groundwater levels are declining in this aquifer.

Table 6.9. Seasonally adjusted Mann-Kendall trend test following Helsel and Hirsch (20022) on groundwater levels in the Matokitoki Gravel aquifer. “Seasons” used in this analysis are: January – March, April – June, July – September, and October – December following White et al. (2012).

Bore	Observations	Median groundwater elevation (msl)	p-value	Trend	Median Annual Sen slope (m)
GPB039	310 observations (Jul 1988 – Dec 2014)	7.300	0.009	Increase	0.029
GPB103	342 observations (Jun 1986 – Dec 2014)	8.870	0.041	Decrease	-0.032
GPB117	373 observations (Dec 1983 – Dec 2014)	5.040	0.190		
GPB126	320 observations (May 1988 – Dec 2014)	9.150	0.121		
GPB128	320 observations (May 1988 – Dec 2014)	9.080	0.021	Decrease	-0.028
GPB129	320 observations (May 1988 – Dec 2014)	5.610	0.985		
GPB130	320 observations (Jun 1988 – Dec 2014)	10.510	0.529		
GPC003	396 observations (Jan 1982 – Dec 2014)	4.580	0.000	Decrease	-0.066
GPC036	281 observations (Aug 1991 – Dec 2014)	4.630	0.002	Decrease	-0.032
GPD132	321 observations (Apr 1988 – Dec 2014)	5.350	0.014	Decrease	-0.030
GPD134	317 observations (Apr 1988 – Dec 2014)	5.060	0.002	Decrease	-0.052
GPD147	243 observations (Dec 1992 – Dec 2014)	5.440	0.251		

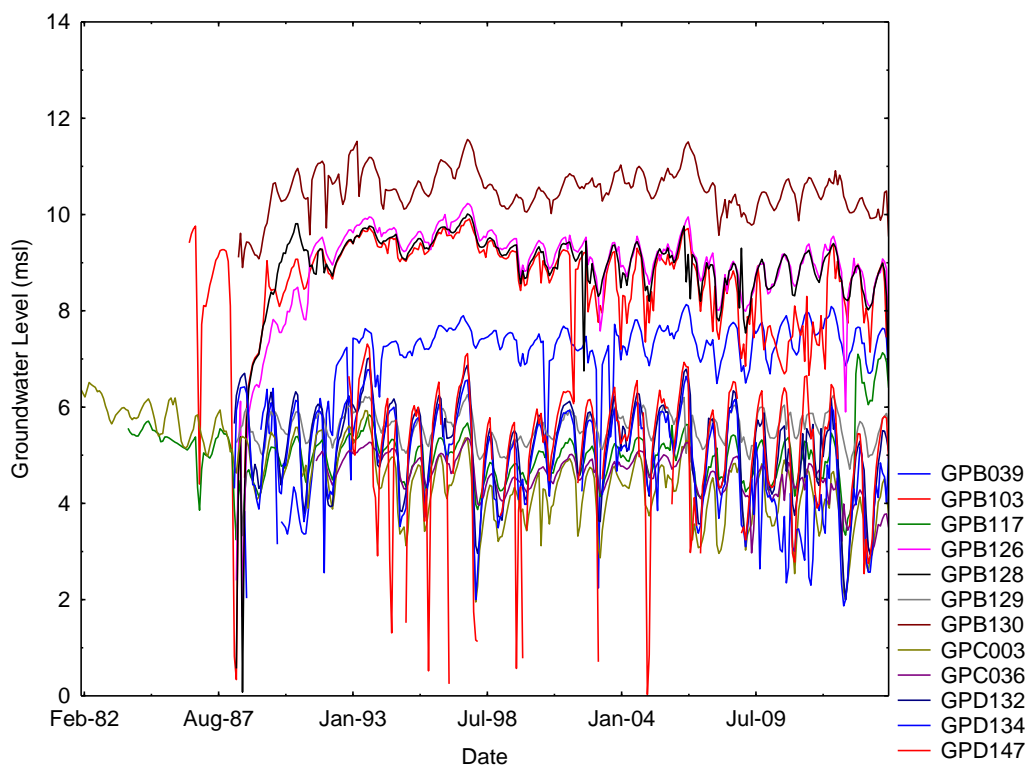


Figure 6.10 Monthly groundwater levels within the Matokitoki Gravel aquifer from January 1982 to December 2014, as monitored by the GDC.

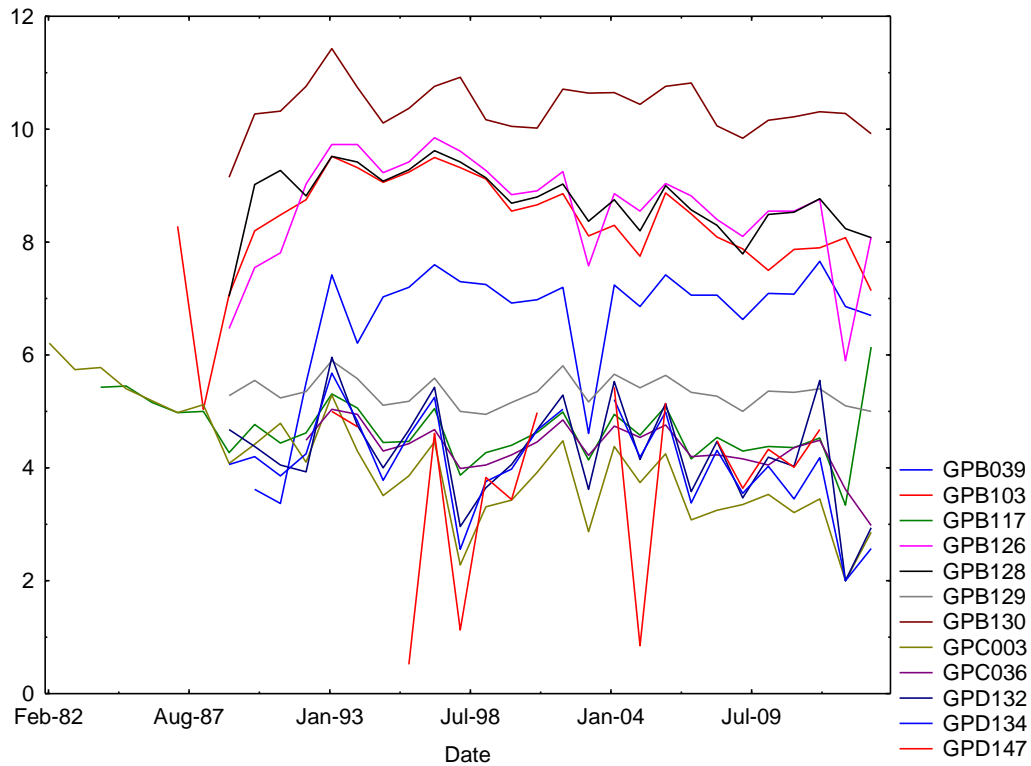


Figure 6.11. Groundwater levels during the months of March in the Matokitoki Gravel aquifer from 1982 to 2014.

Table 6.10. Mann-Kendall trend test following Helsel and Hirsch (2002) on groundwater levels in the Matokitoki Gravel aquifer during the month of March.

Bore	Observations	p-value	Trend	Median Annual Sen slope (m)
GPB039	25 observations (1990 – 2014)	0.469		
GPB103	28 observations (1987 – 2014)	0.040	Decrease	-0.042
GPB117	31 observations (1984 – 2014)	0.020	Decrease	-0.025
GPB126	26 observations (1989 – 2014)	0.047	Decrease	-0.050
GPB128	26 observations (1989 – 2014)	0.002	Decrease	-0.046
GPB129	26 observations (1989 – 2014)	0.389		
GPB130	26 observations (1989 – 2014)	0.320		
GPC003	33 observations (1982 – 2014)	0.000	Decrease	-0.087
GPC036	23 observations (1992 – 2014)	0.025	Decrease	-0.029
GPD132	26 observations (1989 – 2014)	0.193		
GPD134	25 observations (1989 – 2014)	0.088		
GPD147	17 observations (1993 – 2014)	0.773		

Table 6.11. Mann-Kendall trend test following Helsel and Hirsch (2002) on groundwater levels in the Matokitoki Gravel aquifer during the month of September.

Bore	Observations	p-value	Trend	Median Annual Sen slope (m)
GPB039	27 observations (1988 – 2014)	0.000	Increase	0.046
GPB103	29 observations (1986 – 2014)	0.091		
GPB117	31 observations (1984 – 2014)	0.671		
GPB126	27 observations (1988 – 2014)	0.453		
GPB128	27 observations (1988 – 2014)	0.128		
GPB129	27 observations (1988 – 2014)	0.786		
GPB130	27 observations (1988 – 2014)	0.967		
GPC003	33 observations (1982 – 2014)	0.000	Decrease	-0.053
GPC036	24 observations (1991 – 2014)	0.005	Decrease	-0.032
GPD132	27 observations (1988 – 2014)	0.006	Decrease	-0.026
GPD134	27 observations (1988 – 2014)	0.019	Decrease	-0.045
GPD147	22 observations (1993 – 2014)	0.865		

## 6.2 Groundwater Level Changes

Changes in groundwater levels as a result of a rainfall event and associated changes in river stage were characterised by undertaking groundwater level monitoring before, during, and after a rainfall event. Over a 48 hour period beginning at 09:00 am on the 15<sup>th</sup> March through to 09:00 am on the 17<sup>th</sup> March a total of 81.2 mm of rainfall fell at the Gisborne Airport weather station as a result of ex-tropical Cyclone Pam hitting the Gisborne district on the 15<sup>th</sup> March. Waipaoa River flow responded by increasing from 1.556 m<sup>3</sup> s<sup>-1</sup> at 09:00 am on the 15<sup>th</sup> March to 115.07 m<sup>3</sup> s<sup>-1</sup> at 09:00 am on the 17<sup>th</sup> March (Appendix G). River stage rose from 30.158 m aMSL to 31.144 m aMSL over the aforementioned period (Appendix G). Both river flow and river stage then decreased over the following 10 days. At 09:00 am on the 27<sup>th</sup> March Waipaoa River flow was 3.456 m<sup>3</sup> s<sup>-1</sup> and river stage was 30.257 m aMSL (Appendix G). Daily monitoring of groundwater levels between 09:00 am and 11:30 am occurred across 18 bores (Figure 5.4; Figure 5.5) between the 14<sup>th</sup> and 27<sup>th</sup> March to assess the impact that the aforementioned rainfall event and associated changes in river flow and river stage had on groundwater

levels. All groundwater level data was corrected for barometric effects using the methods described in Chapter 5.

### Te Hapara Sands

GPB099 was the only bore monitored within the Te Hapara Sands (Figure 6.12). The barometric efficiency at this bore was 0.23. Groundwater levels rise from 5.636 m aMSL on the 15<sup>th</sup> March to 5.696 m aMSL on the 16<sup>th</sup> March (Figure 6.12). By the 19<sup>th</sup> March groundwater levels declined to pre-event levels (i.e., groundwater levels on the 14<sup>th</sup> March) and then continued to decline beneath pre-event levels throughout the daily monitoring period.

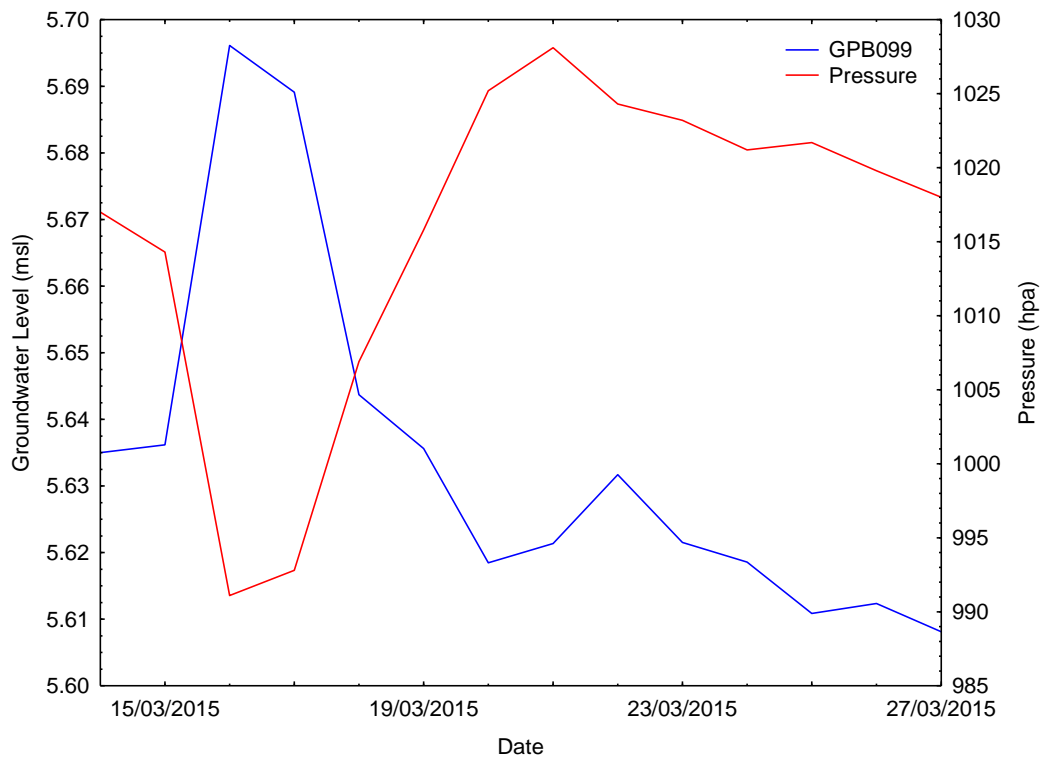


Figure 6.12. Groundwater levels in the Te Hapara Sands (GPB099) and atmospheric pressure from the 14<sup>th</sup> March 2015 to the 27<sup>th</sup> March 2015.

### Shallow Fluvial Deposits

Groundwater levels rise from 13.750 m aMSL on the 15<sup>th</sup> March to 13.813 m aMSL on the 17<sup>th</sup> March at GPG051. While fluctuating slightly throughout the rest of the monitoring period, groundwater levels remain around 13.820 m aMSL (Figure 6.13). At GPG046, groundwater levels increase from 18.460 m aMSL on the 16<sup>th</sup> March to 18.542 m aMSL on the 18<sup>th</sup> March. Whilst groundwater levels decline to baseline levels by the end

of the monitoring period at GPH046, small increases occur on the 20<sup>th</sup> and 23<sup>rd</sup> despite no rainfall occurring and declines in river stage (Figure 6.13). Despite large differences in the change in groundwater levels, GPH005 (increases 0.463 m between the 16<sup>th</sup> and 17<sup>th</sup> March) and GPH047 (increases by 0.070 m between the 16<sup>th</sup> and 17<sup>th</sup> March) respond to the rainfall event/changes in river stage in a similar manner. Groundwater levels peak on the 18<sup>th</sup> March (at 16.106 m aMSL at GPH005 and 10.344 m aMSL at GPH047) a day after river stage peaks and then declined throughout the monitoring period. GPH005 declined to baseline levels whereas GPH047 declined below baseline levels (Figure 6.13). Barometric efficiencies in this aquifer range from 0.12 to 0.23.

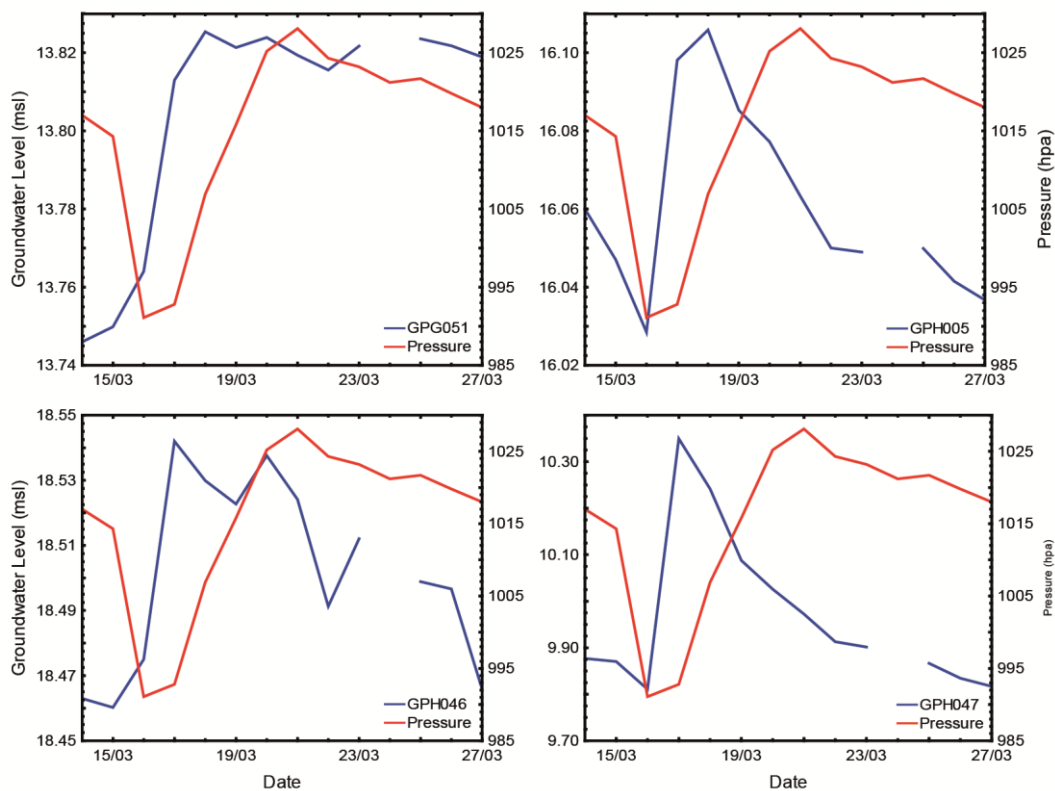


Figure 6.13. Groundwater levels in the Shallow Fluvial Deposits (GPG051, GPH005, GPH046, and GPH047) and atmospheric pressure from the 14<sup>th</sup> March 2015 to the 27<sup>th</sup> March 2015.

### Waipaoa Gravel aquifer

Groundwater levels at GPE032, GPG013, GPG059, and GPH022 respond to the rainfall event and changes in river stage in a similar manner (Figure 6.14). Groundwater levels at all four bores peak between the 17<sup>th</sup> and 20<sup>th</sup> March and the decline throughout the rest of the monitoring period. GPH022 displays the biggest increase in groundwater levels at

0.232 m followed by GPG059 at 0.175 m, whereas GPG013 and GPE032 display small increases of 0.053 m and 0.049 m, respectively (Figure 6.14). Therefore, a bores response to changes in rainfall and river stage appears to be related to its location, as greater changes in groundwater levels are seen in the northern reaches of this aquifer. Barometric efficiencies in these four bores range from 0.07 to 0.42. GPI023 differs from the aforementioned bores in that it is regularly pumped. The increase in groundwater levels between the 14<sup>th</sup> and 15<sup>th</sup> March was due to pumping occurring at GPI023 during monitoring on the 14<sup>th</sup> March. As such, GPI023 did not exhibit any increases as a result of the rainfall event/changes in river stage. Although, it is possible that pumping obscured any effects that otherwise may have been seen.

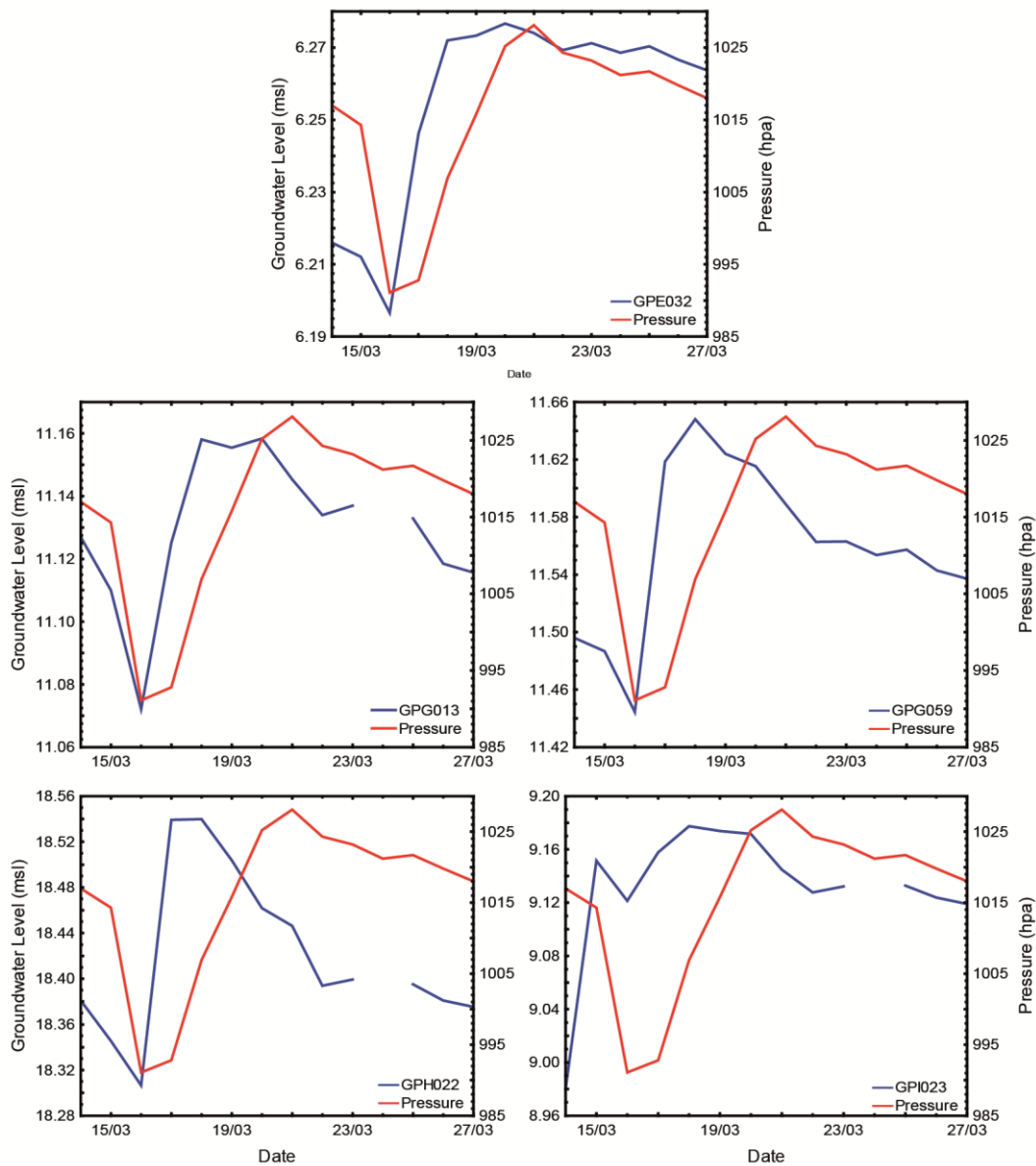


Figure 6.14. Groundwater levels in the Waipaoa Gravel aquifer (GPE032, GPG013, GPG059, GPH022, and GPI023) and atmospheric pressure from the 14<sup>th</sup> March 2015 to the 27<sup>th</sup> March 2015.

### Makauri Gravel aquifer

Bores monitored within the Makauri Gravel aquifer can be broken three groups. The first group are bores located in the northern section of the aquifer (GPH008 and GPH044) (Figure 5.4; Figure 5.5). Groundwater levels peak on the 17<sup>th</sup> March at GPH008 at 17.791 m aMSL, an increase of 0.378 m compared with 16<sup>th</sup> March (Figure 6.15). Groundwater levels peak on the 21<sup>st</sup> March at GPH044 at 14.750 m aMSL and exhibited an increase of 0.253 m between the 16<sup>th</sup> and 17<sup>th</sup> March (Figure 6.15). At both bores groundwater levels decline after peaking but do not return to baseline levels. The second group of bores are located in the middle of the

Makauri Gravel aquifer (GPE002, GPE041, GPG060, and GPG088) (Figure 5.4; Figure 5.5). These four bores all display their greatest daily increases in groundwater levels between the 16<sup>th</sup> and 17<sup>th</sup> March (between 0.206 and 0.322 m) (Figure 6.15). Groundwater levels at all four of these bores continue to increase throughout the monitoring period. The remaining two bores (GPB101 and GPB102) are located in the southern section of this aquifer (Figure 5.4; Figure 5.5). Groundwater levels at GPB101 and GPB102 display the smallest increases in groundwater levels within the Makauri Gravel aquifer between the 16<sup>th</sup> and 17<sup>th</sup> March at 0.154 and 0.129 m, respectively. Groundwater levels at GPB101 and GPB102 peak on the 18<sup>th</sup> March at 3.840 m aMSL and 8.150 m aMSL, respectively (Figure 6.15). Unlike the four monitored bores located in the middle section of the Makauri Gravel aquifer, GPB101 and GPB102 display declines in groundwater levels after peaking. GPB101 does not decline to baseline levels, whereas GPB102 declines below baseline levels (Figure 6.15).

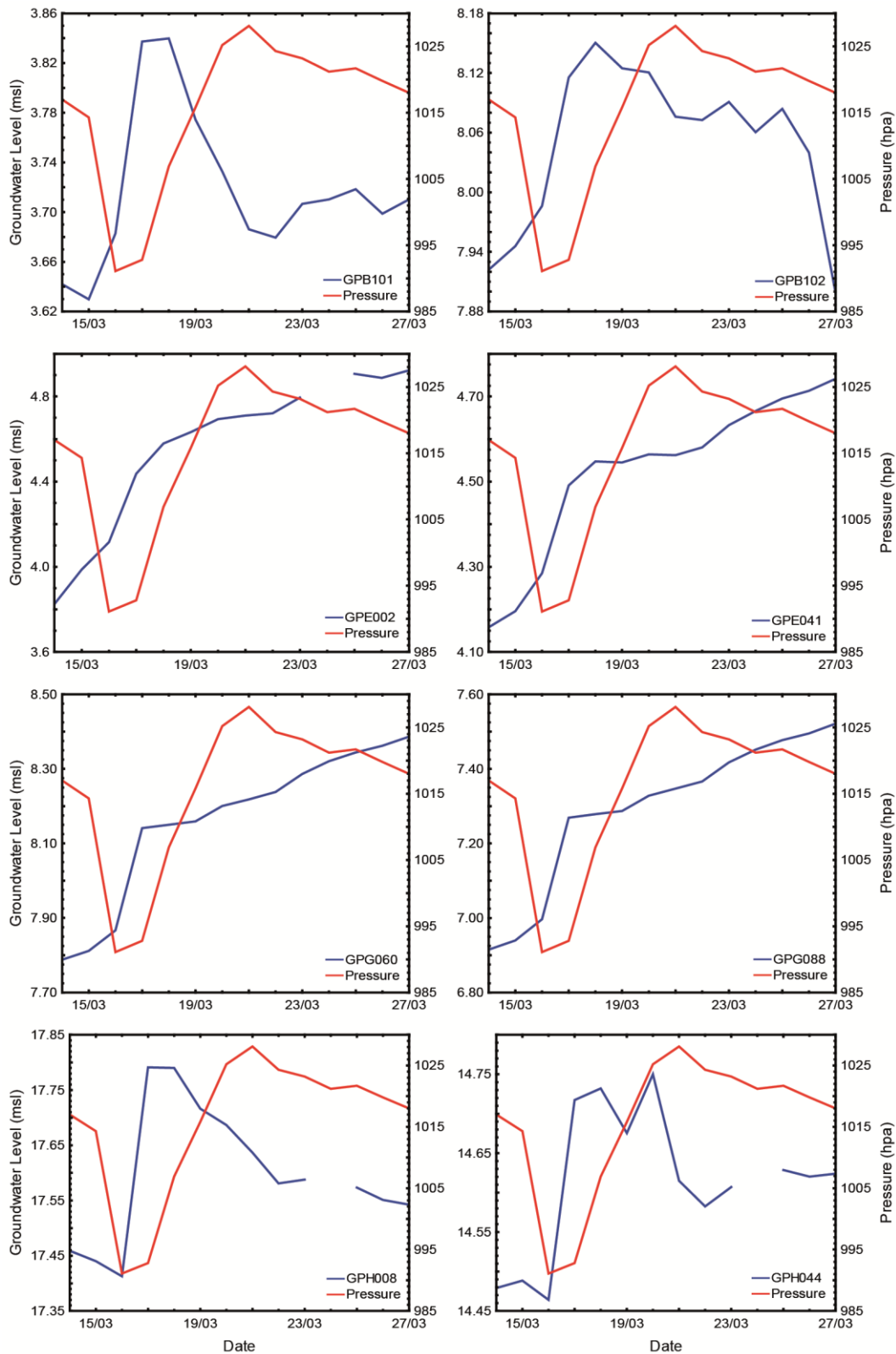


Figure 6.15. Groundwater levels in the Makauri Gravel aquifer (GPB101, GPB102, GPE002, GPE041, GPG060, GPG088, GPH008, and GPH044) and atmospheric pressure from the 14<sup>th</sup> March 2015 to the 27<sup>th</sup> March 2015.

## 6.3 Pumping Test

As mentioned in Chapter 5, a pumping test was undertaken in close proximity to Caesar Road to see if a hydraulic connection existed between the Makauri Gravel aquifer and the overlying Waipaoa Gravel aquifer. Pumping commenced at 8:30 am on the 16<sup>th</sup> June 2015 at GPG036 and lasted for 24 hours at a rate of 100 m<sup>3</sup>/day (which was a lower rate than anticipated based upon conversations with the bore owner). Two bores, GPG064 and GPG062, respectively located 140 and 230 m from GPG036 were monitored throughout the pumping test and for 24 hours following the cessation of pumping (Figure 5.6). Barometric effects were accounted for using the methods described in Appendix B. At both GPG064 and GPG062 the barometric efficiency was calculated to be 0.18.

### **GPG064**

At the commencement of the pumping test groundwater levels at GPG064 were 11.534 m aMSL (Figure 6.16A). After one hour of pumping, groundwater levels begin to increase and continue to do so for three hours, when groundwater levels peak at 11.543 m aMSL (Figure 6.16A). After six hours of pumping groundwater levels begin to decline. After 24 hours of pumping groundwater levels have returned to 11.534 m aMSL (Figure 6.16A). For the first 0.75 hours after the cessation of pumping groundwater levels remain constant at 11.534 m aMSL (Figure 6.16B). From 0.75 to 6.25 hours after pumping stopped groundwater levels increase to 11.541 m aMSL (Figure 6.16B). 24 hours after pumping groundwater levels were at 11.534 m aMSL (Figure 6.16B).

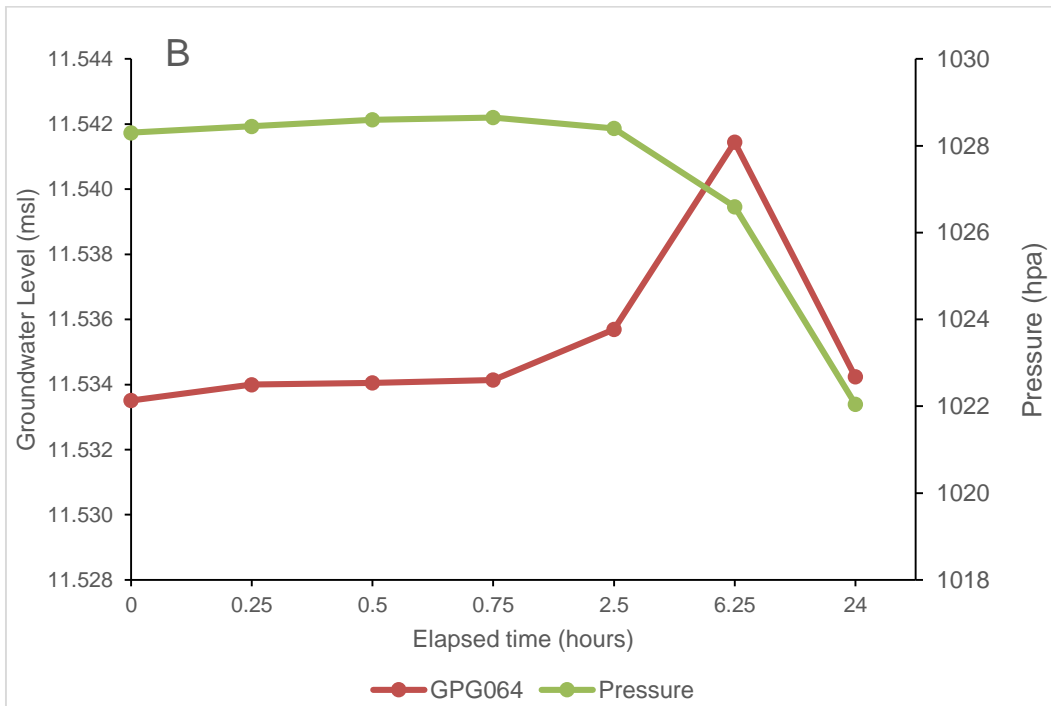
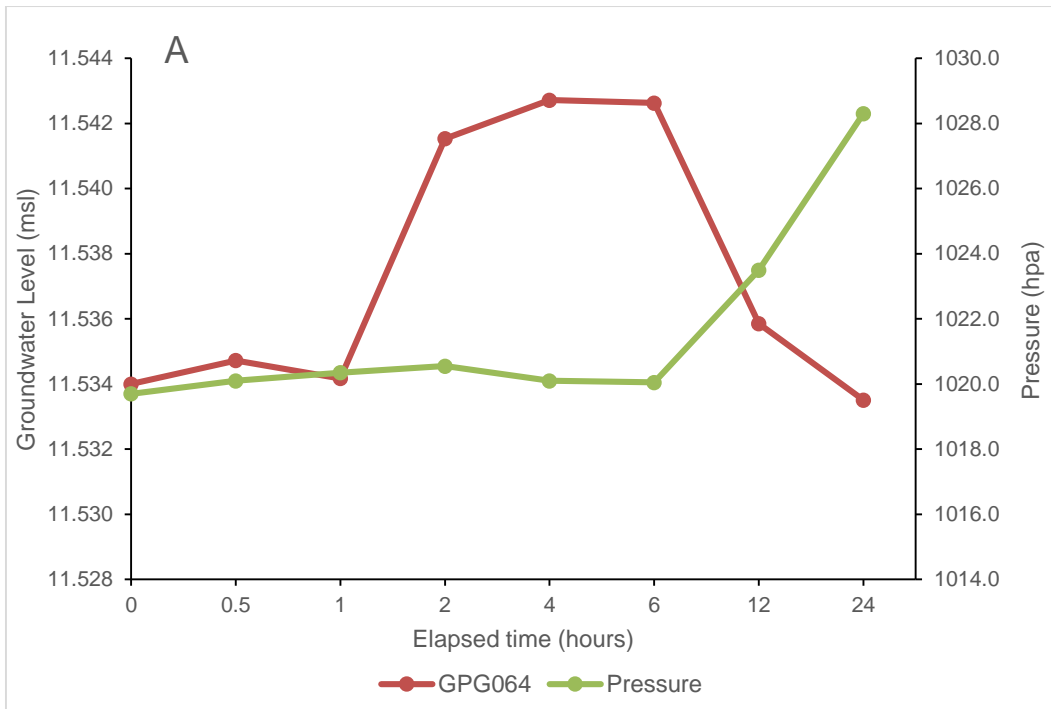


Figure 6.16. (A) Groundwater levels (adjusted for barometric effects) at GPG064 and barometric pressure during the 24 pumping test undertaken at GPG036. (B) Groundwater levels (adjusted for barometric effects) at GPG064 and barometric pressure in the 24 hours following cessation of pumping at GPG036

### GPG062

At the commencement of the pumping test groundwater levels at GPG062 were at 11.716 m aMSL (Figure 6.17A). After four hours of pumping groundwater levels had increased to 11.721 m aMSL (Figure 6.17A). Groundwater levels then continuously declined throughout the rest of the

pumping test ending at 11.714 m aMSL after 24 hours of pumping (Figure 6.17A). Groundwater levels at GPG062 remain relatively constant for the first 2.5 after the cessation of pumping having increased 0.002 m (Figure 6.17B). Groundwater levels then begin to decline. 24 hours after pumping had stopped groundwater levels had declined to 11.706 m aMSL. At both GPG064 and GPG062 no evidence was identified to suggest that a hydraulic connection exists between the Makauri Gravel aquifer and the overlying shallow aquifer.

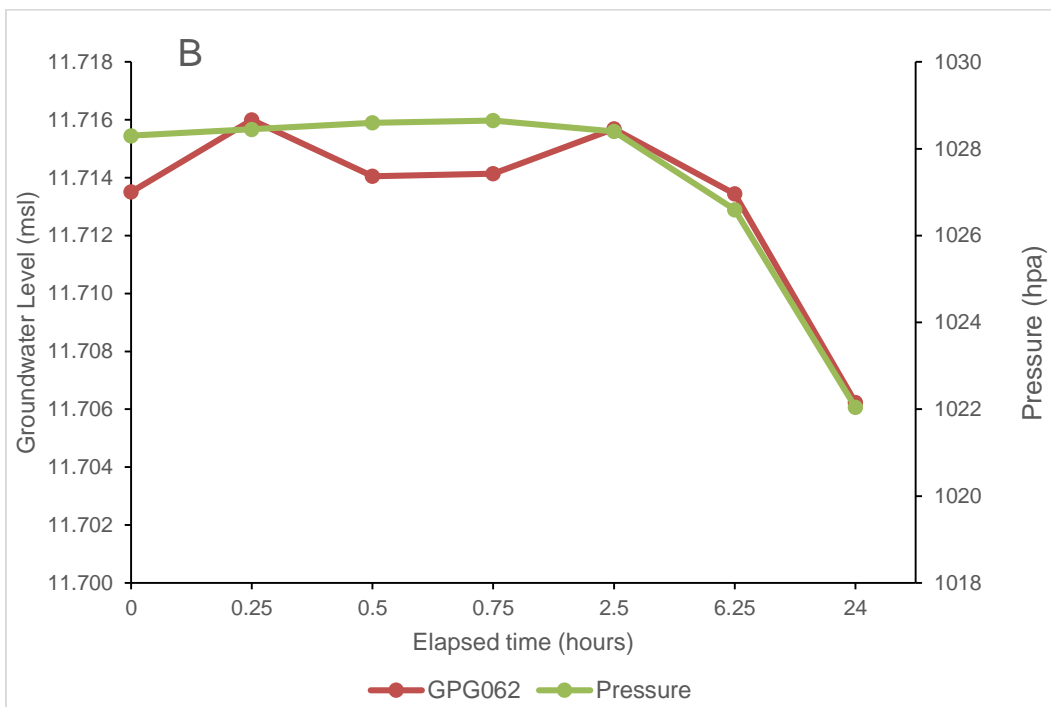
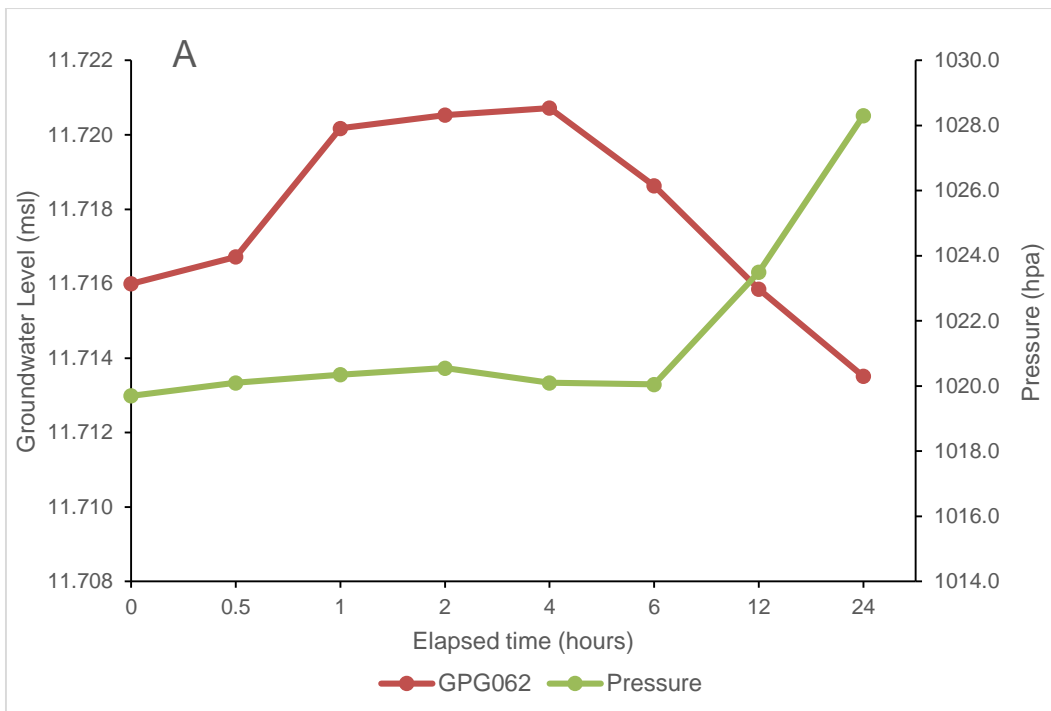


Figure 6.17. (A) Groundwater levels (adjusted for barometric effects) at GPG062 and barometric pressure during the 24 pumping test undertaken at GPG036. (B) Groundwater levels (adjusted for barometric effects) at GPG062 and barometric pressure in the 24 hours following cessation of pumping at GPG036.

## 6.4 Concurrent river flow gaugings

This section examines concurrent river flow gaugings from the Waipaoa River to understand the surface-groundwater interactions between reaches within the Poverty Bay flats. Concurrent river flow gaugings have

been undertaken at low flows at irregular intervals since 1993 at 10 different sites (Table 6.12; Figure 5.2).

Table 6.12. The 10 river flow gaugings sites on the Waipaoa River, when they were first gauged and the number of gaugings at each site.

<b>Site</b>	<b>First Gauged</b>	<b>Number of surface gaugings</b>
Kanakanaia Bridge	26/02/2013	3
Clarke's	11/11/2010	5
Kaiteratahi Bridge	26/02/2013	3
Whitmore Road	16/11/1993	20
Ford Road	16/11/1993	20
Bruce Road	16/11/1993	20
Brown Road	16/11/1993	20
Ferry Road	26/02/2013	3
Tietjens Road	11/11/2010	5
Bloomfield Road	11/11/2010	5

Concurrent river flow gaugings at four gauging sites have occurred 16 times in the middle of the Poverty Bay flats between 16/11/1993 and 29/11/1996. During these gaugings river flow ranged from  $2 \text{ m}^3 \text{ s}^{-1}$  through to  $14 \text{ m}^3 \text{ s}^{-1}$  (Figure 6.18A). River flow displayed gains and losses between reaches ranging from  $-0.76$  to  $0.77 \text{ m}^3 \text{ s}^{-1}$  between each gauging site (Figure 6.18B). All reaches displayed gains and losses and there was no consistent pattern within each reach. However, gains and losses between reaches in excess of  $0.3 \text{ m}^3 \text{ s}^{-1}$  were associated with flows greater than  $4 \text{ m}^3 \text{ s}^{-1}$ . For example, when the Waipaoa River flow was  $14 \text{ m}^3 \text{ s}^{-1}$  (16/11/1993) the Bruce Road gauging site exhibited losses of  $-0.76 \text{ m}^3 \text{ s}^{-1}$ , whereas when the Waipaoa River flow was  $2.3 \text{ m}^3 \text{ s}^{-1}$  (09/01/1995) the Bruce Road gauging site exhibited losses of  $0.15 \text{ m}^3 \text{ s}^{-1}$  (Figure 6.18B).

Concurrent river flow gaugings at seven gauging sites have occurred twice on the 11/11/2010 and 01/11/2011. During these gaugings river flow ranged from  $8 \text{ m}^3 \text{ s}^{-1}$  through to  $16 \text{ m}^3 \text{ s}^{-1}$  (Figure 6.18C). River flow displayed gains and losses between reaches ranging from  $-1.22$  to  $2.35 \text{ m}^3 \text{ s}^{-1}$  between each gauging site with greater gains/losses generally associated with greater river flow (Figure 6.18D). Gains between reaches on both days that gauging occurred were found at Ford and Tietjens and greater gains occurred when river flow was greater at both sites (Figure 6.18C; Figure 6.18D). Conversely, Whitmore Road was the only

gauging site that exhibited losses in river flow on both days that monitoring occurred and greater losses were associated with greater river flow (Figure 6.18C; Figure 6.18D).

Concurrent river flow gaugings has occurred at 10 sites three times between 26/02/2013 and 16/01/2015. During these gaugings river flow ranged from  $1.9 \text{ m}^3 \text{ s}^{-1}$  through to  $3.2 \text{ m}^3 \text{ s}^{-1}$  (Figure 6.18E). River flow displayed gains and losses between reaches ranging from  $-0.32$  to  $0.56 \text{ m}^3 \text{ s}^{-1}$  between each gauging site with greater gains/losses generally associated with greater river flow (Figure 6.18F). Kaiteratahi Bridge and Tietjens Road are the only two gauging sites that exhibited gains in river flow across both gauging days (Figure 6.18F). No gauging site displays losses across both gauging days despite river flow being similar.

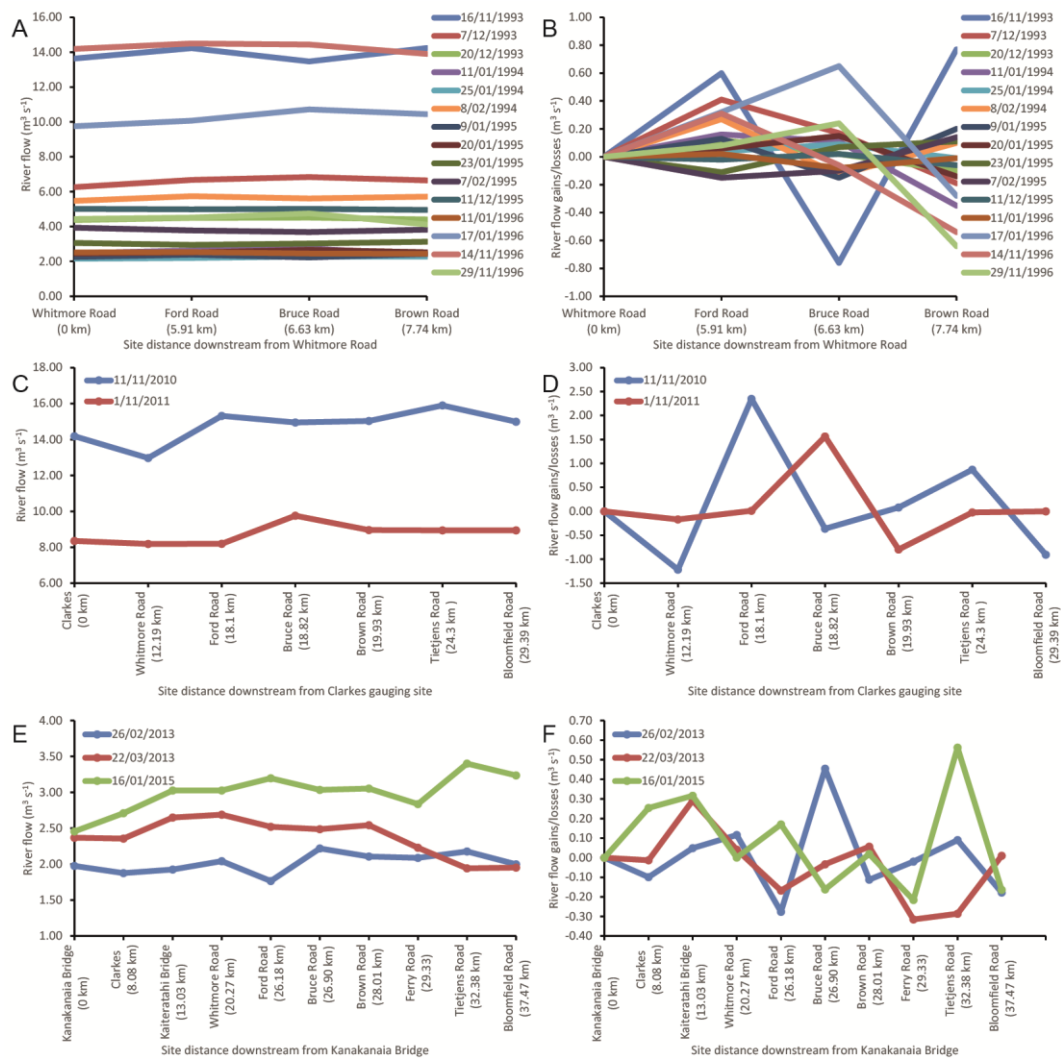


Figure 6.18. Concurrent Waipaoa River flow gaugings. Each line represents gaugings across a particular day. (A) Waipaoa River flow as monitored at four gauging sites. (B) Waipaoa River flow gains/losses between the four gauging sites in (A). (C) Waipaoa River flow as monitored at seven gauging sites. (D) Waipaoa River flow gains/losses between the seven gauging sites in (C). (E) Waipaoa River flow as monitored at ten gauging sites. (F) Waipaoa River flow gains/losses between the seven gauging sites in (E).

## 6.5 Infiltration characteristics

Identifying the infiltration characteristics of the two sites identified using the “HIGGS Index” is important when it comes to evaluating the MAR prospects of each site. The infiltration rate of a particular site must be sufficient so that a MAR scheme can achieve its end goals. The infiltration characteristics of the selected sites were calculated using the methods described in Chapter 5 and are given below.

### 6.5.1 Site 1

The soils found at Site 1 in each of the five tests were very similar (Figure 6.19). A thin layer top soil at the ground surface between 50 and 70 mm thick was present at each of the five holes at Site 1. Between 70 and 250 mm a silt loam layer was present at each hole, which in three holes contained a sand component. From 250 to 500 mm (the depth to which the holes were excavated) a sand layer was present at each hole.



Figure 6.19. (A) Soil types present in Hole 2 at Site 1 to a depth of 500 mm. (B) Soil types present in Hole 4 at Site 1 to a depth of 500 mm. The soils found within these two holes were typical of Site 1.

Five infiltrometer tests were undertaken at Site 1 to estimate the long-term infiltration rate. Infiltration rates ( $i_n$ ) within the infiltrometer during the last measurement taken ranged from 5.00 m/day at Hole 2 to 20.17 m/day at Hole 4 (Table 6.13). The  $i_n$  corresponded with downward flux rates ( $i_w$ ) between 0.12 m/day at Hole 2 to 0.75 m/day at Hole 4 (Table 6.13). The depth of wetting ( $L$ ) across the five tests varied from 0.95 m/day to 1.49

m/day (Table 6.13). Finally, saturated hydraulic conductivity ( $K_s$ ) was calculated.  $K_s$  is equivalent to the long-term infiltration rate within an infiltration basin. Hole 2 exhibited the lowest  $K_s$  at 0.02 m/day while Hole 4 exhibited the highest  $K_s$  at 0.15 m/day at Hole 4.  $K_s$  had an over mean of 0.06 m/day across the five holes at Site 1 (Table 6.13). Two of the holes were excavated to a depth of 1 m to examine why  $K_s$  varied across Site 1. A clay layer was found at depths of 550 to 700 mm below the groundwater surface at each hole. As such, it was the depth to underlying clay layer which controlled infiltration rates during the infiltrometer tests.

Table 6.13. Infiltration rate ( $i_n$ ), downward flow rate ( $i_w$ ), depth of wetting ( $L$ ), and hydraulic conductivity ( $K_s$ ) at Site 1, as calculated using the methods described in Chapter 5 following Bouwer (1999). \*All variables were calculated based upon their respective infiltrometer tests which lasted in duration from 49 to 137 min.

	m/day					
	Hole 1	Hole 2	Hole 3	Hole 4	Hole 5	Mean
<b>Infiltration rate (<math>i_n</math>)</b>	9.06	5.00	10.15	20.17	15.98	12.06
<b>Downward flow rate (<math>i_w</math>)</b>	0.24	0.12	0.25	0.75	0.44	0.36
<b>Depth of wetting (<math>L</math>)</b>	1.08	0.95	0.99	1.49	1.11	1.12
<b>Saturated hydraulic Conductivity (<math>K_s</math>)</b>	0.04	0.02	0.04	0.15	0.07	0.06

### 6.5.2 Site 2

At Site 2 a thick, low permeability layer of finely packed silt was present from the ground surface to a depth of 500 mm (only one hole was excavated at Site 2) (Figure 6.20). After 60 min of the one and only infiltrometer test at Site 2 65 mm of water had infiltrated into the underlying soils. At Site 1 the mean infiltration depth after 60 min across the five tests was 400 mm, and therefore testing was discontinued at Site 2. In spite of ceasing testing at Site 2 the data was used to provide estimates of  $i_n$ ,  $i_w$ ,  $L$ , and hydraulic conductivity ( $K$ ). The  $i_n$ ,  $i_w$ , and  $L$  were calculated to be 0.40, 0.02, and 0.31 m/day, respectively (Table 6.14).  $K_s$  could not be calculated at Site 2 as the soils beneath the infiltrometer did not reach saturation. Therefore,  $K$  was used to estimate the long-term infiltration rate at Site 2.  $K$  was calculated to be 0.01 m/day (Table 6.14).



Figure 6.20. Soil types present at Site 2 to a depth of 500 mm beneath the ground surface (photo was taken approximately 18 hours after infiltrrometer test was stopped and water is still present at the site).

Table 6.14. Infiltration rate ( $i_n$ ), downward flow rate ( $i_w$ ), depth of wetting ( $L$ ), and hydraulic conductivity ( $K_s$ ) at Site 2, as calculated using the methods described in Chapter 5 following Bouwer (1999). All variables were calculated based upon the incomplete infiltrometer test at Site which lasted 60 min.

	<b>m/day</b>
	<b>Hole 1</b>
<b>Infiltration rate (<math>i_n</math>)</b>	0.40
<b>Downward flow rate (<math>i_w</math>)</b>	0.02
<b>Depth of wetting (<math>L</math>)</b>	0.31
<b>Hydraulic Conductivity (<math>K_s</math>)</b>	0.01

## 6.6 Evaluation of MAR potential

The MAR potential of the two sites identified for MAR using an infiltration basin was evaluated using the HIGGS Index. Ratings hydraulic connection, groundwater depth, and groundwater flow direction were estimated based upon data obtained from the GDC. Ratings for impact of the vadose zone media and saturated hydraulic conductivity were estimated based upon data collected from each site.

After assigning ratings to each parameter the MAR potential for each site was then calculated using Eq (4.2). The MAR potential for both sites is low, yet the MAR potential of Site 1 is double that of Site 2 (Table 6.15). The difference in the MAR potential between the two sites is due to the different sediments found within the vadose zones at each site. The results indicate that Site 1 would be the preferred location to investigate MAR using an infiltration basin.

Table 6.15. MAR potential for the two sites identified for MAR using an infiltration basin using the HIGGS Index.

Parameter	Weight	Rating	
		Site 1	Site 2
Hydraulic connection	4	0.5	0.5
Impact of the vadose zone	4	0.2	0.1
Groundwater depth	3	0.6	0.6
Groundwater flow direction	2	1.0	1.0
Saturated hydraulic conductivity	5	0.1	0.1
<b>MAR Potential</b>		2.88	1.44

## 6.7 Hydrogeological modelling

Hydrogeological modelling was undertaken using *Comsol* to ascertain whether an infiltration basin can be used as a MAR technique to artificially recharge the Makauri Gravel aquifer. After calibration and validation (Chapter 5) various MAR scenarios were run within the model. It is important to note that in all of the MAR scenarios the vadose zone has been assumed to have been removed from beneath the infiltration basin to remove the low permeability shallow sediments encountered at Site 1 (Section 6.2). Therefore, there is a direct connection created between the infiltration basin and the underlying Shallow Fluvial Deposits. The following changes were evaluated under the MAR scenarios: changes in hydraulic head, changes in groundwater flow, and changes in Darcy velocity.

### 6.3.1 Changes in hydraulic head

Changes in hydraulic heads as a result of MAR were evaluated by comparing hydraulic heads under nine different MAR scenarios against the baseline (i.e., current conditions). The infiltration rates of the nine MAR scenarios ranged from 0.0425 to 1.5 m/day across a 250 m area (i.e., 10.625 to 375 m<sup>3</sup>/day) (Table 6.16). Eight of the nine MAR scenarios predict that increases in groundwater levels will result in inundation of the ground surface in close proximity to the infiltration basin (Table 6.16). These eight scenarios have infiltration rates equal to or greater than 0.045 m/day (Table 6.16). An infiltration rate of 0.0425 m/day or less is sufficiently low to avoid groundwater levels inundating the surrounding

land (Table 6.16). For this reason only results pertaining to Scenario 9 are discussed henceforth.

Table 6.16. Infiltration rates across the nine MAR scenarios. Inundations at the ground surface denotes scenarios that are predicted to create surface flooding issues as a result of increases in groundwater levels

<b>Scenario</b>	<b>Infiltration Rate (m/day)</b>	<b>Infiltration Rate (m<sup>3</sup>/day)</b>	<b>Inundation at ground surface</b>
<b>Scenario 1</b>	1.5	375	✓
<b>Scenario 2</b>	1	250	✓
<b>Scenario 3</b>	0.5	125	✓
<b>Scenario 4</b>	0.25	62.5	✓
<b>Scenario 5</b>	0.1	25	✓
<b>Scenario 6</b>	0.05	12.5	✓
<b>Scenario 7</b>	0.0475	11.875	✓
<b>Scenario 8</b>	0.045	11.25	✓
<b>Scenario 9</b>	0.0425	10.625	*

Scenario 9 predicts changes in hydraulic head across all of the observation bores. The greatest changes in hydraulic heads are seen in the shallow aquifers. In the Shallow Fluvial Deposits the hydraulic head at GPH047 increases by 2.3 m (Table 6.17; Figure 6.21). In the Waipaoa Gravel aquifer, hydraulic heads increase from 1.3 to 1.4 m (Table 6.17; Figure 6.21). In the Makauri Gravel aquifer, the target aquifer, the increase in hydraulic head is dependent upon the location of the observation bore. Directly beneath the infiltration basin where GPH008 and GPG077 are located (i.e., -5000 in Figure 6.21) no changes in hydraulic heads are observed. From 1000 to 4000 m (i.e., -4000 to -1000 in Figure 6.21) hydraulic heads increase by 0.48 to 0.73 m (Table 6.17). From 5000 to 6000 (i.e., 0 to 1000 m in Figure 6.21) hydraulic head increases are greatest at 0.8 to 0.85 m (Table 6.17). From 6000 m in the model hydraulic head increases under Scenario 9 begin to decrease. In the final 500 m of the Makauri Gravel aquifer hydraulic head increases are 0.04 m (Table 6.17).

Table 6.17. Hydraulic heads as modelled under the baseline (i.e., current conditions), predicted hydraulic heads under Scenario 9, and the difference between hydraulic heads under the baseline and Scenario 9.

<b>Aquifer</b>	<b>Bore</b>	<b>Coordinates</b>	<b>Baseline (m aMSL)</b>	<b>Scenario 9 (m aMSL)</b>	<b>Increase (m)</b>
<b>SFD</b>	GPH047	x=-2850, y=6.55	12.61	14.91	2.30
	GPG059	x=-1350, y=-3.91	11.12	12.52	1.40
<b>WGA</b>	GPG013	x=-1250, y=10.49	10.99	12.39	1.40
	GPG051	x=-1100, y=6.6	10.82	12.20	1.38
	GPG019	x=-540, y=-6.51	9.98	11.28	1.30
	GPH008	x=-5000, y=-55	17.30	17.30	0.00
<b>MGA</b>	GPG077	x=-5000, y=-12.74	17.80	17.80	0.00
	GPH044	x=-3970, y=-27.02	15.20	15.93	0.73
	GPG060	x=1350, y=-58.76	10.02	10.50	0.48
	GPG058	x=-1340, y=-58.85	10.00	10.49	0.49
	GPG088	x=-1310, y=-57	9.95	10.43	0.48
	GPG026	x=400, y=-29.63	7.51	8.36	0.85
	GPF068	x=830, y=-35.5	7.13	7.93	0.80
	GPE002	x=-830, y=-36	7.13	7.93	0.80
	GPF090	x=2100, y=-40.51	6.18	6.59	0.41
	GPF074	x=2500, y=-67	5.65	5.88	0.23
	GPE034	x=4100, y=-59.68	5.89	5.97	0.08
	GPF117	x=-4500, y=-61	5.94	5.98	0.04
	GPF035	x=4570, y=-59.62	5.95	5.99	0.04

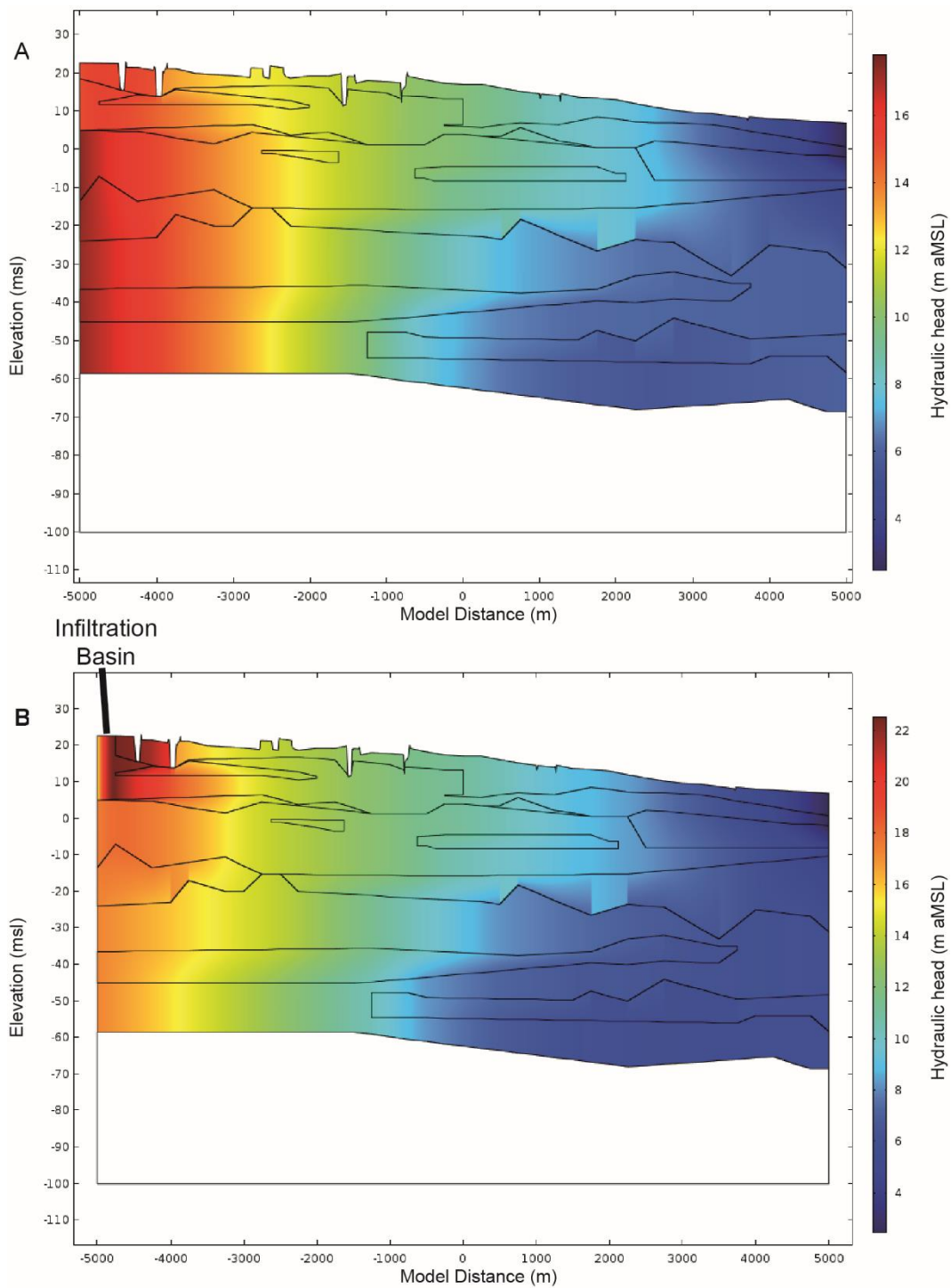


Figure 6.21. (A) Hydraulic heads as modelled under the baseline. (B) Hydraulic heads as modelled in Scenario 9.

### 6.3.2 Changes in groundwater flow

A qualitative description of how an infiltration basin may affect groundwater within the Poverty Bay flats groundwater system was used by analysing changes in groundwater flow (Figure 6.22A; Figure 6.22B).

Overall, groundwater flow paths between the baseline and Scenario 9 are similar except for two locations where groundwater flow paths differ.

The first location is directly beneath the infiltration basin where the infiltrated water is entering the groundwater system. Here, the baseline indicates that groundwater flows downwards from the Shallow Fluvial Deposits and upwards from the Waipaoa Gravel aquifer. The groundwater then converges in the upper regions of the Waipaoa Gravel aquifer and begins to flow horizontally (Figure 6.22A). The introduction of an infiltration basin under Scenario 9 changes groundwater flow paths in this area. Groundwater is now predicted to flow downwards from the infiltration basin and follow one of two paths (Figure 6.22B).

The first groundwater flow path indicates that groundwater flows vertically towards the bottom of the Shallow Fluvial Deposits and then horizontally along the boundary of the Shallow Fluvial Deposits and the Waipaoa Gravel aquifer. The second groundwater flow path flows vertically down into the Waipaoa Gravel aquifer and then horizontally along the Makauri Gravel aquifer.

The second location where groundwater flow paths differ between the baseline and Scenario 9 is where the Waipaoa Gravel aquifer and Makauri Gravel aquifer are connected (i.e., the small circle in Figure 6.22B). In this area the baseline suggests that there is very little groundwater exchanged between the Waipaoa Gravel aquifer and the Makauri Gravel aquifer.

In Scenario 9 the amount of groundwater exchanged between the Waipaoa gravel aquifer and the Makauri Gravel aquifer increases (Figure 6.22B). This increased groundwater exchange can be seen in the increases in hydraulic head shown throughout the Makauri Gravel aquifer (Table 6.17).

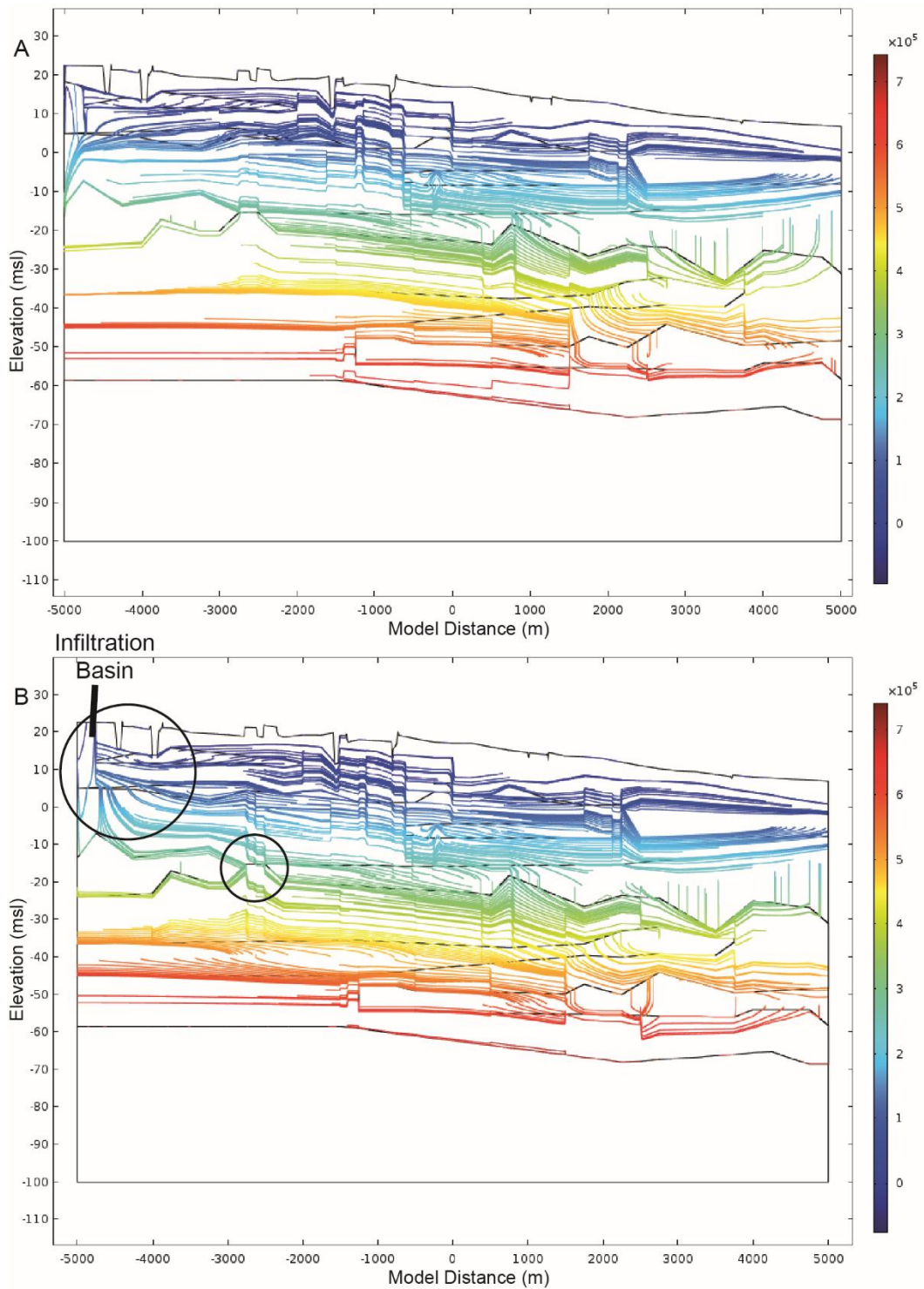


Figure 6.22. (A) Groundwater flow paths as modelled under the baseline. (B) Groundwater flow paths as modelled in Scenario 9. Black circles within (B) highlight areas where groundwater flow differs from (A).

### 6.3.3 Changes in Darcy Velocity

Analysing changes in Darcy's velocity allows a quantitative analysis of the changes in groundwater flow at the observation bores. Changes in Darcy velocity between the baseline and Scenario 9 are given in Table 6.18. Within the Shallow Fluvial Deposits, Darcy's velocity increases

by 0.01050 m/day between the baseline and Scenario 9, the greatest increase exhibited at any of the observation bores. Darcy velocity across all four observation bores in the Waipaoa gravel aquifer increases by 0.00012 to 0.00196 m/day (Table 6.18).

In the Makauri Gravel aquifer, predicted changes in Darcy velocity appear to be related to changes in groundwater flow rather than changes in hydraulic head. For example, both GPH044 and GPF074 exhibited increases in hydraulic head, yet Darcy's velocity decreased at GPH044 and increased at GPF074 (Table 6.17; Table 6.18). Decreases in Darcy velocity are observed at all observation bores between 0 and 4000 m (i.e., -5000 and -1000 in Figure 6.21) (Table 6.18). Increases in Darcy velocities are observed in the observation bores between 5400 and 7500 m (i.e., 400 and 2500 in Figure 6.21) (Table 6.18). In the final 1000 m of the model decreases in Darcy velocity are predicted (Table 6.18).

Table 6.18. Darcy velocity for the baseline and Scenario 9 at the observation bores.

<b>Aquifer</b>	<b>Bore</b>	<b>Coordinates</b>	<b>Baseline (m/day)</b>	<b>Scenario 9 (m/day)</b>	<b>Increase (m/day)</b>
<b>SFD</b>	GPH047	x=-2850, y=6.55	0.00885	0.01933	0.01050
	GPG059	x=-1350, y=-3.91	0.01056	0.01067	0.00012
<b>WGA</b>	GPG013	x=-1250, y=10.49	0.00766	0.00962	0.00196
	GPG051	x=-1100, y=6.6	0.01186	0.01299	0.00113
	GPG019	x=-540, y=-6.51	0.01927	0.02094	0.00167
	GPH008	x=-5000, y=-55	0.01734	0.01551	-0.00183
<b>MGA</b>	GPG077	x=-5000, y=-12.74	0.52731	0.48852	-0.03880
	GPH044	x=-3970, y=-27.02	0.01928	0.01383	-0.00545
	GPG060	x=1350, y=-58.76	0.01537	0.01519	-0.00018
	GPG058	x=-1340, y=-58.85	0.01534	0.01517	-0.00017
	GPG088	x=-1310, y=-57	0.01525	0.01509	-0.00016
	GPG026	x=400, y=-29.63	0.01108	0.01245	0.00137
	GPF068	x=830, y=-35.5	0.00400	0.00493	0.00093
	GPE002	x=-830, y=-36	0.00400	0.00493	0.00093
	GPF090	x=2100, y=-40.51	0.00055	0.00153	0.00098
	GPF074	x=2500, y=-67	0.00037	0.00095	0.00058
	GPE034	x=4100, y=-59.68	0.00121	0.00042	-0.00079
	GPF117	x=-4500, y=-61	0.00100	0.00029	-0.00071
	GPF035	x=4570, y=-59.62	0.00096	0.00017	-0.00069

## 6.7 Summary

Trend analyses were undertaken on rainfall, river flow and stage, and groundwater levels to identify if any trends were exhibited by each variable (Section 6.1). Trend tests showed that groundwater levels were declining at statistically significant rates in the Makauri Gravel and Matokitoki Gravel aquifers. Groundwater levels within the Waipaoa Gravel aquifer were shown to be stable as no statistically significant trends were identified. The datasets for the Shallow Fluvial Deposits and the Te Hapara Sands are limited but groundwater levels are stable in these two aquifers. No statistically significant trends were identified with regard to rainfall at the Gisborne Airport weather station or Waipaoa River flow. A statistically significant increasing trend was shown with regard to Waipaoa River stage.

Changes in groundwater levels as a result of a rainfall event and associated changes in river stage were analysed (Section 6.2). Groundwater levels changes varied between aquifers and spatially within individual aquifers. The Makauri Gravel aquifer was the only aquifer to show consistent increases in groundwater levels across the entire monitoring period.

A pumping test was undertaken in an attempt to identify if a hydraulic connection existed in the Caesar Road area between the Makauri Gravel aquifer and the overlying shallow aquifers (Section 6.3). The pumping rate was lower than expected and no hydraulic connection was identified.

Concurrent Waipaoa River flow gaugings were analysed to understand the surface-groundwater interactions between reaches within the Poverty Bay flats (Section 6.4). The only consistent trend displayed by these river flow gaugings is that gains and losses between reaches in excess of  $0.3 \text{ m}^3 \text{ s}^{-1}$  were associated with flows greater than  $4 \text{ m}^3 \text{ s}^{-1}$ .

The infiltration characteristics of the two sites identified via the HIGGS Index were analysed via infiltration tests (Section 6.5). The mean long-term infiltration rate at Site 1 was 0.06 m/day. Further analysis at this site

showed that it was underlain by a thick clay layer. Site 2 contained very fine silts of low permeability. The infiltration test at Site 2 was abandoned once it was clear that Site 1 was more conducive to MAR using an infiltration basin. The HIGGS Index was used to calculate the MAR potential two different sites (Section 6.6). The MAR potential of both sites is low.

Hydrogeological modelling was undertaken to ascertain what changes an infiltration basin may induce in the Poverty Bay flats groundwater system, particularly in the Makauri Gravel aquifer (Section 6.7). Modelling showed that an infiltration rate of 0.0425 m/day would result in increases in hydraulic heads throughout the Makauri Gravel aquifer. Changes in Darcy's velocity appeared to be related to the bores location and whether it was affected by change in groundwater flow paths rather than changes in hydraulic head.

## Chapter 7 – Discussion

---

The objective of this research is to identify whether an infiltration basin may be successfully used to artificially recharge the Makauri Gravel aquifer beneath the Poverty Bay flats. Supplementary work was also undertaken to characterise the current state of groundwater resources within the Poverty Bay flats, identify interactions surface-groundwater resources, and examine hydraulic connections between aquifers.

This chapter discusses the results of this research in relation to the overarching objective and supplementary work undertaken to characterise the Poverty Bay flats groundwater system. Section 6.1 discusses the current state of groundwater resources and identifies possible drivers of any observed trends. Section 6.2 links the changes in groundwater levels observed as a result of a rainfall event and associated changes in river stage with our current knowledge of the Poverty Bay flats groundwater system. Section 6.3 analyses the hydraulic connection between the Makauri and Waipaoa Gravel aquifers. Section 6.4 describes the surface-groundwater interactions within the Poverty Bay flats. Section 6.5 describes the MAR potential of the two sites identified using the HIGGS Index. Section 6.6 discusses the hydrogeological modelling. Each section includes suggestions areas for further monitoring and/or research.

### 7.1 Groundwater resources

Trend analyses were undertaken on rainfall, Waipaoa River flow and stage data, and groundwater level data to evaluate the current state of groundwater resources and identify possible drivers of any observed trends. The current state of groundwater resources is discussed below across five sections.

#### 7.1.1 Rainfall

Annual rainfall data recorded at the Gisborne Airport weather station did not exhibit any trends (Table 6.1). Therefore, any changes in observed groundwater levels are not driven by rainfall.

### **7.1.2 Waipaoa River flow and stage**

Waipaoa River flow data recorded at the Kanakanaia Bridge did not exhibit any trends (Table 6.2). Therefore, like rainfall, changes in observed groundwater levels are not driven river flow. Conversely, Waipaoa River stage is increasing at a statistically significant rate of 0.016 m/yr (Table 6.2). Theoretically, this means that the amount of groundwater recharge from the Waipaoa River may have increased over time as the elevation of surface water has increased relative to groundwater. Any increasing trends with regard to groundwater levels may have resulted from increases in Waipaoa River stage.

### **7.1.3 Shallow aquifers**

Shallow aquifers within the Poverty Bay flats include the Te Hapara Sands, Shallow Fluvial Deposits, and Waipaoa Gravel aquifers. Limited information is available regarding groundwater level trends within these bores. However, the few bores that are monitored within these aquifers indicate that groundwater levels are typically stable (Table 6.3; Table 6.4; Table 6.5). This indicates that pumping has not affected groundwater levels in these bores. These findings are inconsistent with White et al. (2012) who found that groundwater levels within these aquifers were typically increasing. It should be noted that different bores were monitored within this research compared with White et al. (2012), which is the likely reason for this inconsistency.

Given these results, groundwater abstractions do not affect groundwater levels within the shallow aquifers of the Poverty Bay flats. Further monitoring should be undertaken through each of these aquifers to increase the spatial coverage of monitored bores. Increasing the spatial coverage would allow for a more complete assessment of groundwater resources within each of the shallow aquifers.

### **7.1.4 Deep aquifers**

Deep aquifers within the Poverty Bay flats include the Makauri Gravel aquifer and the Matokitoki Gravel aquifer. Groundwater level trends within the Makauri Gravel aquifer show some spatial variation with regards to

observed trends. In the northern reaches of the aquifer groundwater levels are typically increasing (Table 6.5; Figure 7.1). These two bores also show statistically significant increases during the month of September, indicating that the amount of groundwater recharge these bores receive has increased over time. These trends may be related to increases in Waipaoa River stage.

In the middle reaches of the Makauri Gravel aquifer where groundwater abstractions are greatest groundwater levels are typically stable. In the southern reaches of the aquifer groundwater levels are typically decreasing. Previous work by Barber (1993) identified that the Waipaoa Gravel aquifer likely recharged the Makauri Gravel aquifer around Caesar Road (Figure 3.5). Therefore, groundwater levels are likely stable in the middle reaches of the Makauri Gravel aquifer due to the presence of a recharge zone. As drawdowns in middle reaches of the Makauri Gravel aquifer increase over time it is likely that less groundwater recharge is distributed to the southern reaches of the aquifer, thus why declines are observed in the southern reaches.

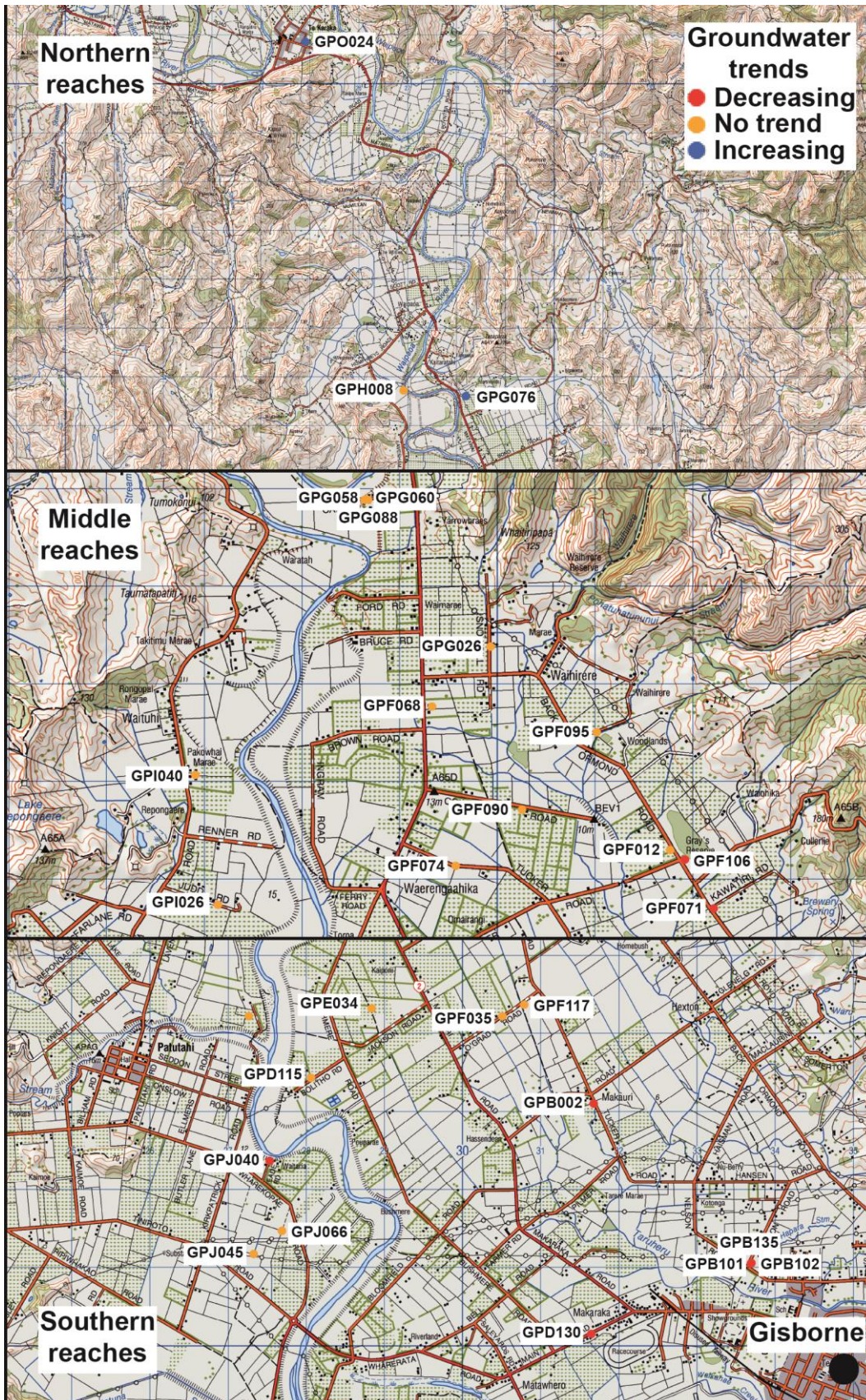


Figure 7.1. Groundwater trends across the 29 bores monitored within the Makauri Gravel aquifer by the GDC. Identified trends are significant at the 95% level.

In the Matokitoki Gravel aquifer groundwater levels declines are observed at six of the seven bores that exhibit trends (Table 6.9). These declines are likely to be related to groundwater abstractions. However, one bore (GPB039) in the Matokitoki Gravel aquifer does exhibit an increasing trend (Table 6.9). It is unknown why this trend has occurred. Therefore, further research is required to identify the underlying cause of the observed trend at GPB039.

Overall, groundwater levels within the Makauri and Matokitoki aquifers are declining, though some spatial variation was observed (Table 6.6; Table 6.9). These declines are likely due to groundwater abstractions as no long-term trends were identified in rainfall or river flow data. These findings are consistent with White et al. (2012).

### **7.1.5 Groundwater abstractions**

Observed declines in groundwater levels within the Makauri and Matokitoki Gravel aquifers are probably caused by groundwater abstractions. This indicates that groundwater abstractions exceed recharge rates in these aquifers, which was first reported by Barber (1993). This is important as groundwater abstraction rates have increased over the last 35 years (Gordon, 2001). This is shown in Table 3.1 which compares groundwater allocations in 1992 and 2015. Furthermore, Table 3.2 shows that there is a large discrepancy between groundwater allocation and average annual groundwater use. As declines have been observed within the groundwater system this discrepancy is an issue.

It is possible, but unlikely, that significantly more water will be abstracted from the Makauri and Matokitoki Gravel aquifers over the coming years exacerbating the pressures facing the groundwater system. This could result in permanent changes to the groundwater system from land subsidence due to over-abstraction of groundwater resources (Domenico and Schwartz, 1998). Alternately, groundwater quality could decrease as the easily abstracted good quality groundwater is abstracted potentially leaving behind groundwater of inferior quality (Brown and Elmsly, 1987;

Konikow and Kendy, 2005). Therefore, the GDC needs to ensure that manages its groundwater resources so these effects do not occur.

Currently, water permits are granted for a maximum of five years to allow adaptation to changes in land use and fluctuations in groundwater levels (GDC, 2011). This will allow the GDC to address the discrepancy between groundwater allocation and actual groundwater use to ensure that water permits holders are only able to abstract what they need. However, by aligning groundwater allocation with actual groundwater use observed declines in the Makauri and Matokitoki Gravel aquifers may not be stabilised or reversed. A water budget for each aquifer within the Poverty Bay flats groundwater system was developed by White et al. (2012) to identify the amount of groundwater available for allocation. In conjunction with the water budget approach, the GDC should undertake further monitoring within the Poverty Bay flats groundwater system to determine recharge rates. This information could then be used to refine water budget estimates to improve groundwater management.

## **7.2 Groundwater level changes**

Groundwater level changes as a result of a rainfall event and associated changes in Waipaoa River stage were characterised by undertaking groundwater level monitoring before, during, and after a rainfall event. Groundwater level changes within the Te Hapara Sands appear to be related to rainfall. Groundwater level changes within the Shallow Fluvial Deposits and Waipaoa and Makauri Gravel aquifers appear to be related to each bores location relative to the Waipaoa River and groundwater recharge zones (Figure 3.5).

### **Te Hapara Sands**

Barber (1993) states that river-derived recharge in this aquifer is greatest in close proximity to the Waipaoa River. GPB099, which taps the Te Hapara Sands, is located approximately 4.5 km from the Waipaoa River. Given the distance between this bore and the Waipaoa River it is likely that rainfall may be the dominant recharge source in this area. The largest increase at this bore (0.07 m between the 15<sup>th</sup> and 16<sup>th</sup> of March) occurred

prior to river stage increasing (Figure 6.12), indicating that groundwater level changes were primarily caused by rainfall. Groundwater levels then declined after the rainfall event ended. This finding is consistent with Barber (1993).

### **Shallow Fluvial Deposits**

Groundwater in the Shallow fluvial Deposits is recharged by river-derived water and rainfall (Barber, 1993; Taylor, 1994). Groundwater level changes in the Shallow Fluvial Deposits were greatest in close proximity to the Waipaoa River. GPH047 is located approximately 50 m from the Waipaoa River near Ormond (Figure 5.5). This bore showed large increases (0.463 m) in groundwater levels as river stage increased, indicating the aquifer is hydraulically connected to the Waipaoa River in this area. GPH005 and GPH046 were located further north near Kaiteratahi. These bores were located approximately 900 and 850 m away from the Waipaoa River, respectively (Figure 5.5). These bores showed small increases in groundwater levels (0.07 m at GPH005 and 0.067 m at GPH047). This indicates that the hydraulic connection with the Waipaoa River weakens with distance from the river.

GPG051 is located east of Caesar Road (Figure 5.5). At GPG051 groundwater levels increase in response to the rainfall event and associated changes in river stage. The increase in groundwater levels is 0.049 m, which is the smallest increase of the bores monitored within the Shallow Fluvial Deposits. This is probably a function of its location as it is at a higher elevation than the Waipaoa River so it cannot be recharged by the river in this location. However, groundwater levels do not decline throughout the monitoring period and instead remain relatively constant. This indicates that this bore is located in close proximity to a recharge source, possibly the hills to the northeast of the Poverty Bay flats which have been identified as a recharge source for the Makauri Gravel aquifer (Barber, 1993; Taylor, 1994). Further monitoring should be undertaken in this area within the Shallow Fluvial Deposits to identify if other bores are potentially recharged by the hills to the northeast of the Poverty Bay flats.

### **Waipaoa Gravel aquifer**

The Waipaoa Gravel aquifer is recharged by the Waipaoa River in its upper reaches as changes in groundwater levels respond to changes in river stage (Barber, 1993). In the Waipaoa Gravel aquifer groundwater level changes as a result of the rainfall event and associated changes in river stage were similar. The greatest groundwater level increase was seen in the northern reaches of this aquifer at GPH022. However, as river stage declined so did groundwater levels. This indicates that GPG022 is hydraulically connected to the Waipaoa River which is consistent with the findings of Taylor (1994).

Around Caesar Road increases in groundwater levels ranged from 0.053 m at GPG013 to 0.175 m at GPG059. These groundwater level increases appear to be relatively small given the bores close proximity to the Waipaoa River. In this area the Waipaoa Gravel aquifer discharges groundwater to the Makauri Gravel aquifer (Figure 3.5). This indicates that groundwater level changes were relatively small because the Waipaoa Gravel aquifer was discharging groundwater to the Makauri Gravel aquifer through the monitoring period. GPI023 was affected by pumping during the monitoring period so groundwater level changes should be interpreted with caution. The observed increase in groundwater levels between the 14<sup>th</sup> and 15<sup>th</sup> March is due to pumping. Groundwater levels at GPI023 remain relatively constant throughout the monitoring period, indicating that GPI023 may be hydraulically connected to the Waipaoa River, which is consistent with Barber (1993).

GPE032 shows the second smallest increase in groundwater levels due to changes in river stage (0.049 m). GPE032 is located adjacent to the Waipaoa River (Figure 5.4). The small increase indicates that the hydraulic connection between the Waipaoa River and the Waipaoa Gravel aquifer is limited. This is consistent with Barber (1993) who did not identify a recharge zone in this area. Recharge zones within the Waipaoa Gravel aquifer affect groundwater across the aquifer to differing degrees. The extent of these recharge zones should be examined, as noted by White et al. (2014).

### **Makauri Gravel aquifer**

The Makauri Gravel aquifer is recharged from a number of different sources (Barber, 1993; Taylor, 1994; White et al., 2012). Groundwater level changes within this aquifer are described by area. GPH008 and GPH044 are located in the northern reaches of this aquifer (Figure 5.5). These two bores show groundwater level increases of 0.378 m (GPH008) and 0.253 m (GPH044). As groundwater levels only increased for a short period of time it is possible that these increases were caused by rainfall upstream of Kaiteratahi which may reach this aquifer (White et al., 2012). GPE002, GPE041, GPG060, and GPG088 are all located in the middle reaches of the aquifer (Figure 5.4; Figure 5.5). Groundwater levels at all of these bores increase throughout the monitoring period indicating that the aquifer a recharge zone is in this area. The location of the recharge zone is shown in (Figure 3.5). The Makauri Gravel aquifer is recharged by a number of sources around Caesar Road (Barber, 1993). Given the number of potential recharge sources in this area, further research should be undertaken in this aquifer to ascertain recharge boundaries and quantify recharge by source.

GPB101 and GPB102 are located in the southern reaches of the Makauri Gravel aquifer (Figure 5.4). These two bores show similar responses to GPH008 and GPH044. These two bores show groundwater level increases of 0.154 m (GPB101) and 0.129 m (GPB102) at the beginning of the monitoring period followed by declines (Figure 6.15). The increases given by these bores are the smallest observed within this aquifer, indicating that recharge zones are some distance from these bores.

Groundwater level changes as a result of a rainfall event and associated changes in Waipaoa River stage varied across the Poverty Bay flats groundwater system. Groundwater level changes were generally greatest in close proximity to the Waipaoa River or recharge zones. Further monitoring is required to examine whether there are seasonal differences in groundwater level changes following a rainfall event. Also, further

monitoring is needed to identify the extent of the recharge zones in greater detail.

### **7.3 Hydraulic connections**

A pumping test was undertaken in close proximity to Caesar Road to see if a hydraulic connection existed between the Makauri Gravel aquifer and the overlying Waipaoa Gravel aquifer. The pumped and observation bores are shown in (Figure 5.6). At both of the observation bores no drawdown was observed. This indicates that no hydraulic connection exists between the Makauri and Waipaoa Gravel aquifers in the area where the pumping test was undertaken, though does not preclude the possibility of a hydraulic connection existing in the wider area.

Previous work by Barber (1993) identified that the Waipaoa Gravel aquifer likely recharged the Makauri Gravel aquifer around Caesar Road. This suggests that further pumping tests need to be undertaken in this area to identify if the two aquifers are hydraulically connected. Alternately, as noted by White et al. (2014), the GDC could drill new monitoring bores in this area and install multiple piezometers within the Waipaoa River recharge zone (Figure 3.5). Drilling new monitoring bores would allow the GDC to collect further information about the geological structure of the Poverty Bay flats around Caesar Road, and thus draw inferences about the hydraulic connection between the Makauri and Waipaoa Gravel aquifers. The installation of multiple piezometers at different depths would enable to GDC to estimate vertical groundwater movement, and thus again draw inference about the hydraulic connection around Caesar Road, and thus draw inferences about the hydraulic connection between the Makauri and Waipaoa Gravel aquifers.

### **7.4 Surface-groundwater connections**

Concurrent river flow gaugings from the Waipaoa River were analysed to understand the surface-groundwater interactions between reaches within the Poverty Bay flats. Given the irregular nature of these gaugings and the inconsistent results little information was available to be drawn from the

data. All reaches analysed displayed gains and losses and there was no consistent pattern between reaches (Figure 6.18). However, greater gains and losses between reaches were associated with higher flows (Figure 6.18). The GDC should undertake concurrent river flow gaugings on the Waipaoa River regularly. In doing this the GDC would be able to build a better understanding of surface-groundwater interactions within the Poverty Bay flats.

As noted in Chapter 4, some tributaries of the Waipaoa River are not gauged, meaning the contribution of such tributaries cannot be accounted for (White et al., 2014). Furthermore, limited information is available regarding surface water abstractions when surface gaugings have been undertaken, meaning the impact of surface water abstractions on concurrent river flow gaugings cannot be accounted for. When the GDC undertakes concurrent river flow gaugings they should also record river flow in the tributaries that enter the Waipaoa River to understand their contribution to river flow. This has been recommended previously by White et al. (2012).

If gains and losses between reaches are small then the surface water abstractions may affect results when analyzing surface-groundwater interactions (White et al., 2014). Typically gains and losses between reaches are less than  $0.3 \text{ m}^3 \text{ s}^{-1}$ . As such, the GDC should account for surface water abstractions on days when gaugings are undertaken. In particular, the GDC should ensure that they understand the volume of surface water abstractions within the Waipaoa River recharge zone identified in Figure 3.5 to ensure that groundwater recharge in this area is not overestimated.

## **7.5 Evaluation of MAR potential of identified sites**

The long-term infiltration rates at Site 1 was 0.06 m/day and 0.01m/day at Site 2. Typical infiltration rates within an infiltration basin range from 0.3 to 3 m/day (Bouwer, 1999). Therefore, the long-term infiltration rates calculated at each site are very low. To increase the long-term infiltration

rate at each site engineering would be required as the sediments of low permeability must be removed. At both sites gravels are found at approximately 6 m below the ground surface according to bore log data. Excavated infiltration basins are commonly used to bypass sediments of low permeability (Bouwer, 1999).

The MAR potential of the two sites identified for MAR using an infiltration basin was evaluated using the HIGGS Index. The MAR potential of Site 1 was 2.88 and Site 2 was 1.44 (Table 6.15). The maximum MAR potential using the HIGGS Index is 480. The MAR potential at each site were low due the presence of sediments of low permeability, as mentioned above, which affected the ratings for impact of the vadose zone and saturated hydraulic conductivity. If these low permeability sediments were not present then the MAR potential would have been higher. However, the desktop study undertaken to identify sites using the HIGGS Index did not identify any areas within the Poverty Bay flats that were likely to have greater infiltration rates than the identified sites. The Poverty Bay flats are located on the flood plain of the Waipaoa River which has led to the deposition of fine silts across the flats (Brown and Elmsly, 1987). Therefore, the presence of sediments of low permeability across the Poverty Bay flats indicates that an infiltration basin is unlikely to be able to successfully artificially recharge the Makauri Gravel aquifer within the Poverty Bay flats without significant engineering.

As such, the GDC must determine whether to continue investigating the possibility of using an infiltration basin to artificially recharge the Makauri Gravel aquifer, but with engineering to overcome identified issues associated with low permeability sediments, or whether it will examine other MAR methods.

While the HIGGS Index was not successful in identifying sites that could be used to artificially recharge the Makauri Gravel aquifer using an infiltration basin, it does not mean that it can not be used successfully. The hydrogeology of the Poverty Bay flats, particularly within the vadose zone, meant that issues were likely to arise. In other areas where the vadose

zone contains permeable sediments (e.g., Canterbury) the HIGGS Index may be used successfully.

## **7.6 Hydrogeological modelling**

Hydrogeological modelling was undertaken to ascertain whether an infiltration basin may be successfully used as a MAR technique to artificially recharge the Makauri Gravel aquifer. The results presented in Section 6.5 (and discussed in Section 7.6) indicated that engineering may be required to remove sediments of low permeability within the vadose zone. Therefore, there is a direct connection created between the infiltration basin and the underlying Shallow Fluvial Deposits.

### **7.6.1 Inundation at the ground surface**

As mentioned in Section 6.7, eight of the nine MAR scenarios predicted that groundwater level increases would result in inundation at the ground surface. Inundation at the ground surface may result direct and indirect effects on surrounding land. Direct damage occurs when groundwater comes into physical contact with humans, property or other objects while indirect damage is induced by groundwater inundation but occurs outside of the actual event (Kreibich and Thieken, 2008). To avoid these adverse effects the GDC should ensure that if an infiltration basin is installed within the Poverty Bay flats that the infiltration rate is equal to or less than 0.0425 m/day (10.625 m<sup>3</sup>/day), as this is the rate at which groundwater level increases will not result in inundation at the ground surface.

### **7.6.2 Changes in hydraulic head & Darcy velocity**

Like Section 6.7, changes in hydraulic heads will only be discussed in relation to Scenario 9 which did not result in inundation at the ground surface. Changes in hydraulic heads within the Makauri Gravel aquifer are dependent on the location of the observations bores. The greatest increases in hydraulic head are observed in bores that tap the Makauri Gravel aquifer after the recharge zone located at Caesar Road (Figure 3.5). Changes in Darcy velocity in the Makauri Gravel aquifer are variable as both increases and decreases are observed (Table 6.17). Like changes in hydraulic head, the greatest increases are observed after

recharge zone located at Caesar Road. This indicates that there will be more water within the Makauri Gravel aquifer where groundwater abstractions are greatest. As such, an infiltration basin may be used to arrest declines in groundwater levels.

However, changes in hydraulic heads and Darcy velocity were greatest in the shallow aquifers (Table 6.16; Table 6.17). This indicates that a majority of the infiltrated water is present within the shallow aquifers. If an infiltration basin is used to manage groundwater resources within the Poverty Bay flats this presents an opportunity to decrease groundwater abstractions within the Makauri Gravel aquifer and increase groundwater abstractions in the shallow aquifers.

While the model does predict increases in hydraulic heads and Darcy velocity the infiltration rates are low at 0.0425 m/day or 10.625 m<sup>3</sup>/day across a 250 m<sup>2</sup> area. These low infiltration rates do not account for any potential clogging layer within the infiltration which may reduce infiltration even further (Bouwer, 1999). It is questionable as to whether the benefits of using an infiltration basin to artificially recharge the Makauri Gravel aquifer would outweigh the costs, although this is something for the GDC to decide.

### **7.6.2 Limitations**

There were a number of limitations associated with the hydrogeological model used within this research. First, the model was a simplified 2-dimensional representation of the Poverty Bay flats. Therefore, the spatial variation of the Poverty Bay flats groundwater system was not modelled. Second, the model was a steady state model. The model did not account for changes over time, and therefore estimates surrounding the time it take for water infiltrated within the infiltration basin could not be ascertained. Third, surface-groundwater interactions were not accounted for. Yet, concurrent Waipaoa River flow gaugings indicate that groundwater is discharged to surface water and vice versa. This means that the contribution of an infiltration basin to Waipaoa River flow could not be estimated even though increases in hydraulic head suggest it may be

significant. Finally, while the model represented the groundwater system sufficiently according to the goodness of fit index  $V$ , the model estimated recharge rates using a trial and error process. At this stage there is not enough data to identify the recharge estimates within each aquifer throughout the Poverty Bay flats, but if this data is obtained it may improve any future modelling undertaken within the Poverty Bay flats.

Given the above limitations, the GDC should develop a 3-dimensional transient model of the Poverty Bay flats groundwater system. This model would allow the GDC to account for the limitations associated with the model developed during this research, thus the GDC could have greater confidence in model predictions. Furthermore, developing such a model would allow the GDC to evaluate different groundwater management strategies within the Poverty Bay flats groundwater. Therefore, the GDC will be able to model multiple strategies to identify the most cost-effective method to arrest declines in groundwater elevations in the Makauri and Matokitoki Gravel aquifer.

## Chapter 8 – Conclusions & Recommendations

---

The Gisborne District Council (GDC) is investigating its groundwater management options to ensure that groundwater resources will be managed sustainably in the future. In particular, the GDC is investigating whether MAR can be used as a groundwater management technique to reverse the trend of declining groundwater elevations. The objective of this research is to identify whether an infiltration basin may be successfully used to artificially recharge the Makauri Gravel aquifer beneath the Poverty Bay flats. Supplementary work will also be undertaken to characterise the current state of groundwater resources within the Poverty Bay flats, identify interactions surface-groundwater resources, and examine hydraulic connections between aquifers.

To identify sites that may be used for MAR using an infiltration basin the HIGGS Index was developed during the course of this research. It was developed using the premise that the MAR potential of a site using an infiltration basin could be evaluated by obtaining a limited number of hydrogeological parameters for a given location. Sites were identified via a desktop study and evaluated further via fieldwork.

This study identified:

- Groundwater levels in the Makauri and Matokitoki Gravel aquifers are declining at statistically significant rates. This is probably due to groundwater abstractions.
- Groundwater level changes as a result of a rainfall event and associated changes in Waipaoa River stage varied across the Poverty Bay flats groundwater system. Groundwater level changes were generally greatest in close proximity to the Waipaoa River or recharge zones.
- Concurrent gaugings did not identify any consistent gaining or losing reaches within the Waipaoa River.

- Long-term infiltration rates at the two sites identified using the HIGGS Index were below typical infiltration rates within an infiltration basin. Consequently, the MAR potential of both sites were low.
- Hydrogeological modelling was undertaken to ascertain what changes an infiltration basin may induce in the Poverty Bay flats groundwater system, particularly in the Makauri Gravel aquifer. Modelling indicated that an infiltration basin could be used to artificially recharge the Makauri Gravel aquifer. However, the infiltration rates are low so the benefits of an infiltration scheme may not outweigh the costs.

It is recommended that the GDC undertakes further monitoring within the Poverty Bay flats to; increase the spatial coverage of bores monitored within the shallow aquifers to obtain a better understanding of groundwater resources in these aquifers; identify the extent of groundwater recharge zones to better understand interactions between aquifers; and identify surface-groundwater interactions between the Waipaoa River and the groundwater system.

Furthermore, the GDC should develop a 3-dimensional transient model of the Poverty Bay flats groundwater system. Such a model would allow the GDC to evaluate different groundwater management strategies within the Poverty Bay flats groundwater.

## References

- Alley, W.M., Reilly, T.E., & Franke, O.L. 1999, *Sustainability of Ground-Water Resources*, United States Geological Survey, Denver, Colorado, United States.
- Barber, J.L. 1993, *Groundwater of the Poverty Bay flats: a brief synopsis*, Gisborne District Council, Gisborne, New Zealand.
- Bardsley, W.E. 2013, 'A good of fit measure related to  $r^2$  for model performance assessment', *Hydrological Processes*, vol. 27, no. 15, pp. 2851-2856, doi: 10.1002/hyp.9914.
- Brown, L.J. 1984, 'Makauri Gravel – A "Blind" Aquifer Underlying Poverty Bay Flats, Gisborne', *New Zealand Geological Survey Record 3*, pp. 69-77.
- Brown, L.J., & Elmsly, T.A. 1987, 'Poverty Bay Flats' Groundwater Chemistry', *New Zealand Geological Survey Record 5*, Lower Hutt, New Zealand.
- Bouwer, H. 1978, *Groundwater Hydrology*, McGraw-Hill, New York, United States.
- Bouwer, H. 1982, 'Design Consideration for Earth Linings for Seepage Control', *Ground Water*, vol. 20, no. 5, pp. 531-537, doi: 10.1111/j.1745-6584.1982.tb01366.x.
- Bouwer, H. 1986, 'Intake Rate: Cylinder Infiltrometer', in A. Klute (ed), *Methods of Soil Analysis, Part 1, Physical and Mineralogical Methods – Second Edition*, American Society of Agronomy, Inc. and Soil Science Society of America, Inc., Wisconsin, United States, pp. 825-844.
- Bouwer, H. 1990, 'Effect of Water Depth and Groundwater Table on Infiltration from Recharge Basins', in S.C. Harris (ed), *Irrigation and drainage, Proceedings of the 1990 National Conference*, American Society of Civil Engineers, pp. 337-384.
- Bouwer, H. 1999, 'Artificial Recharge of Groundwater: Systems, Design, and Management', in L.W. Mays (ed), *Hydraulic Design Handbook*, McGraw-Hill Professional, pp. 24.1-24.44.

- Bouwer, H. 2000, 'The Recharge of Groundwater', *Natural Recharge of Groundwater Symposium Proceedings*, Groundwater Resources Association of California and Arizona Hydrological Society, Arizona, United States, pp. 95-102.
- Brooks, T. 1999, *Review of Roys Hill Artificial Recharge Site*, Hawke's Bay Regional Council, Hawke's Bay, New Zealand.
- Comsol. 2012, *Comsol Multiphysics User's Guide – Version 4.3* (www.comsol.com).
- Daniel, J.F., Cable, L.W., & Wolf, R.J. 1970, *Ground Water –Surface water relation during periods of overland flow*, United States Geological Survey, Professional Paper 700-b, pp. 219-233.
- Dillon, P. 2005, 'Future management of aquifer recharge', *Hydrogeology Journal*, vol. 13, no. 1, pp. 313-316, doi: 10.1007/s10040-004-0413-6.
- Dillon, P., Pavelic, P., Page, D., Beringen, H., & Ward, J. 2009, *Managed aquifer recharge: An Introduction. Waterlines Report Series No. 13*, National Water Commission, ACT, Australia.
- Dillon, P., Toze, S., Page, D., Vanderzalm, J., Bekele, E., Sidhu, J., & Rinck-Pfeiffer, S. 2010, 'Managed aquifer recharge: rediscovering nature as a leading edge technology', *Water Science & Technology*, vol. 62, no. 10, pp. 2338-2345, doi: 10.2166/wst.2010.444.
- Domenico, P.A., & Schwartz, F.W. 1998, *Physical and Chemical Hydrogeology: Second Edition*, John Wiley & Sons, United States.
- Fenemor, A.D., & Robb, C.A. 2001, 'Groundwater management in New Zealand', in M.R. Rosen & P.A. White (eds), *Groundwaters of New Zealand*, New Zealand Hydrological Society Inc, Wellington, New Zealand, pp. 273-289.
- Fenwick, G., Thorpe, H., & White, P. 2004, 'Groundwater systems', in J.S. Harding., P.M. Mosley., C.P. Pearson & B.K. Sorrell (eds), *Freshwaters of New Zealand*, New Zealand Hydrological Society Inc. and New Zealand Limnological Society Inc, Christchurch, New Zealand, pp. 29.1-29.18.
- Ferris, J.G., Knowles, D.B., Brown, R.H., & Stallman, R.W. 1962, *Theory of Aquifer Tests*, United States Geological Survey, Denver, Colorado, United States.

- Freeze, A., & Cherry, J.A. 1979, *Groundwater*, Prentice-Hall, New Jersey, United States.
- Gisborne District Council. 2002, *Regional Policy Statement*, Gisborne District Council, Gisborne, New Zealand.
- Gisborne District Council. 2005, *The State of Our Environment – Gisborne 2003-2004 – Fresh Water Resources*, Gisborne District Council, Gisborne, New Zealand.
- Gisborne District Council. 2007, *The State of Our Environment – Gisborne 2005-2006 – Fresh Water Resources*, Gisborne District Council, Gisborne, New Zealand.
- Gisborne District Council. 2011, *The State of Our Environment – Gisborne 2009-2010 – Fresh Water Resources*, Gisborne District Council, Gisborne, New Zealand.
- Golder Associates. 2013, *Selwyn-Te Waihora Land and Water Planning: Managing Groundwater Replenishment Using Managed Aquifer Recharge (MAR)*, Report No. 09781101119\_009\_R\_Rev0, Prepared for Canterbury Regional Council, Golder Associates, New Zealand.
- Golder Associates. 2014A, *Poverty Bay Groundwater Management – MAR Feasibility Stage 1A – Conceptual Model*, Report No. 1378110136-003, Prepared for Gisborne District Council, Golder Associates, New Zealand.
- Golder Associates. 2014B, *Poverty Bay Groundwater Management – MAR Feasibility Assessment and Goldsim Groundwater Management Tool (Stage 1B)*, Report No. 1378110136-003-R-Rev0-006, Prepared for Gisborne District Council, Golder Associates, New Zealand.
- Gonthier, G.J. 2007, *A Graphical Method for Estimation of Barometric Efficiency from Continuous Data – Concepts and Application to a Site in the Piedmont, Air Force Plant 6, Marietta, Georgia*, United States Geological Survey Scientific Investigation Report 2007-5111, Web-only publication (<http://pubs.usgs.gov/sir/2007/5111/>).
- Gordon, D. 2001, 'Gisborne', in M.R. Rosen & P.A. White (eds), *Groundwaters of New Zealand*, New Zealand Hydrological Society Inc, Wellington, New Zealand, pp. 355-366.

- Gordon, D. 2009, *Roys Hill Aquifer Recharge Review*, Unpublished, Hawke's Bay, New Zealand.
- Grant, P.J. 1972, *Groundwater of the Heretaunga Plains, Hawkes Bay: Report on Project NA/HY/1*, Ministry of Works, Wellington, New Zealand.
- Heath, R.C. 1983, *Basic Ground-Water Hydrology*, United States Geological Survey Water-Supply Paper 2220, Denver, Colorado, United States.
- Helsel, D.R., & Hirsch, R.M., 2002, 'Statistical Methods in Water Resources – Chapter A3', in United States Geological Survey, *Techniques of Water-Resources Investigations of the United States Geological Survey – Book 4. Hydrologic Analysis and Interpretation*, United States Geological Survey.
- Konikow, L., & Kendy, E. 2005, 'Groundwater depletion: A global problem', *Hydrogeology Journal*, vol. 13, pp. 317-320. Doi: 10.1007/s10040-004.
- Krause, P., Boyle, D.P., & Base, F. 2005, 'Comparison of different efficiency criteria for hydrological model assessment', *Advances in Geosciences*, vol. 5, pp. 89-97, doi: 10.5194/adgeo-5-89-2005.
- Kreibich, H., & Thiekern, A. 2008, 'Assessment of damage caused by high groundwater inundation', *Water Resources Research*, vol. 44, pp. no. 9, pp. 1-14, doi: 10.1029/2007WR006621
- Kresic, N. 2006, *Hydrogeology and Groundwater Modeling (Second Edition)*, CRC Press, United States.
- Nash, J.J., & Sutcliffe, J.V. 1970, 'River flow forecasting through conceptual models , Part 1 – A discussion of principles', *Journal of Hydrology*, vol. 10, no. 3, doi: 10.1016/0022-1694(70)90255-6.
- New Zealand Government. 1991, *Resource Management Act*, Ministry for the Environment, Wellington, New Zealand.
- Reid, D., & Scarsbrook, M. 2009, *A review of current groundwater management in Hawke's Bay and recommendations for protection of groundwater ecosystems*, NIWA Client Report: HAM2009-153, Prepared for Hawke's Bay Regional Council, NIWA, Hamilton, New Zealand.

- Robb, C. 2000, *Information on Water Allocation in New Zealand*, Lincoln Environmental Client Report 4375/1, Prepared for Ministry for the Environment, Lincoln Environmental, Wellington, New Zealand.
- Sinclair Knight Merz. 2010, *Managed Aquifer Recharge Feasibility Study*, Prepared for Canterbury Regional Council, Sinclair Knight Merz, Auckland, New Zealand.
- Schwartz, F.W., & Zhang, H. 2003, *Fundamentals of Groundwater*, Wiley, United States.
- Taylor, C. 1994, 'Hydrology of the Poverty Bay flats aquifers, New Zealand: recharge mechanisms, evolution of the isotopic composition of dissolved inorganic carbon, and ground-water ages', *Journal of Hydrology*, vol. 158, no. 1-2, pp. 151-185, doi: 10.1016/0022-1694(94)90051-5.
- Telfer, H. 2013, *Trends and Observations in Land Use on the Poverty Bay Flats 2007 – 2013*, Gisborne District Council, Gisborne, New Zealand.
- Toebe, C. 1972, 'The Water Balance of New Zealand', *Journal of Hydrology (New Zealand)*, vol. 11, no. 2, pp. 127-139.
- Todd, D.K., & Mays, L.W. 2004, *Groundwater Hydrology*, Wiley, United States.
- Weeber, J.H., Brown, L.J., White, P.A., Russell, W.J., & Thorpe, H.R. 2001, 'A History of Groundwater Development in New Zealand', in M.R. Rosen & P.A. White (eds), *Groundwaters of New Zealand*, New Zealand Hydrological Society Inc, Wellington, New Zealand, pp. 5-4.
- White, P.A., & Brown, L.J. 1997, *Assessment of the effects of artificial recharge on groundwater resources and river flows in the Heretaunga Plains*, Client Report 72652C.10, Prepared for Hawke's Bay Regional Council, Institute of Geological & Nuclear Sciences, Taupo, New Zealand.
- White, P.A. 2001, 'Groundwater Resources in New Zealand', in M.R. Rosen & P.A. White (eds), *Groundwaters of New Zealand*, New Zealand Hydrological Society Inc, Wellington, New Zealand, pp. 45-75.

- White, P.A., & Reeves, R.R. 2002, *The volume of groundwater in New Zealand 1994 to 2001*, Client Report 2002/79, Institute of Geological & Nuclear Sciences, New Zealand.
- White, P.A., Moreau-Fournier, M., Tschritter, C., & Murphy, P. 2012, *Groundwater in the Poverty Bay Flats*, GNS Science Consultancy Report 2012/106, Prepared for Gisborne District Council, GNS, New Zealand.
- White, P.A., Bekele, M., & Tschritter, C. 2014, *Advice on characterisation of groundwater and surface water in the Poverty Bay flats to support policy development by Gisborne District Council*, GNS Science Consultancy Report 2014/135, Prepared for Gisborne District Council, GNS, New Zealand.
- Winter, T.C., Harvey, J.W., Franke, O.L., & Alley, W.M. 1998, *Ground Water and Surface Water – A Single Resource*, United States Geological Survey, Denver, Colorado, United States.

# Appendices

**Appendix A. The bores for which groundwater levels are monitored manually once a month by the GDC, the aquifers which each bore taps, and the number of observations at each bore.**

<b>Bore</b>	<b>Aquifer</b>	<b>Observations</b>
GPA004	Te Hapara Sands	381 observations (Jan 1982 – Sep 2013)
GPA005	Te Hapara Sands	396 observations (Jan 1982 – Dec 2014)
GPI007	Shallow Fluvial Deposits	381 observations (Feb 1995 – Dec 2014)
GPG019	Waipaoa Gravel aquifer	281 observations (Aug 1991 – Dec 2014)
GPG059	Waipaoa Gravel aquifer	353 observations (Aug 1985 – Dec 2014)
GPG076	Waipaoa Gravel aquifer	240 observations (Jan 1995 – Dec 2014)
GPH022	Waipaoa Gravel aquifer	386 observations (Nov 1982 – Dec 2014)
GPH030	Waipaoa Gravel aquifer	240 observations (Jan 1995 – Dec 2014)
GPB002	Makauri Gravel aquifer	322 observations (May 1982 – Feb 2009)
GPB101	Makauri Gravel aquifer	373 observations (Dec 1983 – Dec 2014)
GPB102	Makauri Gravel aquifer	371 observations (Feb 1984 – Dec 2014)
GPB135	Makauri Gravel aquifer	281 observations (Aug 1991 – Dec 2014)
GPD115	Makauri Gravel aquifer	240 observations (Jan 1995 – Dec 2014)
GPD130	Makauri Gravel aquifer	321 observations (Apr 1988 – Dec 2014)
GPE034	Makauri Gravel aquifer	237 observations (Jan 1995 – Dec 2014)
GPF012	Makauri Gravel aquifer	239 observations (Jan 1995 – Dec 2014)
GPF035	Makauri Gravel aquifer	284 observations (Jul 1988 – Dec 2014)
GPF068	Makauri Gravel aquifer	232 observations (Jan 1995 – Dec 2014)
GPF071	Makauri Gravel aquifer	281 observations (Aug 1991 – Dec 2014)
GPF074	Makauri Gravel aquifer	254 observations (Nov 1993 – Dec 2014)
GPF090	Makauri Gravel aquifer	239 observations (Feb 1995 – Dec 2014)
GPF095	Makauri Gravel aquifer	281 observations (Aug 1991 – Dec 2014)
GPF106	Makauri Gravel aquifer	318 observations (Jul 1988 – Dec 2014)
GPF117	Makauri Gravel aquifer	240 observations (Nov 1993 – Dec 2014)
GPG026	Makauri Gravel aquifer	240 observations (Jan 1995 – Dec 2014)
GPG058	Makauri Gravel aquifer	353 observations (Aug 1985 – Dec 2014)
GPG060	Makauri Gravel aquifer	353 observations (Aug 1985 – Dec 2014)
GPG077	Makauri Gravel aquifer	309 observations (Apr 1989 – Dec 2014)
GPG088	Makauri Gravel aquifer	257 observations (Aug 1993 – Dec 2014)
GPH008	Makauri Gravel aquifer	362 observations (Nov 1984 – Dec 2014)
GPI026	Makauri Gravel aquifer	362 observations (Aug 1986 – Dec 2014)
GPI032	Makauri Gravel aquifer	224 observations (Feb 1995 – Sep 2013)
GPI040	Makauri Gravel aquifer	300 observations (Jan 1990 – Dec 2014)
GPJ040	Makauri Gravel aquifer	389 observations (Aug 1982 – Dec 2014)
GPJ045	Makauri Gravel aquifer	249 observations (Apr 1994 – Dec 2014)
GPJ066	Makauri Gravel aquifer	281 observations (Aug 1991 – Dec 2014)
GPO024	Makauri Gravel aquifer	240 observations (Jan 1995 – Dec 2014)
GPB039	Matokitoki Gravel aquifer	310 observations (Jul 1988 – Dec 2014)
GPB103	Matokitoki Gravel aquifer	342 observations (Jun 1986 – Dec 2014)
GPB117	Matokitoki Gravel aquifer	373 observations (Dec 1983 – Dec 2014)
GPB126	Matokitoki Gravel aquifer	320 observations (May 1988 – Dec 2014)
GPB128	Matokitoki Gravel aquifer	320 observations (May 1988 – Dec 2014)
GPB129	Matokitoki Gravel aquifer	320 observations (May 1988 – Dec 2014)
GPB130	Matokitoki Gravel aquifer	320 observations (Jun 1988 – Dec 2014)
GPC003	Matokitoki Gravel aquifer	396 observations (Jan 1982 – Dec 2014)
GPC036	Matokitoki Gravel aquifer	281 observations (Aug 1991 – Dec 2014)
GPD132	Matokitoki Gravel aquifer	321 observations (Apr 1988 – Dec 2014)
GPD134	Matokitoki Gravel aquifer	317 observations (Apr 1988 – Dec 2014)
GPD147	Matokitoki Gravel aquifer	243 observations (Dec 1992 – Dec 2014)

**Appendix B. Methods used to correct recorded groundwater levels for barometric effects following Gonthier (2007).**

To correct recorded groundwater levels for barometric effects (when necessary) the following equations were used:

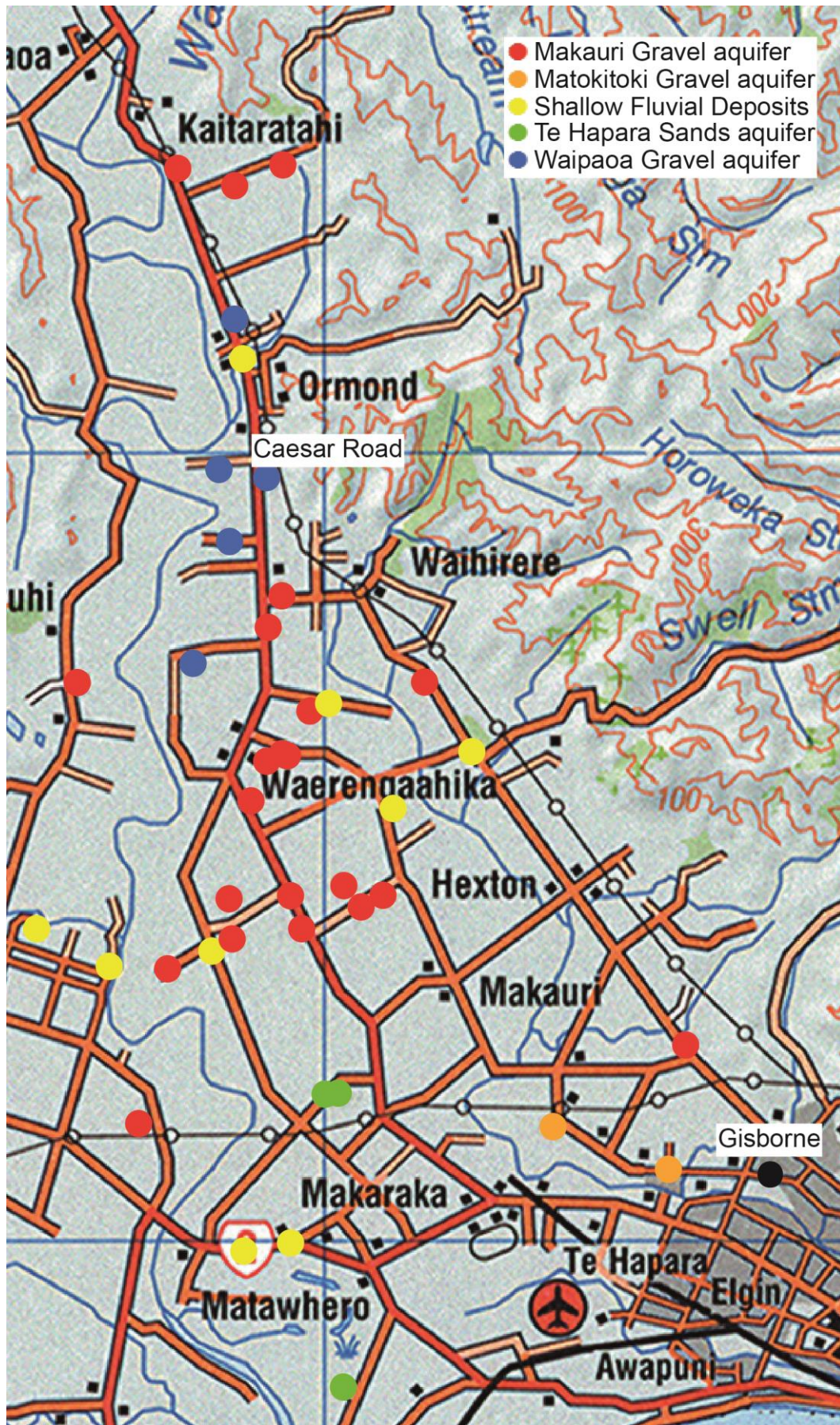
$$\alpha = \frac{\Delta P_{aq}}{\Delta P_{at}}$$

where  $\alpha$  is the barometric efficiency, which describes the rate at which groundwater levels change as a result of changes in atmospheric pressure,  $\Delta P_{aq}$  is the pressure change within the aquifer (m), and  $\Delta P_{at}$  is the change in atmospheric pressure at the land surface (m).

$$W_{t(c)} = W_{t(uc)} - \alpha(B_0 - B_t)$$

where  $W_{t(c)}$  is the recorded groundwater levels at time  $t$  corrected for barometric effects,  $W_{t(uc)}$  is the recorded groundwater levels at time  $t$  prior to correction for barometric effects, and  $(B_0 - B_t)$  is atmospheric pressure at time  $t$  ( $B_t$ ) referenced to an atmospheric pressure datum ( $B_0$ ). After correction for barometric effects inferences can be drawn about groundwater level changes without atmospheric pressure acting as a confounding variable.

Appendix C. Location of the 43 pumping undertaken within the Poverty Bay flats.



**Appendix D. Infiltrometer test procedure at the two sites identified using HIGGS Index.**

**Site 1**

Across Site 1 seven test holes were dug to a depth of at least 500 mm below the ground surface and the soil types found were recorded to determine which area would likely be most conducive to MAR using an infiltration basin. A sand layer was identified at Hole 2, which was not present at the other six holes. The spatial extent the sand layer at Hole 2 was then obtained by digging a further four test holes 50 m from Hole 2 in each direction. All four of the tests holes around Hole 2 had a sand layer present. Therefore, all infiltrometer tests were undertaken at Hole 2 (hereafter referred to as Site 1). Within the area in which the sand layer had been identified by the five test holes at Site 1 a 500 m<sup>2</sup> was marked out consisting of five 10 × 10 m sections. Random selection then identified a 1 × 1 m area in each of the five sections in which an infiltrometer test would be undertaken using the methodology outlined below

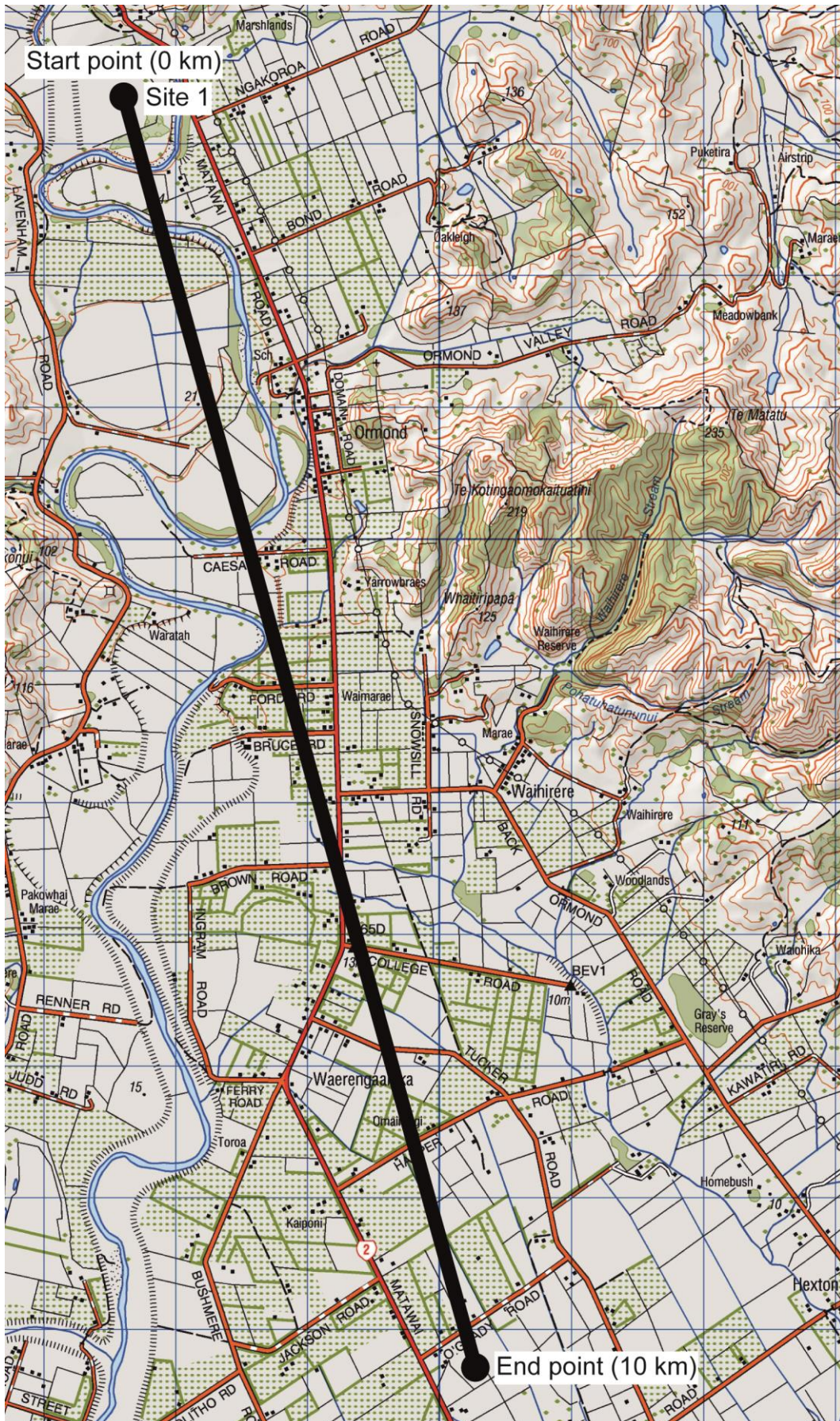
A hole was dug to a depth of 500 mm below the ground surface, a depth at which the sand layer was present. The hole was approximately 2.4 m long and 1 m wide. The inner and outer ring of the double-ring infiltrometer were then installed at depths of 50 and 45 mm, respectively, to prevent water from blowing a hole out beneath the infiltrometer following Bouwer (1986). Prior to filling each ring with water a plate was placed in each ring to minimise erosion following Bouwer (1999). The outer and inner rings were then filled with water to 150 and 250 mm, respectively. The plate was subsequently removed from each ring. The amount of time it took for the water level within the inner ring to drop 100 mm was recorded. After dropping 100 mm, the water level in the inner ring was refilled to 250 mm. The process was repeated four times until the accumulated infiltration reached 500 mm, which was deemed to be the point at which the soil was saturated following Bouwer (1999). At all times during the test the water level in the outer ring was held constant between 100 and 150 mm. Upon completion of the testing the lateral divergence of the water from the infiltrometer was recorded. infiltrometer was recorded.

## **Site 2**

Site 2 is limited in its spatial extent when compared with Site 1. At Site 2 two test holes were excavated to a depth of 500 mm below the ground surface at either end of the Site. The underlying soil conditions were similar, and therefore no further tests holes were necessary.

Initially it was planned to undertake the infiltrometer tests at Site 2 using the same installation depths at those used at Site 1. However, the number of stones present in Hole 1 meant that installing the double-ring infiltrometer at 500 mm below the ground surface risked affecting the infiltration rates. Therefore, the double-ring infiltrometer was installed 250 mm below the ground surface. The inner and outer rings were then installed at depths of 45 and 40 mm, respectively. The installation depths aside, the infiltrometer test was undertaken using the same methods as those at Site 1. No infiltrometer test was undertaken at Hole 2, which is detailed in Chapter 6.

**Appendix E.** Topographic map showing the cross-sectional area of the Poverty Bay flats that was modelled.



**Appendix F. Trend tests during the months of March and September for three of the aquifers within the Poverty Bay flats.**

Mann-Kendall trend test following Helsel and Hirsch (2002) on groundwater levels in the Te Hapara Sands during the months of March and September.

<b>Bore</b>	<b>Observations</b>	<b>p-value</b>	<b>Trend</b>	<b>Median Annual Sen slope (m)</b>
GPA004 (March)	32 observations (1982 – 2013)	0.112		
GPA005 (March)	33 observations (1982 – 2014)	1.000		
GPA004 (September)	32 observations (1982 – 2013)	0.199		
GPA005 (September)	33 observations (1982 – 2014)	0.271		

Mann-Kendall trend test following Helsel and Hirsch (2002) on groundwater levels in the Shallow Fluvial Deposits during the months of March and September.

<b>Bore</b>	<b>Observations</b>	<b>p-value</b>	<b>Trend</b>	<b>Median Annual Sen slope (m)</b>
GPI007 (March)	32 observations (1982 – 2013)	0.284		
GPI007 (September)	33 observations (1982 – 2014)	0.417		

Mann-Kendall trend test following Helsel and Hirsch (2002) on groundwater levels in the Waipaoa Gravel aquifer during the months of March and September.

<b>Bore</b>	<b>Observations</b>	<b>p-value</b>	<b>Trend</b>	<b>Median Annual Sen slope (m)</b>
GPG019 (March)	24 observations (1991 – 2014)	0.874		
GPG059 (March)	30 observations (1985 – 2014)	0.836		
GPG076 (March)	20 observations (1995 – 2014)	0.603		
GPH022 (March)	32 observations (1983 – 2014)	0.277		
GPH030 (March)	20 observations (1995 – 2014)	0.127		
GPG019 (September)	24 observations (1991 – 2014)	0.082		
GPG059 (September)	30 observations (1985 – 2014)	0.521		
GPG076 (September)	20 observations (1995 – 2014)	0.048	Increase	0.024
GPH022 (September)	32 observations (1983 – 2014)	0.807		
GPH030 (September)	20 observations (1995 – 2014)	0.745		

**Appendix G. Waipaoa River flow and stage, and atmospheric pressure during the period when groundwater levels were monitored for changes as a result of ex-tropical Cyclone Pam hitting the Gisborne District.**

<b>Date</b>	<b>River flow (m<sup>3</sup> s<sup>-1</sup>)</b>	<b>River stage (msl)</b>	<b>Pressure (hpa)</b>
14/03/2015	1.554	30.158	1017.0
15/03/2015	1.556	30.158	1014.3
16/03/2015	1.928	30.182	991.1
17/03/2015	115.07	31.144	992.8
18/03/2015	52.357	30.753	1006.9
19/03/2015	19.04	30.476	1015.8
20/03/2015	11.049	30.391	1025.2
21/03/2015	7.062	30.345	1028.1
22/03/2015	5.469	30.317	1024.3
23/03/2015	4.764	30.298	1023.2
24/03/2015	4.224	30.282	1021.2
25/03/2015	3.883	30.272	1021.7
26/03/2015	3.558	30.261	1019.8
27/03/2015	3.456	30.257	1018.0